LUND UNIVERSITY

MASTER'S THESIS

DIVISION OF MATERIALS ENGINEERING
DEPARTMENT OF MECHANICAL ENGINEERING
FACULTY OF ENGINEERING, LTH
OCTOBER 2014

Thermodynamics and Kinetics of Tungsten Oxidation and Tungsten Oxide Sublimation in the Temperature Interval 200°–1100°C

AUTHOR: **Johan Wendel**

SUPERVISOR: YONGJOONG LEE, EUROPEAN SPALLATION SOURCE AB, LUND

EXAMINER: SRINIVASAN IYENGAR, LUND UNIVERSITY, MATERIALS ENGINEERING

ISRN LUTFD2/TFMT --13/5047--SE

EUROPEAN SPALLATION SOURCE

Division of Materials Engineering

Department of Mechanical Engineering

Faculty of Engineering, Lund University

SE-223 63 Lund, Sweden

European Spallation Source ESS AB

Box 176

SE-221 00 Lund, Sweden

Abstract

The characteristics of tungsten oxidation and tungsten oxide sublimation have been examined to aid in the design of the target station of the European Spallation Source, ESS. Experiments were set up using thermogravimetric analysis methods to investigate mass changes of various samples. A wide temperature interval, 200°–1100°C, was chosen to accommodate different scenarios. Atmospheres of air (p_{O_2} = 0.21), pure argon ($p_{O_2} \leq 5$ ppm), pure helium ($p_{O_2} \leq 5$ ppm), and pure helium containing water vapor ($p_{O_2} \leq 5$ ppm, $p_{H_2O} = 0.0316$ atm) were used to determine under what conditions oxidation and sublimation occurs.

Tungsten foil samples kept at 575°and 625°C in argon for two hours acquired a total mass gain of around 0.1 % of the initial sample mass. Oxidation was observed at 200°C to a lesser extent. Longer experiments indicated that oxidation at 500°, 550°, and 600°C follows a linear trend in mass gain per unit time over the experiment length of 48 h.

Tungsten discs kept at 500°C in helium for two hours indicate parabolic oxidation behavior and the total mass gain was close to 0.1 % of the initial sample mass whereas at 900°C, the mass gain reached upwards of 1 %. Electropolished (EP) discs oxidized to a lesser extent than unpolished (UP) discs, indicating a finer surface quality. Rate constants were acquired and plotted according to an Arrhenius relationship. The activation energies corresponding to the chemical reaction between tungsten and oxygen were calculated to 40 and 94 kJ/mol for UP and EP samples, respectively, whereas the activation energies for the parabolic oxidation were calculated to 142 and 153 kJ/mol UP and EP samples, respectively.

Thermogravimetric analysis of WO_3 sublimation showed no evidence of sublimation below 1100°in dry helium or air. A helium atmosphere containing water vapor at 1075°C was needed to sublimate tungsten trioxide. The rate constant for sublimation was determined to be 1.77 mg/cm^2h.

Keywords: Tungsten, Tungsten Oxide, Oxidation, Sublimation, Thermodynamics, Kinetics, High temperature, STA, TGA.

Acknowledgements

This master's thesis was completed at the Division of Materials Engineering at the Faculty of Engineering at Lund University in collaboration with the European Spallation Source, ESS.

I would like to thank Professor Srinivasan Iyengar for his assistance in guiding me through this work with his vast knowledge in materials science and engineering. I would also express my gratitude to Hossein Sina, PhD student, and Zivorad Zivkovic for their support regarding my experiments. A special thanks to Jemila Habainy, PhD student, for her guidance and inspiring me to complete this thesis. Finally, I am grateful to ESS and Dr. Yongjoong Lee for the opportunity to conduct this thesis.

Contents

List of Figures

List of Tables

List of Acronyms

$\mathbf{CaWO_4}$	Scheelite
ESS	European Spallation Source
$\mathbf{(Fe,Mn)WO_4}$	Wolframite
$\mathbf{O_2}$	Molecular oxygen
$\mathbf{O^{2-}}$	Oxygen ion
STA	Simultaneous Thermal Analysis
TGA	Thermogravimetric Analysis
W	Tungsten
$\mathbf{W^{+4,5,6}}$	Tungsten ions of different valency
$\mathbf{WO_2}$	Tungsten dioxide
$\mathbf{WO_{2.72}}$	Tungsten oxide
$\mathbf{WO_{2.90}}$	Tungsten oxide
$\mathbf{WO_{2.96}}$	Tungsten oxide
$\mathbf{WO_3}$	Tungsten trioxide
$\mathbf{WO_3 \cdot H_2O}$	Tungstate

Chapter 1

Introduction

This section is intended as a brief introduction to the subject of tungsten as a spallation target material and how adequate environmental control is paramount for the use of tungsten at elevated temperatures. First, a short description of the European Spallation Source, ESS, will be provided followed by an overview of the literature survey that was made.

1.1 The European Spallation Source

The European Spallation Source is a large scale science and technology facility currently being built in Lund, Sweden. It is a joint European project in which 17 member states are currently involved. At the time of its completion, it will encompass one of the most extensive neutron imaging capabilities in the world and is believed to aid unique research in a great variety of scientific fields, e.g. fundamental physics, materials chemistry and structure biology.

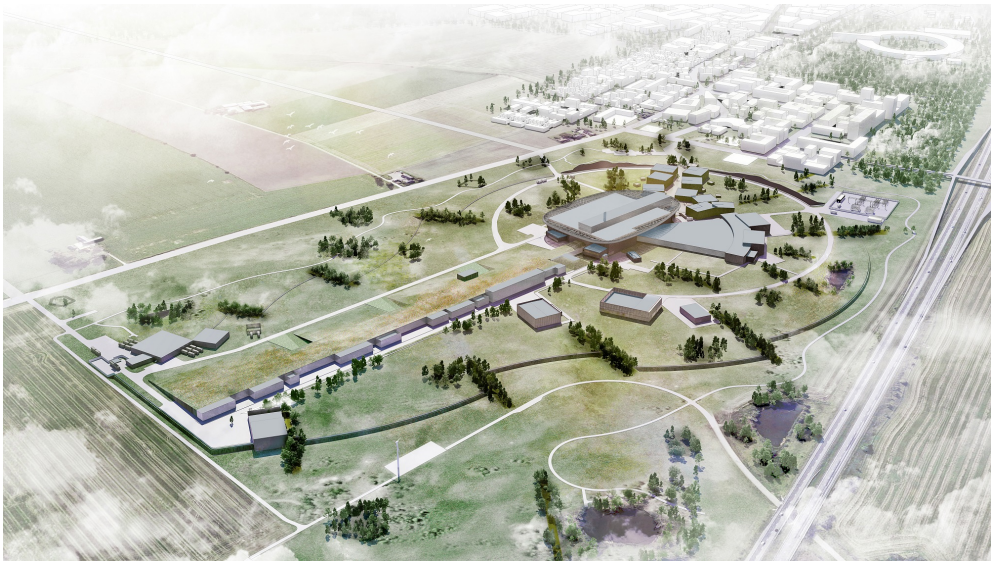

Figure 1.1: The latest conceptual rendering of ESS [1].

In the heart of the facility lies the so called target station in which the high power proton beam is directed towards a rotating wheel of tungsten slabs. When exposed to the high energy protons, some of the neutrons of the tungsten will be knocked out in the spallation process. This is illustrated in Figures 1.2 and 1.3.

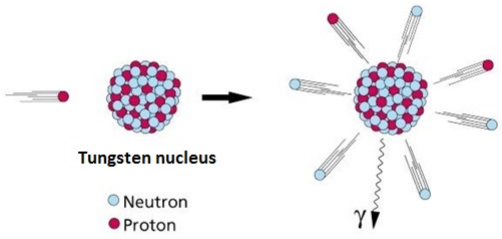

Figure 1.2: The spallation process.

The technical design report on the target system summarizes its function: 'The main function of the target station is to convert the high-energy proton beam from the accelerator into low-energy neutron beams with the greatest possible efficiency, safety and reliability.' [5].

The spallation process induces considerable amounts of heat inside the tungsten material and sufficient cooling by helium gas is crucial for the operation. Despite flowing through a purification loop, small amounts of oxygen impurities will inevitably be present in the helium gas and the strong tendency for tungsten to oxidize in the presence of oxygen is problematic when designing the spallation target. At the time of writing this thesis, the designated operating temperature is set to a maximum of 500°C. At these elevated temperatures, tungsten reacts with oxygen and forms various tungsten oxides and this can cause contamination of the facility. If some kind of accident takes place that introduces even more oxygen into the environment or raises the target temperature to higher levels, the effect will be even more severe. It is easy to see that limitation of oxidation is an important design parameter.

During the operation, the tungsten metal will be subject to a temperature cycling process. The reason for this is the placement of 33 segments of tungsten on a rotating wheel that will each sequentially align with the proton beam window which will allow for beam exposure. The designated temperature of 500°C will be induced as soon as the spallation process is initiated by protons from the accelerator, after which the segment will immediately cool down as alignment with the beam is lost. The helium gas flowing past the rotating tungsten segments will cool each segment to around 400°C prior to the next beam exposure. The helium gas will also cycle in temperature, from 30°to 230°C, due to heat exchange with the target. As the helium

gas is flowing with a high velocity around the tungsten target, erosion will also be a problem in the target design.

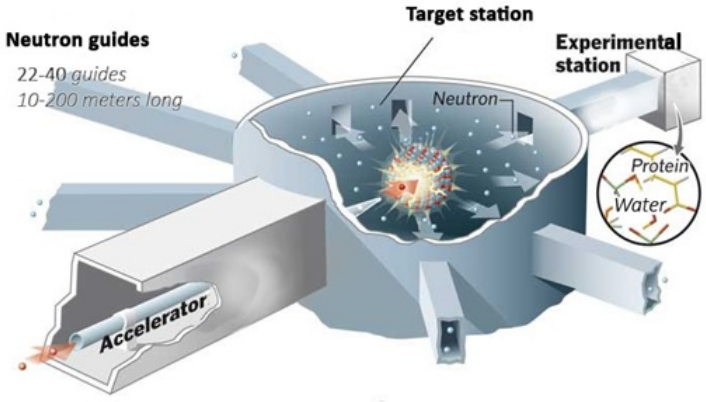

Figure 1.3: Spallation inside the target station.

It is unclear whether the temperature cycling of the tungsten target or the cooling gas could have any significant implications on the operation but it is possible that the tungsten oxide could be more prone to crack formation under these conditions and that the helium gas could solve more contaminants. These implications will not be investigated in this thesis.

In the target station design report it is stated the surface area of the wheel is large enough that, in the event of a loss of power and/or coolant, passive cooling would prevent unsafe target temperatures with a significant safety margin [5]. What this means in terms of limitation of oxidation and sublimation is unclear, as e.g. oxidation can be a problem even below the designated operation temperature.

Given these ramifications, a literature survey was made to assess previous work on oxidation and sublimation of tungsten under different conditions. It is worth noting that very few sources discuss the use of tungsten as a spallation target.

1.2 Objectives

This thesis will focus on the oxidation and sublimation characteristics of the tungsten spallation target of ESS.

A review of existing literature on this subject will be made in order to gather relevant information. Theoretical aspects of oxidation and sublimation will be made with a focus on tungsten and tungsten oxides. Experiments based primarily on thermogravimetric analysis will be set up to determine the thermodynamic and kinetic characteristics of these processes. Different temperatures, experiment lengths, atmospheres, and sample types will be used as the basis for conclusions. The objectives can be summarized by the following points.

- The extent of oxidation in pure helium in the interval 200°–1000°C.
- Determine the temperature range where sublimation of tungsten oxide is significant.
- From this data, acquire rate constants and activation energies describing the kinetics of oxidation and sublimation.

Additionally, previously established kinetic models are investigated and, based on results, correlated with the acquired results of this thesis.

Special concern will be taken to discuss the implications that the results may have on spallation target in ESS in terms of normal operation or due to an elevated temperature in an accident scenario. The results can e.g. confirm previous findings on the kinetics of oxidation or establish the sublimation temperature of tungsten trioxide.

1.3 Literature review

This section is intended as a brief introduction to previous work on the subject of oxidation and sublimation of tungsten and its different oxides. The general idea here is to present the most relevant and up to date results in a conclusive form. Naturally, a lot of information exists in the literature which describes various aspects of e.g. oxidation, but the findings are often inconclusive and spread out. Numerous discrepancies of the results can also be found when cross referencing articles. The inconsistency in the literature is most apparent for reported values of the activation energies of oxidation processes, and for the sublimation temperature of tungsten trioxide. This is mainly a result of the difference in experimental setups the authors have used. Furthermore, some articles or book extracts lack a clear description of the conditions of the experiments and these results can therefore be complicated to compare with other reported values. In this thesis, the experimental conditions are reported as accurately as possible to ensure repeatability.

Pure tungsten, tungsten alloys and tungsten oxides have all been studied extensively over the past fifty years or so. There appears to have been a significant surge

in research of tungsten in various forms during the 1960's. The cause of this can probably be attributed to the post-war interest in tungsten as a structural material for aeronautics and astronautics as well as for military use.

The mechanical properties of tungsten are well documented for many situations as a result of the research. Although pure tungsten and various alloys with tungsten as a key component have one of the best high-temperature mechanical integrities, the properties deteriorate rapidly with an increase in working temperature [6]. Despite this, tungsten is one of the materials that can be used with some success in structural applications when the temperature reaches high levels. The tungsten slabs used in ESS as the spallation target material will not have any structural requirements other than those imposed by the thermomechanical fatigue issues. One major drawback with tungsten however is the lack of environmental resistance. The reason for this is the relatively poor resistance to oxidation that tungsten exhibits. In order to counteract this, the pure metal needs protective coatings.

The majority of the literature that is reviewed is based on articles from a broad range of well-known journals. The experiments are most often conducted in air or in pure oxygen gas which is a particularly ill-suited atmosphere for pure tungsten. The high partial pressure of oxygen will essentially turn pure tungsten to pulverized WO_3 in days. There are fewer experiments conducted which pin-point the oxidation kinetics of pure tungsten in atmospheres with a very low partial pressure of oxygen, which is central to the approach of ESS for having tungsten as a spallation source material.

1.3.1 ESS Target Station reports

A natural basis for this thesis is various technical reports provided by the Target Station Division of ESS. Mainly two reports are used, one providing an overview of the function and role of the target station itself by Peggs [7], and the other containing a more detailed description of the designated target material tungsten [8].

In the ESS target station report [7], some experiments are discussed in which two tungsten alloys, W-Ni-Cu and W-Ni-Fe, are exposed to a He+5% O_2 gas mixture. Despite a brief contact with this gas, there was a significant level of oxidation above 600°C. It is obvious that further oxidation studies are of interest to ESS.

Since then, the spallation target is designed to consist of pure tungsten slabs. This thesis will therefore focus on the oxidation of pure tungsten and sublimation of tungsten oxide, and not be concerned with any tungsten alloys.

1.3.2 Technical translations: NASA and others

A great source of information on the oxidation of tungsten is a literature review collection published by NASA in august 1969 [9]. In this technical translation it is reported that a study conducted in 1956 observed two different oxide layers on an oxidized tungsten sample. The outer layer was found to be WO_3 while the inner layer was not determined. However, the authors observed that the thickness of this

inner layer did not change with an increase in the duration of the oxidation.

The authors discuss whether or not it is possible to consider the oxide layers to be homogeneous and isotropic phases, but they conclude that it is too simplified. The crystal orientation of the oxide film on the surface of the grain-oriented metal is directly linked with the orientation of the oxidizing metal. The rate of growth of the film depends on its crystal orientation. For example, one research group found that during the process of oxidation, some of the crystals in the oxide film grow more rapidly because of a more advantageous orientation.

This is further supported in another experiment where scientists were able to determine that the crystal orientation influences the oxidation rate in a significant way. The crystallographic planes were ranked (100)>(111)>(110) in order of susceptibility to oxidation. The (100) face oxidized roughly 6 times more rapidly than the (110) face. This trend was observed in single crystals of tungsten in dry oxygen at a temperature of 2050°±50°C and an oxygen partial pressure of 10^{-6} atmospheres.

This technical translation also houses numerous reported values for the activation energy of different processes. The most interesting ones are arguably those related to the oxidation process, e.g. both for the chemical reaction between tungsten and oxygen and for oxygen ion diffusion in tungsten oxide. The figures are often conflicting and can deviate much from each other. Gulbransen and Andrew found three different values of the activation energy at different regions and conditions. When the oxidation follows a parabolic rate law, the process has an activation energy of 186 kJ/mol but when deviations from the parabolic region are found, the activation energy was found to be 228 kJ/mol. Above 800°C the authors obtained a value of 136 kJ/mol. Arzhanyy *et al.* reports a value of 97 kJ/mol, whereas Gulbransen and Wysong [10] found that the oxidation followed a parabolic behavior between 400°and 500°C and that the activation energy was 191 kJ/mol in this range. Deviations were found over 500°C and below 400°C. Clearly, there is a discrepancy in these reported values which is likely explained by the differences in experimental setups. It is important to stress that the reported activation energies correspond to the migration of oxygen ions, O^{2-}, through the tungsten oxide scales. This will be explained in the theory section.

Furthermore, Gulbransen and Wysong could not observe any weight loss in a thick film until 800°C was reached. At 850°C, the sublimation rate was much faster. On thin films, the oxide was stable until 900°C and was appreciable at 1000°C. As the sublimation proceeded, the rate decreased. They concluded that the volatility of the tungsten oxide is not only dependent on temperature but also on film thickness.

1.3.3 Books devoted to tungsten

A great source of information about tungsten and its compounds is found in a book authored by Lassner and Schubert [3]. Tungsten metal is stable in dry and humid air only at moderate temperature. It starts to oxidize at about 400°C. The oxide layer is not dense and does not offer any protection against further oxidation. Above 700°C the oxidation rate increases rapidly, and above 900°C, sublimation of the

oxide takes place, resulting in catastrophic oxidation of the metal. Any water vapor content of the air enhances the volatility of the oxide. Another section summarizes that oxidation starts at approximately 400°C, that above 500°C the oxide layer will start to form cracks, and at 800°C, sublimation of WO_3 takes place.

Tungsten also reacts with water to some extent from room temperature up to 2000°C. The reaction rate is determined by the temperature and the p_{H_2O}/p_{H_2} ratio. As a reaction product, the presence of H_2 always has to be considered. The reaction rate as well as the O:W ratio of the oxide formed increases with temperature and p_{H_2O}/p_{H_2} ratio. Water increases the volatility of the tungsten oxides by the formation of the volatile oxide hydrate $WO_2(OH)_2$. Another section indicates that bulk tungsten does not react with water but oxidizes in presence of water vapor at elevated temperature, e.g. 600°C.

The authors point out that although tungsten exhibits a very high melting point, its sensitivity towards oxidation is a big advantage which in turn limits all high-temperature applications to a be confined to a protective atmosphere or vacuum.

1.3.4 Journal articles

Oxidation of tungsten

The tungsten oxides obtained during many types of oxidation experiments will yield compounds that are colored. The phenomenon is described by electrochromics and many different transition metals have oxides which are subject to this effect. The electrochromic colors derive from the intervalence charge-transfer optical transitions taking place within the material. These transitions are a consequence of the electron-transfer processes occurring during the oxidation reactions and will give rise to a variety of different colors [11]. The stoichiometric compound tungsten trioxide, WO_3, will e.g. exhibit a pale yellow look whereas tungsten dioxide, WO_2, will be more blue.

A paper on electrochromic oxides by Granqvist [12] describes that the crystals of all well-known metal oxides that exhibits electrochromism are composed of MO_6 octahedra arranged in an array by corner- and/or edge-sharing. The crystal structure of tungsten trioxide, WO_3, is of perovskite-type, as is many binary compounds of MO_3-type, where M is a hexavalent metal cation and O is a divalent oxygen anion. Various atomic displacements and rotations of the octahedra can occur which in turn makes the WO_3-oxide stable in a number of different forms, including tetragonal, orthorhombic, monoclinic and triclinic symmetries. These are temperature dependent meaning that it might be possible to control this polymorphism phenomenon by regulating the temperature of the oxide.

In addition to this, it has been shown in various articles that tungsten has a tendency to form a wide range of substoichiometric Magnèli phases. These phases are very complex with large unit cells and where the octahedra can be arranged so that tunnels through the oxides can be formed which have pentagonal or hexagonal cross sections. These tunnels can promote ion transport, which in turn possibly increases the extent of the oxidation [12]. Depending on what crystal structures exist

in the oxide layer, it will exhibit different colors due to the electrochromic effect. Electronic band theory can then be established in order to explain the coloration of the oxides, but this will not be described in this report.

In an article by Dunn [13], the complexity of tungsten oxide is reviewed through a series of oxidation experiments. Dunn states that it has been observed in some metals, e.g. copper, that a sintering process takes place at higher temperatures, which could lead to a densification of the otherwise porous oxide, thereby reducing the oxidation rate and altering the appearance of the mass curve slightly. Dunn rejects this idea as the oxidation curve at 900°C follows a perfect parabolic curve and concludes that tungsten trioxide must be in equilibrium with its surroundings since it is not sintered. The polymorphism of tungsten oxides is also discussed in the article and the kink in the oxidation curves observed at 800°–900°C is attributed to a transition between two allotropes of tungsten trioxide. The oxide is not being a unary substance, but rather a mix of α-WO_3 and β-WO_3. The β-modification is formed in excess at higher temperatures and is less permeable to oxygen, reducing the oxidation rate. Dunn concludes that some evidence for this is given by the color changes, from "lemon-yellow" at ordinary temperatures to "deep-orange" at higher temperatures. This color-based conclusion cannot be strengthened in this thesis, however, as samples subjected to higher temperatures emerges green-grey rather than "deep-orange". It is notable though, that all samples were orange in color immediately after being removed from the furnaces of each experiment in this thesis.

Volatilization of tungsten oxides

Compared with studies regarding the oxidation of tungsten, there are relatively few sources discussing the sublimation of tungsten oxides. Some of those will be reviewed in this section.

Poluboyarinov *et al.* [14] state that the thermomechanical and heat-physical properties of refractory ceramics have been studied before, but that their suitability for prolonged use is also dependent on volatilization, which is not as commonly described. If the ceramic, e.g. WO_3, can be described as a porous ceramic, the volatilization may not only occur from the external surface but also from the internal interfaces. Since it is hard to determine the effective surface area of a porous specimen, one can adopt a standard volatilization rate based on the external dimensions of the specimen.

Belton and McCarrin [15] investigated how water vapor could react with tungsten trioxide and form $WO_3 \cdot H_2O$ or similar tungstate species. The water vapor aided the sublimation rate of tungsten oxide by forming these tungstate species. The reaction lowered the partial pressure of trioxide gas over the surface, allowing more solid trioixde to become gaseous. This in turn enhanced the rate of sublimation.

No humid atmospheres are used in this thesis, but the notion that some species could aid in the volatilization of tungsten oxides should still be kept in mind when reading through it.

Hargittai *et al.* [16] investigated different species formed by sublimation of tungsten through electron diffraction methods with experiments conducted at 1400°C. The authors state that the sublimation of oxide is not appreciable below 1000°C either in vacuo or a stream of neutral gas. However, tungsten oxides volatilize readily in the presence of water vapor at 1000°C and at a pressure of 1 atm.

Webb *et al.* [17] further strengthens this idea and discusses different allotropes of tungsten.

Chapter 2

Theoretical Background

The theoretical concepts governing the nature of the oxidation and sublimation processes of pure metals are generally well understood, although, as pointed out earlier, there are still some inconsistencies found in the literature. This section of the thesis will present an overview of the subject, divided into several subsections dedicated to important aspects of oxidation and sublimation.

A convenient way to think about these physical and chemical processes is to divide them into two parts; thermodynamics and kinetics. A convenient and simply way to think of it is that the thermodynamics answers why the reactions proceed, whereas kinetics describe how they proceed.

First, however, an overview of the physics and chemistry of tungsten and its oxides will be provided as an introduction to the subject.

2.1 The history and uses of the element tungsten

The history of tungsten began in 1781 when two Swedes, Carl Wilhelm Scheele and Torbern Bergman suggested that it might be possible to reduce an acid made from the mineral Scheelite (at that point known as tungsten), $CaWO_4$, to obtain a new, unknown metal. Two years later, in 1783, two Spanish chemists, José and Fausto Elhuyar managed to reduce acid made from the similar mineral Wolframite, $(Fe, Mn)WO_4$, and isolate this new metal which was named tungsten. Since then, tungsten has become known as a metal with many uses and is utilized for its unique properties in everything from micron-sized eukaryotic cells to advanced military equipment.

Tungsten, with the chemical formula W, is the 74th element in the periodic table. The elements of this row are commonly called the transition metals. Tungsten is not found in its pure form in nature but is trapped in various types of minerals like Scheelite and Wolframite. The density of tungsten is very high, $19.25 g/cm^3$, comparable to that of gold and additionally has the highest melting point and lowest vapor pressure of all pure elements.

Tungsten has a high elastic modulus and is commonly used on its own or as an alloying element for high-strength alloys. Furthermore, it retains much of its

strength and excellent mechanical properties even beyond the point where other materials have already melted. Unfortunately, tungsten is susceptible to various corrosion scenarios which limits its use in these environments. The corrosive attacks such as oxidation are often accentuated at higher temperatures which paradoxically limits the utilization of the high-temperature properties of tungsten. This is the primary cause for restriction when using tungsten for high-temperature applications [6] and successful limitation of the impacts of e.g. oxidation is the key to utilizing the unique properties of tungsten in oxidizing environments. The oxidation characteristics of tungsten are determined by the interplay between thermodynamics and kinetics.

2.2 Thermodynamics of oxidation

The tendency for tungsten to oxidize is indicated by the change in Gibbs free energy, ΔG, accompanying the formation of the oxide.

$$\Delta G = \Delta H - T\Delta S \tag{2.1}$$

where ΔH is the change in enthalpy, T is the temperature and ΔS is the change in entropy upon formation of the oxide. The second law of thermodynamics states that when $\Delta G<0$, a spontaneous reaction is expected, and this is the case for oxide formation. The combination of a fixed amount (1 mol) of the oxidizing agent, e.g. O_2, with the metal, e.g. W, is given by $\Delta G^\circ$and is called the standard Gibbs free energy of the reaction [18]. The value of ΔG is related to how much free energy the system can release upon oxide formation, and since the system by default wants to minimize its energy, the oxide will form if it is thermodynamically favorable. The oxidation of tungsten is governed by the second law of thermodynamics.

The numerical value of ΔG for the oxidation reaction progressively becomes smaller as the temperature increases. This indicates that the tendency for oxide formation decreases, and consequently the oxides become less stable.

The reason for this is a decrease in entropy for the reaction which becomes apparent when analyzing the reaction further. Entropy is a measure of disorder in a system and the entropy change of the reaction thus gives information about how much the order is changing when the reaction is taking place. When the oxide is forming, a solid metallic component, e.g. W, is combining with a gaseous component, e.g. O_2, which then subsequently combines to the oxide in its solid form. Both solids are highly ordered relative to the gas molecule and thus the overall change in entropy is negative, as the system becomes progressively more ordered with the extent of the oxidation. The slope in the so called Ellingham diagram is almost the same for all oxides, owing to the fact that the entropy change of the reaction is approximately equivalent to the entropy of oxygen, as the metal reactant and the oxide product are both solids. This is evident when comparing the Gibbs equation for the formation of a variety of tungsten oxides and plotting the results in an Ellingham diagram.

Because of the positive slope of the ΔG°versus T line for most oxides in an

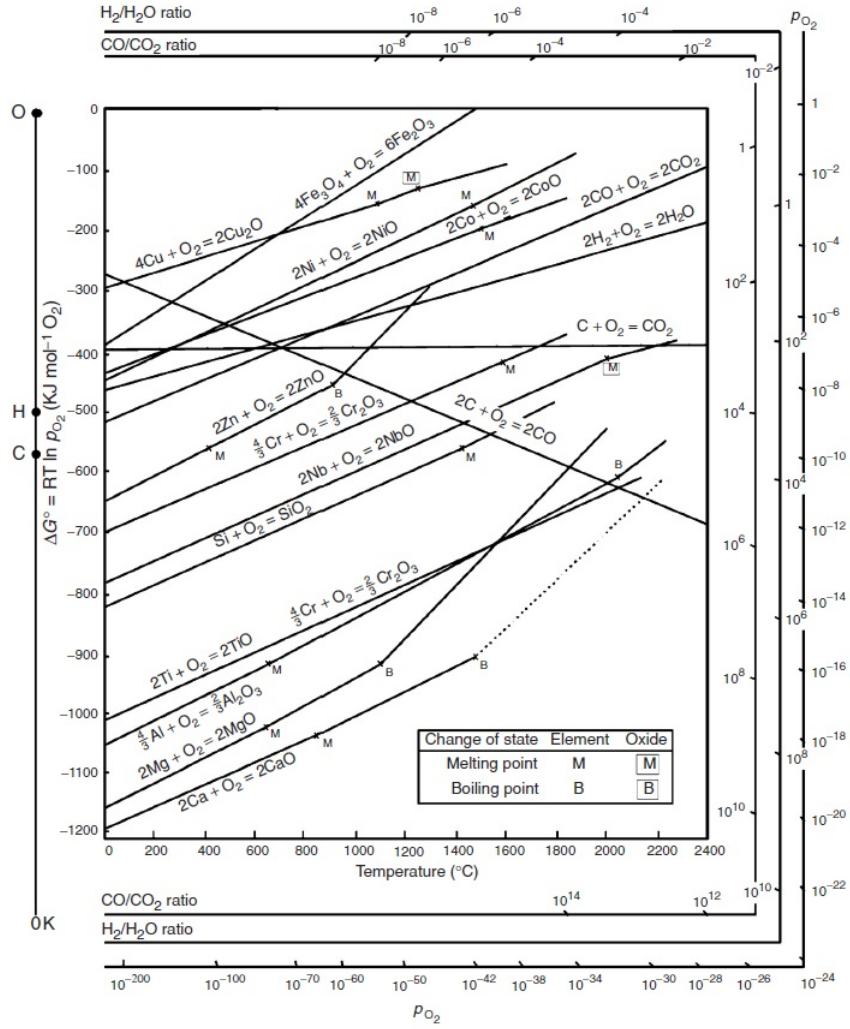

Figure 2.1: Standard free energy of formation of selected oxides as a function of temperature [2].

Ellingham diagram, ΔG°will approach zero at some elevated temperature. This is known as the standard dissociation temperature when the oxide is in equilibrium with the pure element and oxygen at a pressure of 1 atm. The temperature at which this phenomena occurs is affected by pressure according to.

$$p_{O_2} = e^{-\frac{\Delta G^{\circ}}{RT}} \tag{2.2}$$

This equation describes the equilibrium dissociation pressure of the oxide at the temperature T. If the pressure is lowered below this value the oxide will dissociate, if raised above it, the oxide is stable. As mentioned earlier, this can be graphically represented in an Ellingham diagram which gives a good overview to quickly estimate the appearance of the slope. The various tungsten oxides are often not presented in the Ellingham diagrams as they only tend to show the most common oxides. If thermodynamic data of the formation is tungsten oxides is available though, it

is possible to add these curves into another Ellingham diagram. In addition to graphically determining the equilibrium partial pressure for oxygen, it is possible to calculate it analytically by using the simple thermodynamic equilibrium equation. This can be illustrated by regarding the equilibrium constant for the formation of tungsten dioxide.

$$W(s) + O_2(g) \rightleftharpoons WO_2(s) \tag{2.3}$$

The equilibrium constant for the reaction is

$$K = \frac{a_{WO_2}}{a_W \cdot a_{O_2}} \tag{2.4}$$

where a_{WO_2}, a_W and a_{O_2} are the activities of the tungsten dioxide, tungsten metal and oxygen gas, respectively. Both the oxide and the metal exist in their standard states and their activities are defined as unity, whereas the activity for the oxygen is related to its partial pressure by a fugacity constant. The partial pressure of the oxygen in the atmosphere is defined as the pressure the oxygen would have while occupying the total volume by itself, at the same temperature. The oxygen is considered to be an ideal gas, then the fugacity constant is unity and the activity of the oxygen is equal to its partial pressure.

$$K = \frac{1}{p_{O_2}} \tag{2.5}$$

As discussed in the previous section on the thermodynamic principles, the key driving force for the formation of oxides in the first place lies in the tendency for the system to minimize its free energy. Formation of different oxides is a convenient way for metals to do this, as is evident by the negative change in Gibbs' free energy upon oxide formation. The change is affected by both pressure and temperature, but the pressure is taken to be constant. Some oxides are more advantageous from a thermodynamic point of view, yielding the most negative change in free energy when the metal oxidizes. The appropriate thermochemical data is available for a collection of tungsten oxides which makes it possible to construct graphs representing the differences in the change of free energy.

In a book describing the high temperature oxidation of metals [2], it is stated that an atmosphere with the active oxidizing species diluted with an inert species, the active molecules will rapidly become depleted in the gas layers immediately adjacent to the specimen surface. The reaction can then only continue if the active molecules can diffuse through the denuded gas layer to the metal surface. However, this may not be applicable if there is a gas flow continuously supplying new molecules to the system.

2.2.1 Tungsten oxides

Tungsten has an intricate and complex relationship with oxygen and will form a large variety of different oxides. This is evident when looking at the following figure originally from Lassner and Schubert [3].

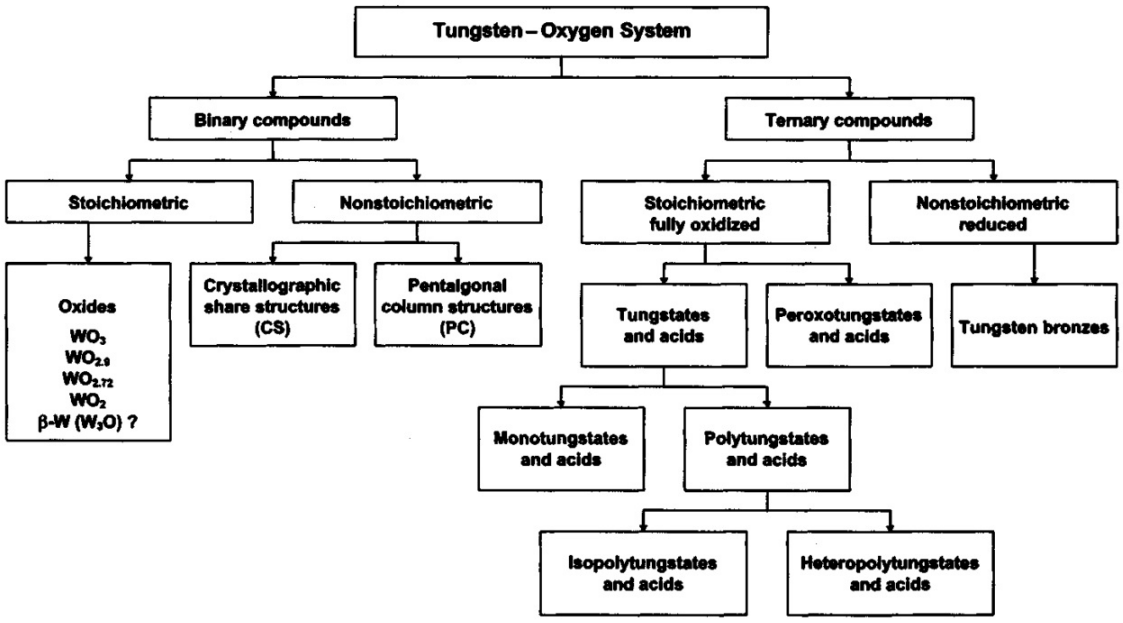

Figure 2.2: Flow chart of compounds of the Tungsten-Oxygen System [3].

Wriedt [19] wrote an exstensive article describing the nature of these compounds. It is stated that at 1 atm pressure, the equilibrium phases of the W-O system are the αW, the monoclinic oxide WO_2, the monoclinic oxide $W_{18}O_{49}$, the monoclinic oxide $W_{24}O_{68}$, the homologous series of monoclinic oxides W_nO_{3n-2} and W_nO_{3n-1}, and WO_3 with at least 11 different types.

It has been confirmed that the tungsten trioxide, WO_3 occurs sequentially as monoclinic, triclinic, monoclinic, orthorhombic and tetragonal crystals.

Wriedt points out that the range of stability for some of these oxides are unknown. Additionally, the literature is sometimes ambiguous as there are problems when distinguishing these phases from each other and from O-deficient WO_3. The following phase diagram of the W-O system illustrates the complexity, particularly due to the W_nO_{3n-2} and W_nO_{3n-1} series at 74-75 at-% O.

The presence of tungsten dioxide, WO_2 is supported by many sources. On its oxygen-deficient side, WO_2 is in equilibrium with and coexists with $\alpha - W$ at all temperatures, whereas on its oxygen-rich side, WO_2 is coexisting with a range of different oxides, depending on which temperature the system is subjected to.

Tungsten forms a variety of different oxides when exposed to oxygen as is evident when evaluating the expression for the change in Gibbs free energy. There are many reported oxides but the best well documented ones include WO_2, $WO_{2.72}$ ($W_{18}O_{49}$), $WO_{2.90}$ ($W_{20}O_{58}$), $WO_{2.96}$ ($W_{50}O_{148}$). The driving force of oxide formation can be determined by calculating the change in Gibbs free energy from their respective oxidation reactions, seen below. Note that each reaction is normalized to 1 mol of oxygen for easier comparison of the reactions.

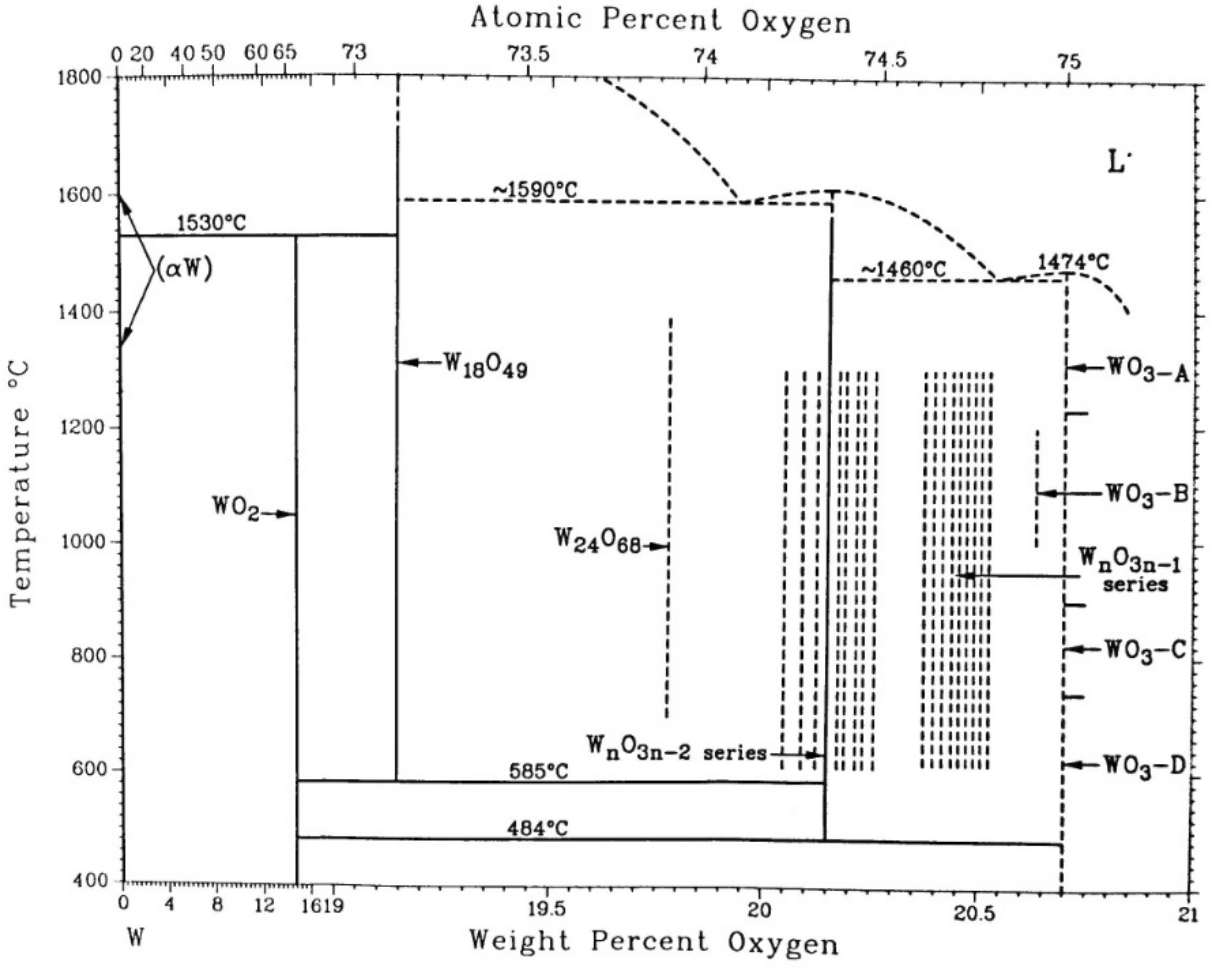

Figure 2.3: Phase diagram of the W-O system, condensed form [4].

$$W(s) + O_2(g) \rightleftharpoons WO_2(s) \qquad \Delta G_f$$

$$\frac{18}{49}W(s) + O_2(g) \rightleftharpoons \frac{18}{49}WO_{2.72}(s) \qquad \Delta G_f$$

$$\frac{20}{58}W(s) + O_2(g) \rightleftharpoons \frac{20}{58}WO_{2.90}(s) \qquad \Delta G_f$$

$$\frac{50}{158}W(s) + O_2(g) \rightleftharpoons \frac{50}{158}WO_{2.96}(s) \qquad \Delta G_f$$

$$\frac{2}{3}W(s) + O_2(g) \rightleftharpoons \frac{2}{3}WO_3(s) \qquad \Delta G_f$$

Each of these equations is associated with a specific free energy of formation, ΔG_f, which describes the thermodynamic conditions for stability in the case when oxygen reacts with tungsten. The stability changes with temperature as is evident from the Ellingham diagram seen in Figure 2.4.

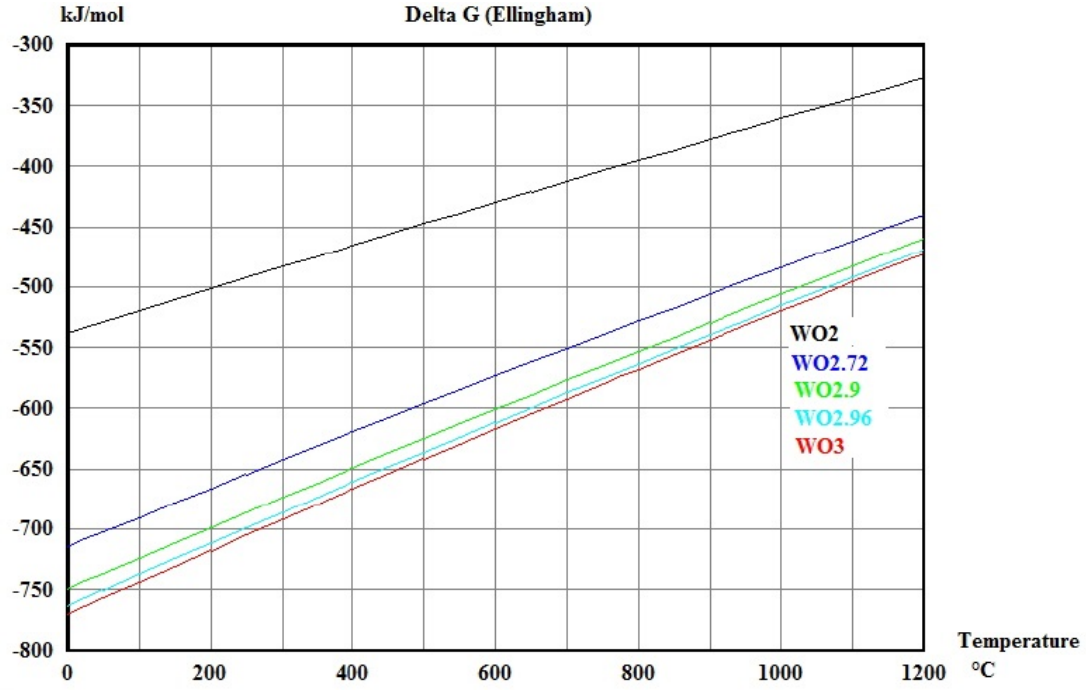

Figure 2.4: Ellingham diagram for various tungsten oxides.

In Figure 2.4, it is confirmed that tungsten trioxide, WO_3, is the most thermodynamically stable oxide over the temperature range but the Ellingham diagram only represents equilibrium conditions for the formation of these oxides. In fact, tungsten dioxide, WO_2 is the first oxide that is formed as small amounts of oxygen attacks the pure metal surface. This oxide is only metastable and will continuously oxidize to a higher oxide as more oxygen enters the metal. The subsequent oxidation of WO_2 to higher oxidation states is a spontaneous reaction as is illustrated by the greater stability of the higher oxides. Eventually, all oxides are oxidized to WO_3, which have the highest stability.

This oxide corresponds to the highest oxidation state of tungsten and will be the main product in the oxidation experiments. WO_3 will, due to its hexavalent charge, be coordinated in an oxygen octahedron as represented in Figure 2.5. The locations of the centers of the atoms are shown in (a), where the black dot is the tungsten atom and the white dots are the oxygen atoms. The relative sizes of the atoms are shown in (b). Here, the oxygen atoms are considerably larger due to their large electron cloud.

This octahedron-structure of representing a metal ion and its oxygen neighbors

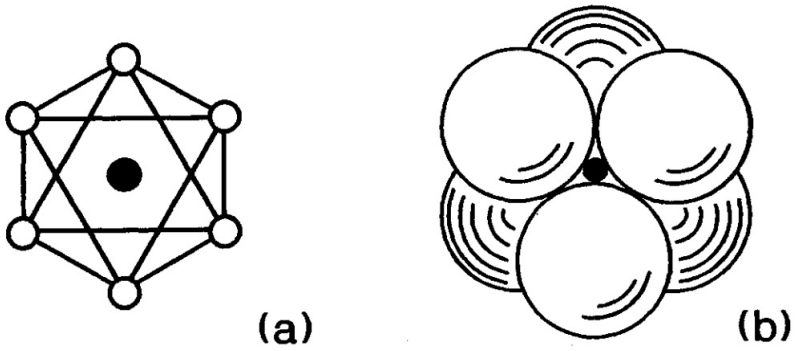

Figure 2.5: Locations of the centers of the atoms in the W-O octahedra and their relative sizes [3].

is commonly seen in materials chemistry. Extending this structure yields the full structure of WO_3.

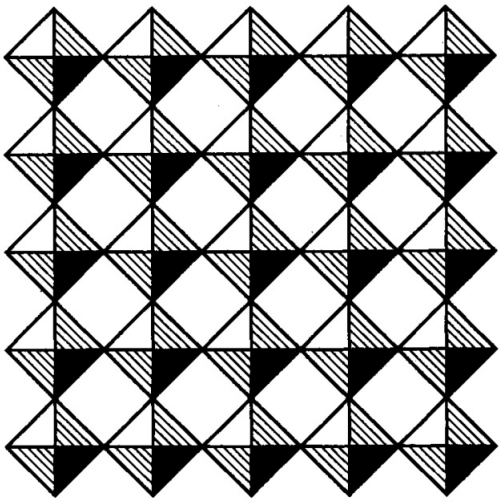

Figure 2.6: Idealized WO_3 structure of corner-sharing octahedra [3].

The idealized structure of WO_3 can be represented as an infinite array of corner-sharing octahedra. The real structure will inevitably contain small deviations which distort the symmetry of the lattice. The cubic symmetry is e.g. reduced to monoclinic at room temperature [3].

2.2.2 Layered oxide films of transition metals

A few studies, [20], [17] and [21] report multiple oxides building up layers or overlapping each other in various ways and it could be interesting to evaluate the prevalence of these in relation to a set of given conditions. The studies determine the character

of the different oxides but they have yet to be combined with studies explaining why they occur. This theory is further supported by Wriedt's work on the complexity of the W-O system, specifying that e.g. WO_2 can be in equilibrium with different oxides at the same time depending on whether the connecting oxides are present on the oxygen-deficient or oxygen-rich side of the WO_2 oxide layer. The formation of each oxide is governed by the equilibrium equation between the reactants, the oxidizing species and the product. The general formula can be written

$$M^{(4+)} + 2O^{2-} \rightarrow MO_2 \tag{2.6}$$

This formula describes a tetravalent metal cation binding two divalent oxygen anions and subsequently forming a dioxide. This is further complicated by the fact that many transition metals have a wide range of oxidation states meaning that a large variety of oxides can be formed. For instance, tungsten has been shown to assume the following oxidation states; W(+III), W(+IV), W(+V) and W(+VI).

Pergament and Stefanovich [22] analyzed the phase composition of anodic oxide films present on transition metals by using a set of thermodynamic calculations. They constructed a model based on a dual layer of oxides with the metal cation in different oxidation states and how these layers could exist relative to each other. This is explained by comparing the changes of the Gibbs free energy of reaction ΔG_r for the reduction and oxidation taking place at the oxide/oxide interface.

They reported that lower oxides, i.e. lower oxidation state of W, always exist near the pure metal and that the oxide structure in whole can be thought of as a being composed of multiple layers of oxides of different compositions. This could be interpreted as an oxygen deficiency gradient downwards through the multi-layer oxide structure, from the highest oxygen deficiency at the gas/oxide interface, i.e. the location of the oxide of the highest oxidation state, WO_3, rising again towards the metal/oxide interface, i.e. W/WO_2. Thermodynamic models can be established at each and every one of these interfaces, predicting the formation of the most stable oxide through the equilibrium equations of each interface. The general formula representing each interface can be written as

$$M_kO_l/M_mO_n \tag{2.7}$$

where M_kO_l is the higher oxide and M_mO_n is the lower one. The initial oxide formed is based on tetravalent tungsten, W^{4+}, and follows the simple electrochemical relation

$$M + O_2 \rightarrow MO_2 \tag{2.8}$$

This redox reaction is based on the oxidation of tungsten taking place at the metal-scale interface and the reduction of oxygen taking place at the scale-gas interface.

$$W \rightarrow W^{4+} + 4e^- \tag{2.9}$$

$$O_2 + 4e^- \rightarrow 2O^{2-}$$

For the oxide layer to increase in thickness, electrons from the oxidation reactions needs to diffuse through the oxide scale to the scale-gas interface, where the reduction process is initiated. Tetravalent tungsten metal ions also need to diffuse away from the metal-scale interface and/or O^{2-} ions must diffuse towards this same interface.

There are some limitations with this Stefanovich and Pergaments model and the extension presented within this thesis. The assumption that the oxide layers are plane parallel to each other is clearly a gross simplification as the true microstructure of the oxide layers relative to each other will greatly influence the prevalence of each oxide species. Additionally, one must consider that there may be competing side reactions occurring simultaneously in the oxide layers, e.g. oxygen evolution, dissolution of the oxide or possibly oxidation of impurities within the supposedly pure tungsten metal.

Extension of the transition oxide layer model

Pergament and Stefanovich acknowledges that although the lower oxides form preferentially as intermediate layers between the metal substrate and a higher oxide, it may be a possibility that other, very thin oxides of a different oxidation state may also be present [22]. The idea behind this section of the thesis is to expand this theory to include a few more layers. Due to limited thermodynamic data however, this may prove difficult.

The previous two-layer model is a good starting point for further derivation of the thin transition metal oxides which serve as intermediate layers. For an arbitrary intermediate oxide layer

$$M_kO_l + O \rightarrow M_mO_n$$

Repeating addition of oxygen anions by diffusion through the subsequent oxide layer cause further oxidation according to the expression seen below.

$$M_mO_n + O \rightarrow M_pO_q$$

Thermodynamic data regarding the equilibrium equations describing the relationship between each neighboring oxide layer can be extracted from a suitable thermochemical database or software. Outotec's HSC thermodynamic software is used.

It is intuitive enough to understand that the oxidation reaction proceeds so that the pure metal substrate is initially oxidized so that it holds very low oxygen content. As oxygen molecules continuously physically and chemically adsorb on the substrate surface, the oxygen content rises, allowing the metal atoms to reach a higher oxidation state.

It might be possible that there is a whole set of different layers in a fixed interlayer relation to each other and that this whole structure may move as more oxide is added.

2.3 Kinetics of oxidation

The thermodynamic principles which govern the feasibility of oxide formation at given conditions are a solid ground when assessing the process of oxidation. Changes in the free energy as a result of the oxide formation gives a good idea about the probable stable reaction products but make no prediction of the rate at which these products are formed. This is where the kinetics of oxide formation can be utilized.

Considering that the designed lifetime of the ESS tungsten spallation target is 5 years, establishing an accurate model of the oxidation kinetics is highly desirable. More specifically, determining the governing rate laws of oxidation over an extended period of time is of interest. Some background on oxidation kinetics will be given in this section in order to understand how this can be done.

The kinetics of oxidation can be divided into two sections; (1) the availability and transport of oxidizing species to the material surface and (2) the diffusion of ionic species inside the material. Each subsection represents a distinct set of processes which will affect the oxidation kinetics. Some brief introduction will be given to both sections but the main focus will be on the description of how ionic species migrate through the oxide scale as predicted by Wagner's theory.

2.3.1 Transport of oxidizing species

The concept of availability and transportation of oxidizing species is rather intuitive and straightforward; if there are no oxidizing species present in the surrounding atmosphere of the tungsten metal substrate, it cannot oxidize. Unfortunately, the concentration of reactive molecules will never reach zero despite good atmospheric control and purification systems. As predicted by the Ellingham diagram in the theory section, extremely low oxygen partial pressures are required to keep tungsten in its unoxidized form and these pressure are impossible to obtain. Commercial helium gas which is readily used as "pure" helium contains an oxygen impurity of maximum 5 ppm. Thus, it is essential to evaluate what factors that play a part in the transport of the oxidizing species and how they can be controlled and manipulated. This section will give a brief introduction to this topic.

In the oxidation process, oxygen molecules will be transported from the impure helium cooling gas and adsorb on the metal surface. The oxygen molecules will initially be adhered to the surface by weak physical bonds in a physisorption process, before they dissociate into their atomic components, i.e. oxygen ions with a valence of -2, and become chemically bonded to the surface atoms of the metal in a chemisorption process. Additional oxygen ions will adsorb and migrate into the material as the process proceeds.

Adsorption of oxygen molecules

A couple of the notions presented here are adopted from thin film technologies but can be implemented to some extent in oxidation reactions as an oxide layer initially develops as a thin film and behave accordingly. The deposition stage of

thin films is typically divided into six sequential sub-steps. The arriving oxygen molecules must first (1) adsorb on the surface, (2) diffuse some distance before being incorporated, (3) react with each other and the surface to form the film, (4) initial aggregation (nucleation), (5) morphology changes (topography and crystallography) and (6) diffusional interactions within the bulk of the film and with the substrate [23]. This sixth step is essentially what happens when oxygen ions diffuse and migrate into the bulk material, oxidizing tungsten metal.

If the transitional oxide layer model states that the lower oxides exist near the metal surface, and assuming that these layers are very thin, it is reasonable to also assume that some physical principles developed for thin films are also valid for all layers that are between the metal substrate and the outermost layer. As explained with the transitional layer oxide structure, the majority of oxide thickness growth is accompanied in the outermost tungsten trioxide layer which continuously expands downwards.

As explained previously, the answer to why the oxidation takes place can be addressed by reviewing some basic thermodynamic concepts which will predict if a certain oxidation product will form. This is the interplay between the Gibbs equation and the equilibrium equation describing the interaction between the reactants, i.e. the metal surface, the oxidizing species, and the reaction products, i.e. the oxide. Some sources indicate the presence of a layered oxide structure, ranging from lower oxides near the pure metal surface and higher oxides closer to the external environment. Furthermore, it has been suggested that the inner layers of oxide remain at constant thicknesses throughout the oxidation process whereas the outermost layer of oxide, typically only one oxide species, continually increases in thickness. This effectively creates a graded oxide structure which is moving downwards towards the bulk metal as new material is oxidized at the metal/oxide interface.

Numerous different tungsten oxides are reported throughout the literature. However, there appears to be some debate whether or not these oxides can be considered non-stoichiometric or if they can instead be viewed as stoichiometric, albeit with very large unit cells. An example of this is the oxide $WO_{2.8}$ which is also reported as W_5O_{14}. A consequence of this indecisiveness is that it is unclear exactly how the oxidation mechanism should be treated. A stoichiometric compound typically follows the Wagner theory whereas a non-stoichiometric compound is interpreted as different kinds of semiconductors, i.e. of n- or p-type. The reality is most likely a mix of several interpretations.

2.3.2 Wagner's theory of oxidation

After the oxygen molecules have been transported to and incorporated into the metal surface as free oxygen ions, they will seek out and create chemical bonds with tungsten and form tungsten oxide. At some point, the incoming oxygen molecules will have to cross a growing oxide layer in order to reach the metal ions. This ionic motion relies on diffusion of the different ionic species down their respective chemical potentials. This process has been studied extensively for the past 100 years and a

good overview of a generalized oxidation model was given by Wagner.

Wagner's theory of oxidation is probably one of the most acknowledged theories regarding the oxidation of metals. Recognizing that metal oxides are ionic in nature, Wagner's theory describes the transport of ionic species and electrons through an oxide layer. When discussing the oxidation of tungsten, the oxygen ion movement through the oxide layer is the most relevant kinetic model.

It was assumed that the oxidation of a pure metal M by an oxidizing agent X from the gas phase will result in the formation of one or more compounds of M and/or X. Furthermore, if a compound initially nucleates on the surface of the metal and subsequently grows and eventually forms a continuous layer on the metal, then diffusion mechanisms of M and/or X through this layer will be required for further oxidation [24].

Starting from a metal in a completely unoxidized state, the rate-limiting step in the oxidation reaction will be the transport of oxidizing species to the metal surface. At some point, however, the thickness of the oxide layer will be sufficiently thick for the diffusion of ionic species through the oxide layer to become the rate-limiting step and will control the overall rate of the reaction. The thickening of a layer is observed to follow the equation

$$\frac{dx}{dt} = \frac{k_p}{x} \tag{2.10}$$

where dx/dt denotes the change of oxide thickness per unit time and k_p is called the parabolic rate constant.

It is important to remember that Wagner's theory of oxidation is an idealized model for oxide formation and is based on a set of assumptions:

- The resulting oxide layer is a compact and perfectly adherent scale.
- Migration of ions or electrons across the scale is the rate-controlling process.
- Thermodynamic equilibrium is established at both the metal-scale and scale-gas interfaces.
- The scale shows only small deviations from stoichiometry.
- Thermodynamic equilibrium is established locally throughout the scale.
- The scale is thick compared with the distances over which space charge effects (electrical double layer) occur.
- Nonmetal solubility in the metal may be neglected.

There are many variants of these assumptions but most points are covered in this list by Davis [24]. Although some of these points can be difficult to estimate or measure properly, using the model to explain oxidation can still be successful.

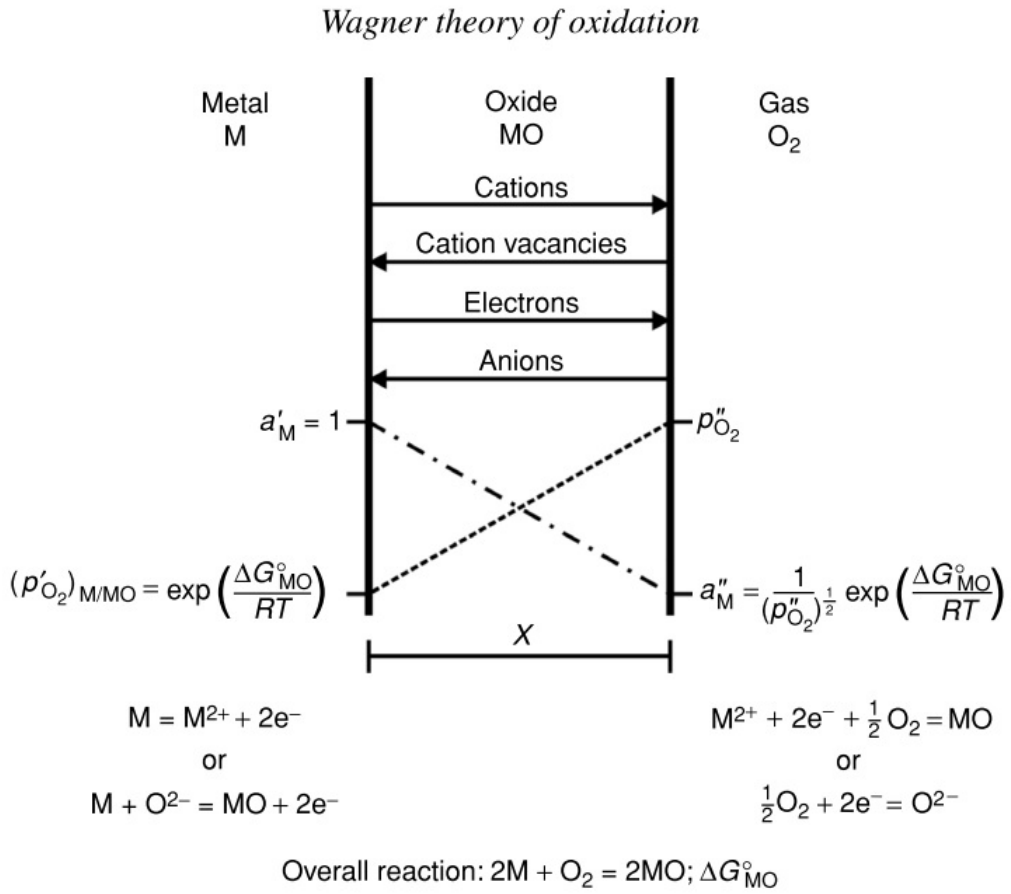

Figure 2.7: The Wagner model of metal oxide formation [2].

Wagner's theoretical model is often accompanied by a graphic representation of oxide formation as seen in the figure below.

The diffusion of ionic species, electrons, and vacancies for a typical oxidation scenario can be followed in Figure 2.7. Additionally, the reactions at each interface can be identified along with the overall oxidation reaction. Note how the partial pressure of oxygen is decreasing with the depth of the oxide which represents how it the oxygen ions are joined with metal ions to form oxide.

Consider a general oxidation reaction

$$M(s) + O_2(g) \rightleftharpoons MO_2(s) \tag{2.11}$$

Where M (s) denotes a general metal in its solid form, combining with oxygen O_2 (g) in its gaseous form to form a solid dioxide MO_2 (s). The oxide layer that is initially formed will be located between the pure metal and the oxygen gas, so that it forms a barrier between the two reactants. It therefore becomes obvious that any oxide formation must be accompanied by the movement of the reactant species through the oxide layer. This can in principle proceed in two ways. The

metal can move through the oxide layer to the oxide-gas interface and react there, or the oxygen can move through the oxide layer to the metal-oxide interface and react there. The oxide layer growth then has its origin at the location where the reaction takes place. In reality however, oxide growth probably takes place at the two interfaces at the same time, albeit at different rates.

Metal oxides are ionic in nature, so the transport of material through the oxide layer cannot be thought of in terms of neutral metal or atomic oxygen diffusing through the oxide. Instead, the transport of ions is considered. The mechanisms which describe material transport in ionic solids are often classified as belonging to either stoichiometric compounds or non-stoichiometric compounds. Various defects are innate of the respective crystal type, but in reality the case is often that all types of defects exist in the material to some extent. The ionic mobility that is present in highly stoichiometric compounds is dominated by Schottky and Frenkel defects. Schottky defects explain ionic mobility with the presence of vacancies in the sub-lattices of the anions and cations, respectively. To maintain electroneutrality, the vacancy densities are identical and this indicates that both ionic species will be mobile. Schottky defects are common in alkali halides, e.g. NaCl. Frenkel defects explain cation mobility by assuming that the anion sub-lattice is perfect but that the cation lattice contain vacancies and interstitials. The concentrations of these must be equivalent to ensure electroneutrality in the crystal. Frenkel defects are common in silver halides, e.g. AgBr [2].

Neither Schottky nor Frenkel defects can explain oxidation however, since they do not provide any mechanism by which electrons can migrate through the oxide layer. To explain the simultaneous transport of ionic species and electrons, it is necessary to assume that the oxides are not perfectly stoichiometric, but rather non-stoichiometric. If a material is non-stoichiometric, it is implied that the ratio between the metallic and non-metallic atomic species in the oxide is not an integer as is given by the chemical formula. This is possible if either one of the two ionic species shows a variable valency. However, electroneutrality is still upheld in the crystal [2].

Diffusion

Diffusion is perhaps the most important concept of Wagner's theory of oxidation, as it explains why the different ions migrate through the oxide scales to each interface. Fick's first law of diffusion denotes the flux of ionic species passing from regions of high concentration to regions of low concentration with a magnitude that is proportional to the concentration gradient. This law is valid as the conditions can be approximated as being in a steady-state, the concentration difference between the ionic species on each side of the interfaces will be high at all times. For a one dimensional diffusion problem, the expression can be written as

$$J = -D\frac{dC}{dx} \tag{2.12}$$

where J is the diffusion flux, e.g. the amount of oxygen ions which enters a unit

area per unit time. D is the diffusion coefficient and describes at what rate the diffusing species will be transported under the given conditions and is influenced by e.g. temperature and size of the ions. dC/dx represents the concentration gradient in one dimension through the material.

In addition to the diffusion phenomena explained by Fick's law, which dictates at what rate the materials transport is possible, there is a geometrical aspect of the problem as well. If the diffusing oxygen ions are somehow obstructed from a clear path towards the metal substrate interface, the oxidation process will be severely hindered.

2.3.3 Factors affecting the oxidation kinetics

Crystal orientation

There are a lot of factors which affect the kinetics of oxidation. One of them is the crystal orientation of the unit cells of the metal substrate which is being oxidized. The metal substrate is typically polycrystalline with a variety of grain sizes. This is a result of the processing of the metal slab and the mechanisms of formation will not be covered in this thesis. Various studies collected in the NASA technical translation [9] report specimens which oxidize at different rates depending on their crystal orientation. Some of the studies were made on polycrystalline samples while the majority was conducted on single crystals with a defined crystal orientation. There is an inconsistency of the results found in literature, but most studies indicate that a (100) surface oxidizes at a higher rate than others. The complexity of these measurements makes it rather hard to replicate the results, and no such attempt will be made. One could however expect that on a polycrystalline sample, heterogeneous oxidation rates could lead to creation of oxide islands which eventually could result in mechanical failure of the oxide layer due to e.g. stress build-up and island collapse.

As mentioned previously, another experiment indicated a significant different between crystallographic planes in terms of oxidation rate. The planes were ranked (100)>(111)>(110) in order of susceptibility to oxidation where the (100) face oxidized roughly 6 times more rapidly than the (110) face. It is therefore reasonable to assume that if care is taken when manufacturing tungsten pieces, it is possible to tailor the resistance to oxidation to be as high as possible.

The samples used in this thesis are all polycrystalline and no experiments were done to investigate the effects that a difference in crystal orientation could have on the oxidation and sublimation characteristics of pure tungsten.

Surface coverage

Whether or not the oxide layer can adequately cover and protect the pure metal surface can be indicated by the Pilling-Bedworth ratio, defined as the molecular volume of the oxide relative to that of the metal from which the oxide is formed. A ratio less than one indicates that the oxide layer is unable to cover the metal which gives rise to oxide islands separated by bare metal. If the ratio is much larger

than one, the oxide will be bulky and may tend to spall. The exceptions to the P-B theory are many but can function as a rule of thumb when assessing the extent of the oxide layer [18].

Additionally, as oxidation is a surface process, the effective surface area of the sample will also be a factor when determining the extent of oxidation. Samples that have undergone a surface treatment which raises the surface quality of the sample, e.g. by electropolishing, have a lower effective surface area and are thus expected to oxidize more slowly than untreated samples.

2.3.4 Derivation of the rate constants

A crucial step in characterizing the oxidation behavior is determining different rate constants that are involved in the oxidation process where the most important ones are from the chemical reaction between tungsten and oxygen, and from the parabolic behavior of oxygen diffusion in tungsten oxide. By doing so, it is possible to estimate e.g. the evolution of oxide thickness over time as well as the recession of the metal/oxide interface as the oxidation proceeds. Additionally, the activation energies associated with each process can be determined, giving indications of how much energy input is required for the different oxidation processes to continue. When discussing the activation energies, it is important to remember that the parabolic oxidation corresponds to the movement of oxygen ions, O^{2-}, throughout the oxide lattice.

The first step when determining the rate constants is to translate the vast number of data points into a more convenient form, i.e. a polynomial. For the best fit, a tenth-degree polynomial is used on each data set. Some problems can arise when the selected interval has a bad overlap with the curve in the sense that it does not cover the parabolic region in a good way. It might include some parabolic section and some irregular parts, or it may miss the parabolic part all together. Both cases will lead to distorted results which affect the value of the rate constant that is acquired from each oxidation curve. Therefore, care is taken to avoid these problems as much as possible.

Below the sublimation temperature at any given set of conditions, the oxidation curve and mass change is only dependent on the addition of oxygen to the sample. Thus, it is possible to obtain the oxidation-relevant rate constants from any experiment conducted below this temperature without concern of interference from the sublimation kinetics.

To explain how the rate constants are determined from each sample, the procedure is illustrated for a typical oxidation curve. This procedure is then repeated for each sample as seen in the chapter on results and discussion.

Consider the oxidation curve for an electropolished sample kept at 900°C for 2 hours in pure He, seen in Figure 2.8.

In the beginning of the experiment, when $t = 0$, the oxide thickness is considered non-existent and oxygen is assumed to react freely with tungsten without the involvement of any diffusion through the oxide. Because of this, the mass gain of

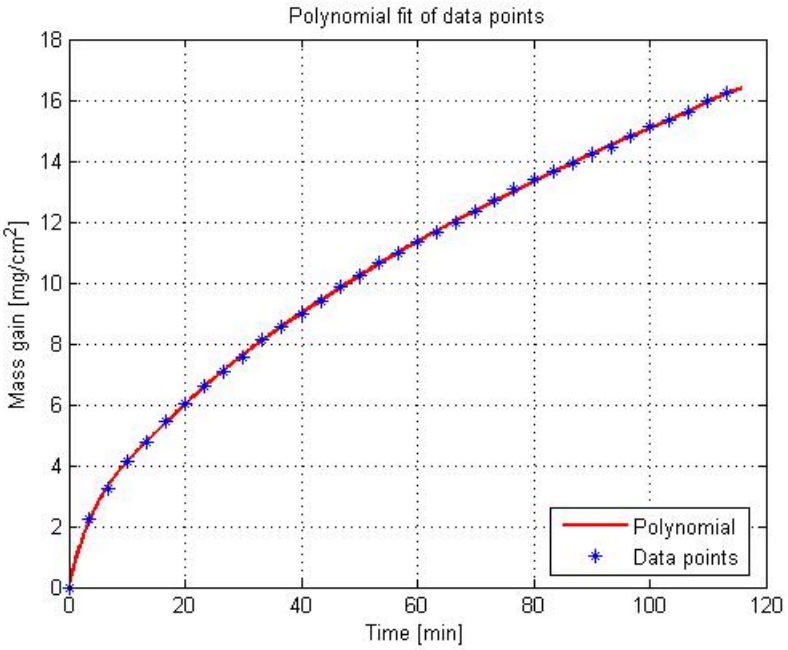

Figure 2.8: Ideal appearance of an oxidation curve. This sample is kept at 900°C.

the sample obeys a linear law according to

$$x = k_{cr}t \tag{2.13}$$

where x is the change in mass corrected for specimen area, t is the time, and k_{cr} is the chemical reaction rate constant. The value of k_{cr} is extracted from the slope of the linear region in the immediate beginning of the experiment, before any oxide layer is built up.

Beyond this initial region, the oxidation curve assumes a typical parabolic appearance that is consistent with theory. As stated previously, the mass addition can be said to follow a parabolic rate of the form

$$x^2 = k_p t \tag{2.14}$$

where x is the change in mass corrected for specimen area, t is the time, and k_p is the parabolic rate constant. The polynomial is then squared with respect to the mass change corrected for area which yields the curve seen in Figure 2.9.

It becomes evident from the linear fitting in this figure that the untreated curve was almost parabolic. From this, the parabolic rate constant, k_p, is then acquired from the linear fitting of the squared polynomial according to

$$k_p = \frac{x^2(t)}{t} = 2.3682\frac{g^2}{cm^4 s^2} \tag{2.15}$$

Note that this value is the slope of the whole curve and that some segments of the squared polynomial expression can deviate to a large extent from parabolic

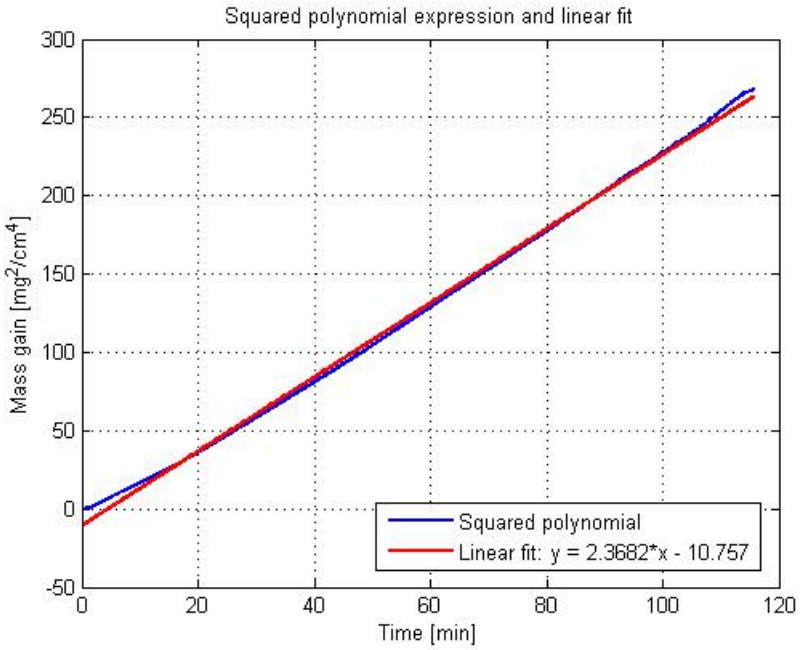

Figure 2.9: The squared polynomial expression with a linear curve fitted to it.

behavior. Difficulties with determining where the linear curve should start and end and which segments should be included inevitably leads to inaccuracies that are hard to avoid. This is discussed further in the chapter on results.

To determine the activation energies, it is first recognized that the rate constants obey an Arrhenius relationship

$$k_p = k \cdot e^{-\frac{Q}{RT}} \tag{2.16}$$

where k is a rate constant that is not used further, Q is the activation energy, R is the gas constant and T is the absolute temperature. Taking the natural logarithm of this expression thus yields

$$\ln k_p = \ln k - \frac{Q}{R}\frac{1}{T} \tag{2.17}$$

Plotting the natural logarithm of several of these rate constants obtained at their respective temperatures versus those temperatures finally yields the activation energy for the process or reaction that is being investigated. This is because the slope of a linear curve fitted to the results is equal to the activation energy divided by the gas constant, so that the slope multiplied with the gas constant yields the activation energy

$$Slope = -\frac{Q}{R} \tag{2.18}$$

$$Q = -R \cdot Slope \tag{2.19}$$

All rate constants and activation energies that was acquired from experiments in this thesis is presented in the chapter on results and discussion.

2.4 Thermodynamics of sublimation

Sublimation denotes the phase transition where a solid material is converted into a gaseous compounds, without ever entering the liquid phase. Many compounds, such as water, can only enable this transition if the pressure is sufficiently low but tungsten oxides can make this transition even at regular atmospheric pressure as indicated by its phase diagram. At the point of sublimation, the solid phase is in equilibrium with the gas phase and they both coexist. Furthermore, the gaseous oxide can only be produced in a quantity that is determined by its vapor pressure in the vicinity of the solid oxide. At some point, the surroundings are saturated by oxide gas and the material stops the sublimation reaction. However, this equilibrium can be shifted into a steady-state of continuous sublimation of new material if the oxide gas is continuously removed from the solid oxide.

Figure 2.10 represents a phase diagram as a function of vapor pressure which can give an idea of which oxides are most stable at a particular atmosphere. A helium atmosphere containing maximum 5 ppm O_2 corresponds to $\log p_{O_2}(atm) = -12.2$.

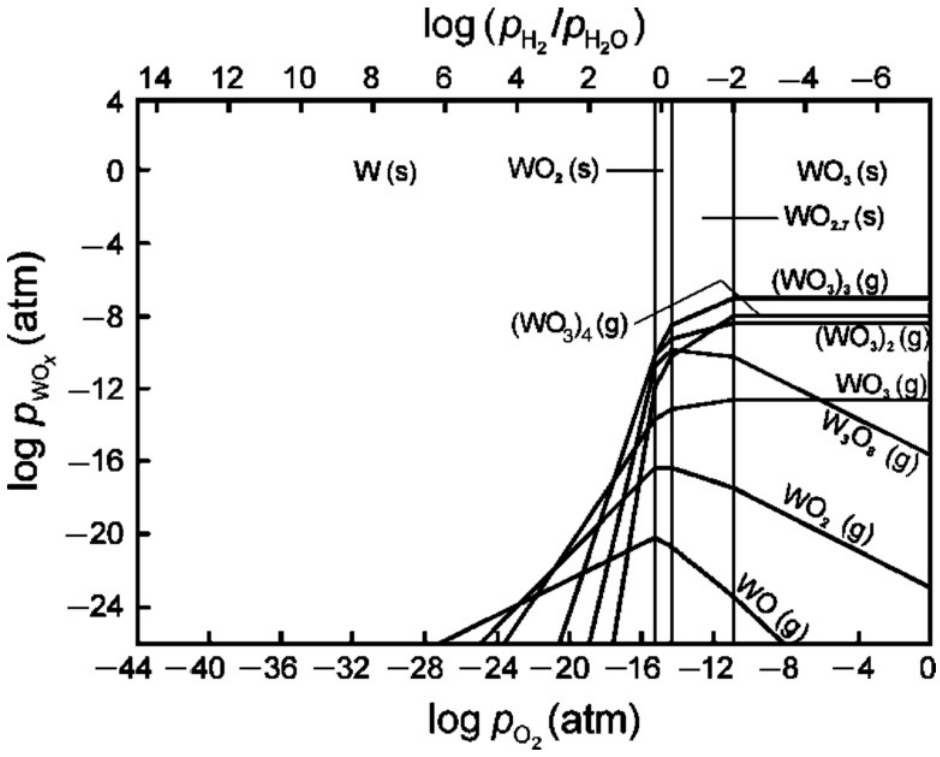

Figure 2.10: The volatile species of the W-O system at 1250 K [2].

At sufficiently high temperatures, the oxide layer will dissociate and transition into a gaseous state. The oxide species, mainly WO_3, then leave the material surface and join the surrounding atmosphere. Another important concept is volatilization, i.e. the tendency for a solid phase to become increasingly unstable in terms of its thermodynamics, eventually leaving the material surface as a gaseous species.

It is important to determine the temperature at which sublimation is possible since this can cause significant problems in various applications, including the spallation target design of ESS. Radioactive particles that escape the target, either by sublimation or erosion, can e.g. enter the cooling circuit or invade other areas of the facility, increasing the risks of safety concerns.

2.5 Kinetics of sublimation

Sublimation can severely limit the protective qualities of an oxide layer or remove it altogether as the sublimation rate can increase rapidly with temperature [6]. The platinum and refractory type metals, including W, tend to have volatile oxides and thus the problems of sublimation can be especially pronounced for an application where these kinds of materials are going to be used.

The kinetics of sublimation treat how fast solid oxide material is converted into gaseous compounds. The rate of sublimation, i.e. the loss of solid material, can be measured simply by noting the initial mass of the sample and then subtracting the final mass. This, of course, requires the mass to only be lost due to sublimation and not some other type of removal, e.g. from vigorous airflow or mechanical ablation. It is generally accepted that sublimation adopts a linear kinetic behavior so that mass loss proceeds at a constant rate over time.

$$\frac{dx}{dt} = -k_s \tag{2.20}$$

where dx/dt is the mass loss per unit time and k_s is the sublimation rate constant.

The notion that sublimation kinetics is a linear mass loss with unit time is only valid if the surface area of the sample is kept constant throughout the experiment. Loss of material can lead to dimensional changes, in which case the shrinkage in effective surface area must be corrected for if the true sublimation kinetics is to be determined. If the change in surface area is only minor compared to the overall area, the results will not be severely flawed.

The surface area parameter can be hard to determine if the sample is porous or otherwise exhibits additional surface geometries. A generalized macro-scale surface area can be adopted to get reasonably accurate results from e.g. powder samples which will be used for experiments in this thesis.

2.5.1 Volatile oxide species

Various literature sources indicate that the sublimation products of WO_3 will polymerize at elevated temperatures. For example, certain ring structures of $(WO_3)_n$,

where n = 1, 2, 3 can be formed [25], [26] [16], [19].

It is unclear how the polymerization of oxides will affect e.g. the size of eroded oxide particles or sublimated species which in turn could affect the contamination of the helium cooling loop. This is not further investigated.

Chapter 3

Experimental Setup

There are a couple of possible ways to measure and evaluate the extent of oxide formation on a sample. If the specimens are removed from the experimental equipment, e.g. a simple furnace or more advanced instruments, the thickness of the residual metal layer and the oxide layer can be measured. If the layers are separated, they can also be weighed. However, this procedure can be problematic when handling small samples or if the oxide layer is adherent to the metal surface.

A far more efficient way to assess the extent of the reaction is to determine the amount of consumed oxygen. This is done by either observing the weight gain of the specimen or monitoring the amount of oxygen pumped in through the gas flow and the oxygen leaving the system. Both of these methods may be used on a continuous and automatic recording basis.

Most previous studies have been conducted at isothermal heat treatment conditions, i.e. a set temperature for the duration of the experiment. This is obviously the best procedure when samples are expected to operate under such conditions. However, as the ESS tungsten target will be subject to a cyclic heating and cooling procedure due to the proton beam, it is reasonable to assume that the kinetic models generated by isothermal experiments will deviate slightly from the real heating conditions at the ESS target.

3.1 Simultaneous Thermal Analysis

The simultaneous thermal analysis instrument is a powerful tool when investigating e.g. thermochemical reactions. The equipment is utilized in this thesis to acquire a greater understanding of the oxidation process of tungsten. Due to risks of contamination of the equipment, the STA will not be used when investigating the sublimation of tungsten oxides.

3.1.1 Theoretical principles

A simultaneous thermal analyzer combines the strengths of a differential scanning calorimeter with thermogravimetric analysis capabilities. The machine works on

the principle that heat is supplied to two separate crucibles in order to raise their temperature. The sample is put in one of the crucibles, whereas the other crucible is left empty as a reference. When a phase transition or a similar thermochemical or thermophysical reaction occurs in the material, the heat supply needed to keep the two crucibles at the same temperature is shifting. If an exothermic reaction is taking place, energy will be released which heats up the crucible. Because of this, less external heat needs to be supplied, which is indicated by a change in the STA thermograph. The same is true for an endothermic reaction, where more energy needs to be supplied to the sample crucible. While this is the calorimetric part of the STA, it also houses thermogravimetric capabilities, allowing it to continuously measure mass changes during a reaction with a an accurate internal balance (min. mass sensitivity 10 μg). In addition to this, the STA offers good environmental control through programmable gas flows, and options to tailor specific heat programs. It is not possible to mimic the thermal cycling of spallation target in ESS with the STA instrument as the maximum heating and cooling rates are 15 K/min, whereas the thermal cycles of the spallation target are about $\Delta T = 100°C$ with a frequency of about 14 Hz. Obviously, there is no way to replicate these conditions using conventional instruments. It is unclear if or how this may affect the oxidation characteristics, but this is not investigated further in this thesis.

Note that the calorimetric capabilities of the STA was not used for any experiments in this thesis.

3.1.2 Equipment setup and sample preparations

The instrument which is used for the main thermal analysis of the tungsten in this thesis is a simultaneous thermal analyzer of the type NETZSCH STA 449 F3 Jupiter, seen in Figure 3.1 below. The temperature interval in which thermal analysis can be conducted is approximately -150°to 2400°C. The instrument can be used to measure many different phenomena related to materials science, e.g. changes of state, solid-solid transitions, specific heat capacity changes etc. In this thesis, however, it will mainly be used to observe mass changes. Prior to conducting each experiment, a so called correction file must be created. This file contains the calorimetric, mass change and gas flow data corresponding to the reference pan and the empty sample pan. The correction is used to compensate for any fluctuations and variations of these parameters when executing the real experiment. The correction files are simply subtracted from each experiment file to acquire their true results.

A large rectangular foil of pure tungsten was machined to produce a series of smaller circular tungsten foils, approximately 6 mm in diameter and 0.1 mm thick. The edge of this thin cylinder was not considered when calculating the surface area but both the top and bottom areas were considered which yields a surface area of around 0.565 cm^2. The foils were then cleaned in acetone, weighed on an accurate scale, and put inside a ceramic crucible of Al_2O_3. The crucible is then placed inside the STA instrument and the experiment is initiated according to the prescribed heating program in which the heating rate, isothermal temperature, experiment

Figure 3.1: The STA equipment used for oxidation experiments.

time and gas flows are determined. This setup and procedure ensures that many parameters of each experiment can be reproduced if needed but there are still some errors which may arise.

3.1.3 Sources of error

As mentioned previously, ESS will operate with helium as a cooling gas but due to the so called buoyancy effect, argon gas has to be used in this STA setup. The buoyancy effect is caused by the low density of helium gas which will distort the readings of the internal balance of the STA. Argon gas is heavier, and will not influence the balance in the same way. The amount of oxygen that is present in the argon gas is equal to the amount of oxygen present in the helium gas, so the oxidizing capabilities of both gases will be identical. Both helium and argon are inert gases and will not contribute to any oxidation of the tungsten and will not react with it in any other way.

Minor deviations in the results and correction files can probably be traced to the conditions in the laboratory that the STA instrument is in, e.g. by the effects of humidity and temperature. This is not further investigated in this thesis.

Two sources of error which are present when conducting the STA measurements

can be divided into two categories; geometry and gas purging. The explanations of these follow in the section below.

To acquire accurate results when performing the STA measurements, it is a wise idea to eliminate as many parameters as possible that could influence the oxidation behavior. One of those is whether or not to use a lid during on the STA crucible. A lid, although having a small hole, could affect the oxidation behavior by trapping air close to the substrate, thereby effectively simulating an oxidation behavior in air. If this is not desirable, as in this case where the sample is required to be in contact with an 'inert' atmosphere such as argon gas, having a lid on top of the crucible is not recommended.

When conducting the STA measurements, the sample is placed in the crucible which is then put inside the STA chamber. The chamber is at this point filled with air and thus it needs to be evacuated in order to acquire the desired atmosphere. This is done by switching on a vacuum pump and subsequently filling the chamber with the desired gas, e.g. 'pure' argon. As the vacuum technology can only be so good, precautions need to be taken in order to secure the atmosphere so that it does not interfere with the specifications set up before the measurements. If an atmosphere of argon is needed, one cannot simply evacuate and purge the chamber a single time, thinking that the correct atmosphere is achieved. Sequential cycles of evacuation and purging the chamber is needed in order to minimize influences from some air remains still in the STA chamber. This can be shown by some simple calculations.

Consider first the initial chamber atmosphere, i.e. air, with an oxygen content of C_{O_2} 20 % =200 000 ppm. A single evacuation and filling cycle, going to 98 % vacuum with 2 % of the previous atmosphere remaining, brings down the oxygen content in the new chamber atmosphere to $C_{O_2} = 2\,\% \cdot 20\,\%$ =4000 ppm. This means that after one cycle, the air remnants from the start of the sample loading is roughly thousand times higher than the 5 ppm impurity which supposedly exist in the argon gas and is the desired atmosphere. Consequently, should the measurements be conducted at this stage, the results will be severely flawed, as the oxidizing atmosphere is not based on 5 ppm oxygen content but rather on 4005 ppm oxygen content. Needless to say, repeated cycles of evacuation and filling are required. A second cycle yields $C_{O_2} = (2\%)^2 \cdot 20$ % =80 ppm, but this is still clearly unacceptable conditions. A third cycles yields $C_(O_2) = (2\%)^3 \cdot 20\% = 1.6ppm$, or roughly 30 % of the value of the oxygen impurity of the argon gas. A fourth cycle yields $C_(O_2) = (2\%)^4 \cdot 20\% = 0.032ppm$. Only at the fourth evacuation and filling cycle does the oxygen content from the remnant atmosphere drop to an appreciable level so as to not interfere significantly with the impurity of the oxygen gas. Based on these calculations, it is obvious that care must be taken when conducting the STA experiments in order to improve accuracy and repeatability of the results.

3.2 Thermogravimetric Analysis

3.2.1 Theoretical principles

The principles behind a TGA experiment are rather straightforward, and this setup particularly so. The sample is connected to an external balance via a series of metal rods and a hanger. The sample is then inserted into the heated oven for oxidation. While oxidation takes place, oxygen reacts with, and attaches to the tungsten metal discs, increasing the overall weight of the sample. This in turn affects the scale which sends a weight reading every fifth second to a computer.

As in the case with the STA setup, there is no way to replicate the inherent temperature cycling of the spallation target in ESS and investigate how the oxidation and sublimation characteristics are affected by this condition.

3.2.2 Equipment setup and sample preparations

The tube furnace used for the thermo-gravimetric analysis was a Carbolite STF 15/75/450, seen in Figure 3.2 below. It has a temperature capability of up to 1500°C and can accommodate any chosen atmosphere by connecting gas canisters to the gas inlet of the furnace. In this way, the atmosphere can be tailored to different partial pressures of oxygen e.g. pure He (5 ppm O), He + 0.5 % O2, air, pure O2. Figure 3.2 shows the tube furnace.

For these TGA experiments, discs of tungsten were used rather than thin foils. The discs measured 20 mm in diameter and 3 mm in thickness which gives a surface area of around 8.164 cm^2. They and had an approximate mass of around 18 grams so they were about 1000 times heavier than the foil samples used in the STA. Additionally, the increased surface area of the discs allowed for more extensive oxidation. As such, the mass gains of the disc samples are considerably larger and are also measured more easily with the external balance.

Two different samples were tested, unpolished and electropolished. The electropolished samples had undergone a cleaning and polishing sequence by TianLong Company prior to the experiments at LTH. Both samples were subjected to an ultrasonic bath immediately before the experiments.

The discs are suspended inside a vertical hanger of 0.5 mm Chromaloy O ® - Resistance Alloy (Fe75/Cr20/Al5) wire. The hanger itself is mounted at the end of a series of thin stainless steel wires that allow for height adjustments. These setup equipment materials are oxidation resistant so that the recorded mass gain can only be attributed to the oxidation of the tungsten discs.

The measurement procedure was as follows:

1. The tungsten disc is cleaned with acetone and put in an acetone-filled beaker in an ultrasonic bath for 180 s. This is done to remove any particles that might contaminate the surface of the samples during handling.

2. The disc is then suspended inside the Chromaloy hanger which is mounted on the stainless steel rods directly below the external mass balance. This cage prevented loosening of the sample during handling and measurement, but may impair oxidation

Figure 3.2: The TGA equipment used for both oxidation and sublimation experiments.

behavior in a minor way due to blocking areas of the sample. 3. At this point, the disc is hanging in a zone in the TGA which is water cooled to prevent premature oxidation. The furnace is started.

4. When the target temperature is reached, additional steel rods allow the disc to be inserted into the middle of the tube furnace and the oxidation starts. This point is defined as the zero time and the balance is set to deliver a reading to a computer every five seconds.

5. After approximately two hours, the steel rods are removed and the furnace is opened so that the disc can be retrieved. The balance recording is stopped.

6. The data points can now be retrieved and plotted versus time.

This procedure is repeated at all temperatures.

3.2.3 Temperature calibration of the vertical tube furnace

The tube furnace of the TGA is set to a desired temperature via a control panel but this may not be the true temperature of the furnace due to the existence of a non-homogeneous temperature distribution. There will inevitably be some temperature gradient that can cause the sample to be placed in an area where the temperature

is unknown. This problem is solved by analyzing the temperature distribution with a K-type thermocouple. The calibrated position inside the tube furnace is then located and the sample is required to be placed at this location during the experiments for a correct temperature reading.

3.2.4 Sources of error

There are a number of different parameters during the TGA measurements which could have affected the results in unforeseeable ways. As with the STA measurements, the external balance was rather tricky to calibrate so as to get accurate readings. Additionally, the balance was set to operate non-stop during a couple of hours as it gave readings to a computer. Some kind of drift phenomena as well as unquantifiable disturbances due to environment effects might occur during this time, resulting in slightly flawed results.

3.3 High-temperature furnaces

A series of regular heating furnaces were used for the oxidation experiments conducted in air, seen in Figure 3.3 below. The furnaces were set to the designated oxidation temperatures 400°, 500°and 600°C. At these temperatures, the 1x1 cm tungsten foil samples were put in. The time was noted and the samples were kept in the furnaces for 48 hours at which point they were extracted and set to cool in room temperature. The crucibles with the oxidized foils were they measured on an analytical balance to acquire the weight change, i.e. mass gain due to oxidation.

As explained in previous sections, there is a theoretical limit of mass gain of the samples due to oxidation which corresponds to tungsten being in its highest oxidation state of +VI. Each tungsten atom is coordinated to three oxygen atoms with a valency of +II, via an octahedron structure. The maximum weight a fully oxidized tungsten sample can have can therefore be calculated. If that mass is noted in the sample after oxidation, then it can be concluded that the sample is fully oxidized. The calculations will look like the following for a tungsten foil mass of 12.79 mg with the molar mass of tungsten and oxygen as $M_W = 183.84 g/mol$ and $M_O = 15.999 g/mol$, respectively.

$$n_W = m_W / M_W = 6.9571 \cdot 10^{-5} mol \tag{3.1}$$

$$n_O = 3 \cdot n_W = 2.0871 \cdot 10^{-4} mol \tag{3.2}$$

$$m_O = n_O \cdot M_O = 2.0871 \cdot 10^{-4} mol \cdot 15.999 g/mol = 3.3 mg \tag{3.3}$$

An experiment to exemplify this was conducted in a regular heating furnace set at 700°C. A small circular piece of tungsten foil, similar to those used in the STA experiments, was weighed, put in an alumina crucible and subsequently set inside the furnace. After 5 hours, the crucible was removed and weighed. Due to brittleness, it is impossible to handle fully oxidized sample without them crumbling apart and

Figure 3.3: The high-temperature furnace equipment used for both oxidation and sublimation experiments.

so the crucible was weighed with the sample inside. The mass increase was noted to 3.3 mg, which corresponds very well with the theoretical limit explained above.

Of course, the mass ratios of tungsten and oxygen will hold for all samples that are fully oxidized.

$$m_{frac,O} = m_O/m_W + m_O = 0.2051 \tag{3.4}$$

So oxygen will add and make up roughly 20 % of the mass of a fully oxidized sample.

3.3.1 Temperature calibration of the furnace

In order to ensure the validity of the experimental results, it is a good idea to calibrate the furnace with respect to temperature. This certifies that the true temperature of the furnace is equal to the designated temperature. The calibration was done by repeatedly measuring the temperature at different locations inside the furnace to acquire the temperature distribution.

Also important is how this distribution shifts with increasing temperature, which is why the calibration is redone at different temperatures. The calibration of the furnace is done solely with the purpose of attaining a temperature reading during

the sublimation analysis with good accuracy.

3.4 Sublimation Analysis

The sublimation experiments were carried out in regular heating furnaces with temperature capabilities upwards of 1000°C. As explained previously, in the theoretical background section on sublimation, the sublimation rate is only a function of the temperature. This is true as long as the sample remains fully oxidized and an oxygen-rich atmosphere is therefore the preferred environment when determining the sublimation temperature.

The samples used for the sublimation measurements are based on tungsten trioxide in powder form. The WO_3-powder was placed in a regular STA crucible and put on an analytical balance. The starting weight was noted and the crucible was then put inside the furnace pre-heated to the specified temperature. The sublimation mechanism requires a certain temperature before it initiates and, as discussed in the literature section, lies somewhere around 750°C.

Even though reported to begin at this particular temperature, there was reason to believe that the sublimation of the oxide would initiate at a lower temperature. At a lower temperature, the rate of sublimation could have been as low as it would have gone undetected from contemporary analysis equipment. The idea here was to determine if the sublimation did begin at lower temperatures than previously reported.

The effect of water vapor on the sublimation process was also investigated as some literature suggested that the volatilization of tungsten trioxide was enhanced in the presence of water vapor. These sets of experiments were conducted using the TGA setup and included a procedure for preparing the gas with water. Helium gas was passed through a gas-tight glass beaker containing water prior to being supplied into the furnace chamber. As such, the helium was saturated with water vapor equal to the vapor pressure of water at 25°C, 3.2 kPa. This pressure is compared with the total pressure in the setup, i.e. atmosphere pressure. The partial pressure of water vapor in the final gas mixture was thus $p_{H_2O} = 3200/101325 = 0.0316$. An important remark to make here is that the partial pressure of water vapor is significantly higher than the normal oxygen impurity of maximum 5 ppm used for the oxidation experiments. This atmosphere can therefore be thought to represent an environment that is heavily contaminated by water vapor.

An attempt was made to sublimate tungsten trioxide by first oxidizing a piece of tungsten foil and subsequently heating it with a gas burner. The burner flame can possibly work upwards of 2000°C. The reason for this experiment was the lack of an adequate furnace at the time this thesis was written which could work in excess of 1100°C.

Chapter 4

Results and Discussion

The results from all experimental work and measurements will be presented in this chapter. The discussion of each result will take place in the respective section, starting with the oxidation experiments conducted by STA, followed by oxidation experiments by TGA and then finally the sublimation experiments, performed by both TGA and with regular heating furnaces. In addition to some selected figures and plots shown here in the results section, the entirety of all data can be found in the respective appendices.

4.1 Simultaneous Thermal Analysis

The section below will give an overview of the results acquired from the STA experiments, called thermographs. A number of runs were used to get an estimation of the extent of oxidation at and around the designated operating temperature of ESS, 500°C. Note that only oxidation experiments were conducted by STA as gaseous oxide species will contaminate the sensitive equipment.

As stated in the procedure, the general idea with the STA measurements is that the samples are heated up to the selected temperature and held there for a period of several hours, i.e. an isothermal experiment. The pure argon gas with a small oxygen impurity is continuously supplied to the STA chamber and the sample is thus exposed to the oxidizing species. At increased operating temperatures, the rate of oxidation is enhanced due to more thermal energy being supplied to the sample which can initiate the oxidation processes. The oxidation of the sample leads to a mass increase as a function of time as oxygen molecules attack the surface and attaches to it by forming oxide compounds. The result is a series of oxidation curves, generated at different temperatures, describing how rapidly the oxidation of the tungsten sample proceeds. A number of parameters determine the appearance of the curves; temperature, time, oxygen partial pressure, gas flow, and sample dimensions are the most important.

Experiments were conducted starting from 200°C and ranging up to 625°C with isothermal sections for either 2 or 48 hours. These are presented in the subsections below. A reminding remark about the appearance of the thermographs seen below is

the effect of buoyancy, which, as stated in the sources of error for the STA setup, can cause significant errors and anomalies, especially in the beginning of an experiment.

As a result of the closed STA system, there is no way to insert the sample foils into the machine once it is operating. Consequently, the samples must be exposed to the heating section before reaching the isothermal section of the experiment. The heating section is roughly 30-40 minutes long depending on the target temperature and the heating rate which was 15 K/min for all experiments.

Some literature sources say that ESCA investigations show that oxidation begin at room temperature, forming WO_3, and that the thickness of the oxide layer increases slowly up to 200°C after which it grows rapidly [3]. However, it is unclear what 'slowly' and 'rapidly' refers to in this case. Assuming that some oxide is formed at these low temperatures, the overall mass gain should be affected by oxygen uptake occurring below the isothermal sections of each experiment. Therefore, the isothermal section alone cannot be seen as the starting point of the oxiation. Due to the buoyancy effect and the fact that oxidation is thought to be very slow below 200°C, a reasonable assumption is that this first part of each thermograph can be discarded or omitted without any considerable loss of accuracy.

For convenience, the thermograph is broken down into three sections; each representing a distinct part of the heat treatment program that the tungsten foils are subjected to. These are the heating section, the isothermal section, and the cooling section.

4.1.1 STA experiments conducted for 2 hours

A series of STA experiments were conducted isothermally for 2 hours in order to assess the oxidation characteristics. Two of the advantages with a shorter measurement period is that more experiments can be executed in the same time frame and that the use of gas is lowered. Additionally, if the chemical reaction kinetics of the oxidation is sought for, i.e. the activation energy for the chemical reaction between tungsten and oxygen, then a shorter experiment is preferred as no information is gained from an additional exposure time.

The first set of 2-hour STA runs were conducted at 575°and 625°C. The resulting thermographs can be seen below.

These results proved unsatisfactory for several reasons. The first one is the obvious contradiction that the sample kept at 575°C shows considerably more oxidation than the sample kept at 625°C where it in theory should be the other way around. This flaw is possibly connected with the second error in these thermographs, manifested as a large disturbance in the solid green mass change curve during the heating section, particularly at the higher temperature. In the case of the 625°C curve, it was determined that the correction file which was used was faulty and caused the large disturbances. Also, there is an unknown anomaly in the 575°C curve causing the mass gain curve to have a negative slope at the end of the isothermal section. This is possibly due to interference from the heating elements in the STA.

Even though the results may be flawed to some extent, there are still some

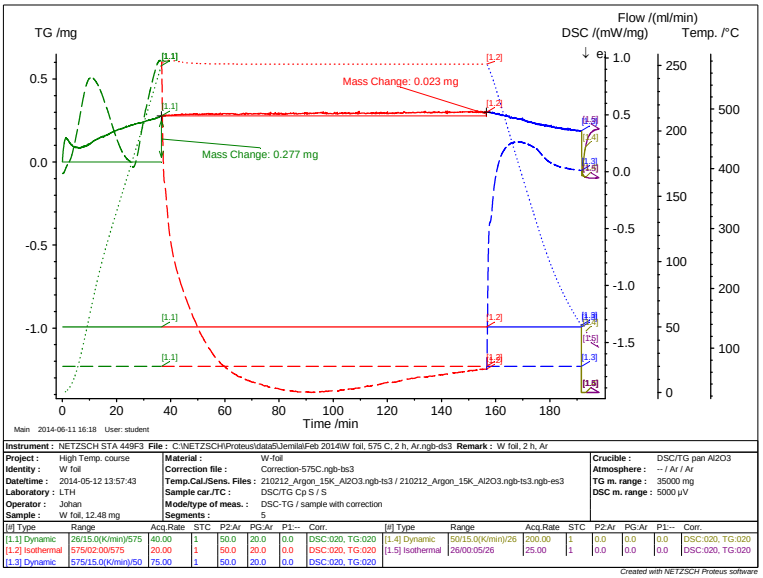

Figure 4.1: The first STA run at 575°C

interesting things that can be pointed out. For example, the majority of the mass gains of both these curves are found in the heating section, and there is only a very gentle rising slope during the isothermal section. Consequently, it appears as if a large portion of the total mass increase of the sample due to oxidation will be present on the sample even at temperatures as low as 200°–300°C This is very interesting and only a few literature sources tell that oxide may indeed be present at these low temperatures for tungsten samples.

It was decided that both of these experiments should be redone in order to address whatever errors might have been included. The new thermographs can be seen below.

The second STA run at 575°C turned out very well. The mass gain curve assumes a smooth parabolic appearance in the beginning of the experiment and then transitions into a linear region. Consistent with both previous thermographs, the largest portion of mass gain is added during the heating section with only a very low mass gain during the isothermal section. Again, this would indicate that significant oxidation takes place even at low temperatures and that once the sample reaches the isothermal section, the oxidation is effectively negligible. Still, this needs additional confirmation.

The second STA run at 625°C shows practically no oxidation at all for some unknown reason. Visual inspection after the experiment disproves this as the sample has clearly been oxidized. In light of this, the experiment is seen as a failure and its result is not to be considered as useful.

As stated previously, three of the four STA runs show indications that there may be a significant mass increase of the samples initiating at as low as 200°C. Therefore,

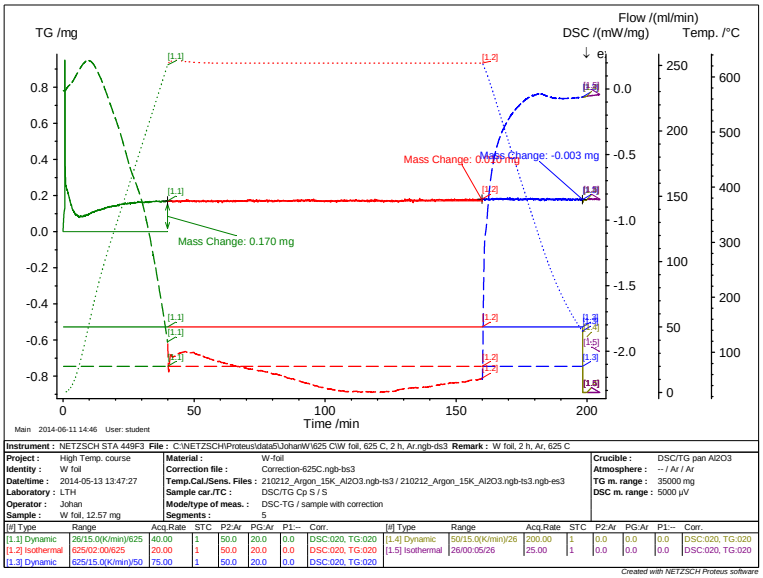

Figure 4.2: The first STA run at 625°C

an experiment was conducted at this temperature in order to verify the results. This is shown in the thermograph below.

This thermograph shows a very low increase in mass and cannot verify the previous findings but the small downwards slope in the beginning of mass curve may be caused by some unknown interference with the balance. It would be preferable if this experiment could be redone for additional accuracy.

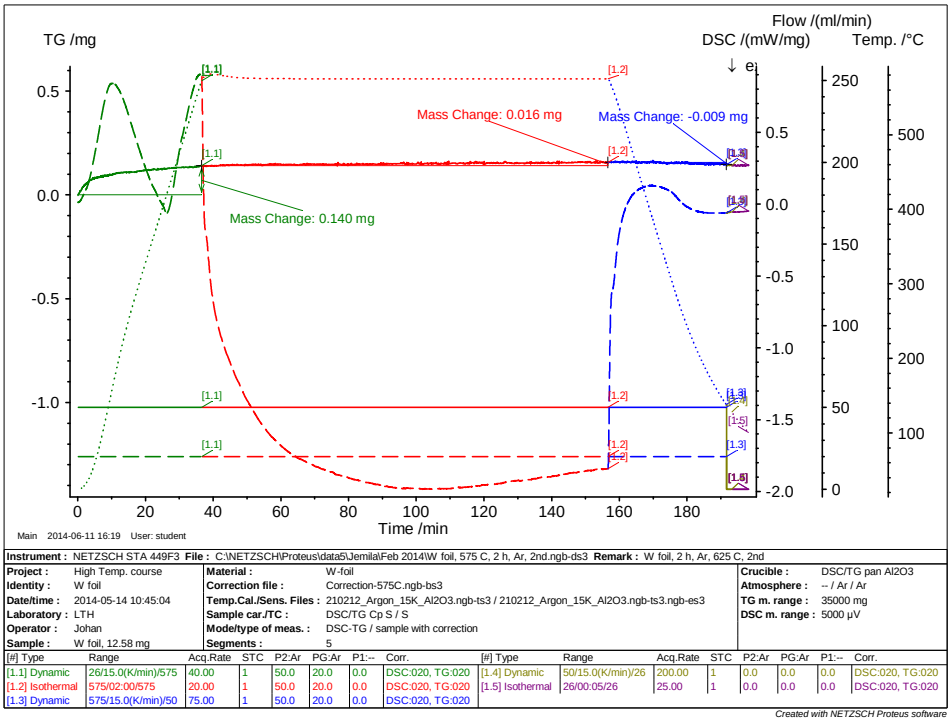

Figure 4.3: The second STA run at 575°C

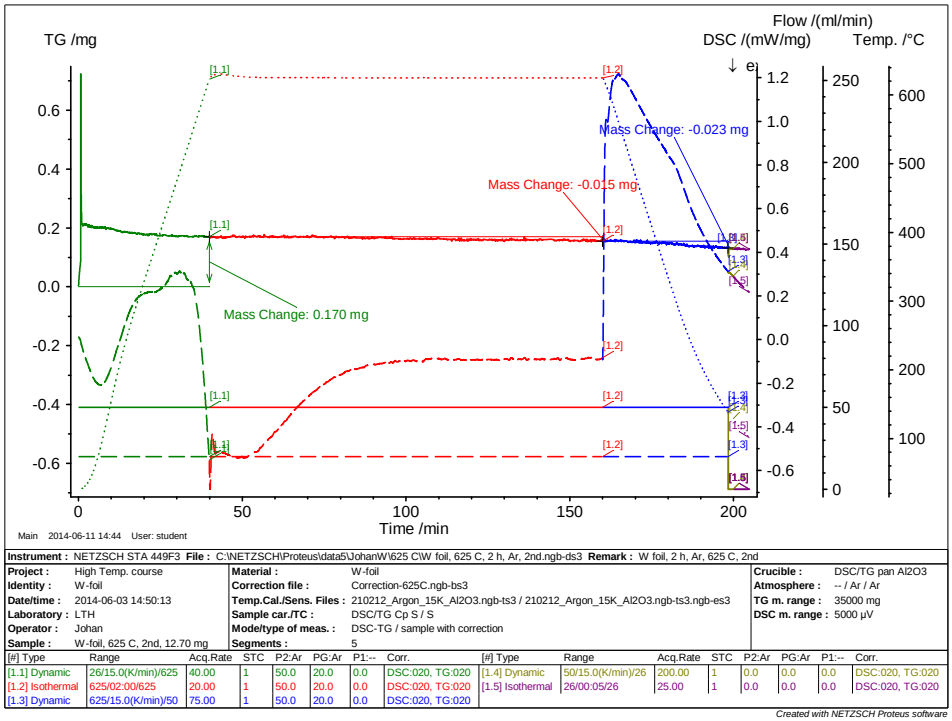

Figure 4.4: The second STA run at 625°C

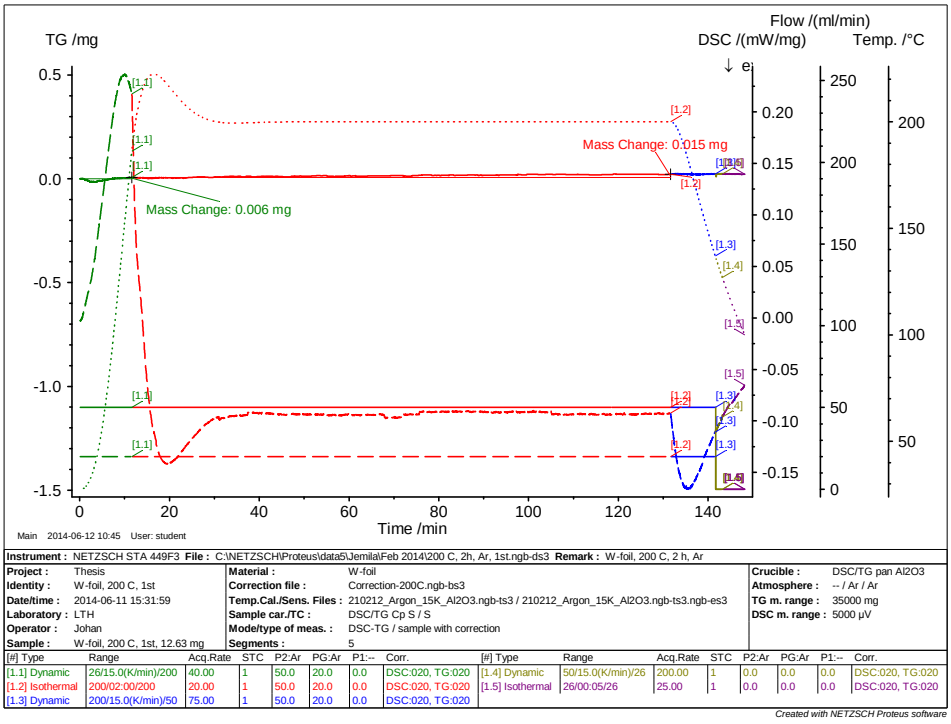

Figure 4.5: The first STA run at 200°C

4.1.2 STA experiments conducted for 48 hours

In the first phase of this thesis, the STA experiments were conducted for 48 hours in order to acquire information about the oxidation characteristics. This idea was abandoned, however, as these experiments were too time-consuming. The only advantage is that they give information about the evolution of the oxide at longer times, something the 2-hour STA runs are unable to give.

The 48-hour runs were conducted at 500°, 625°and 600°C. These can be seen below.

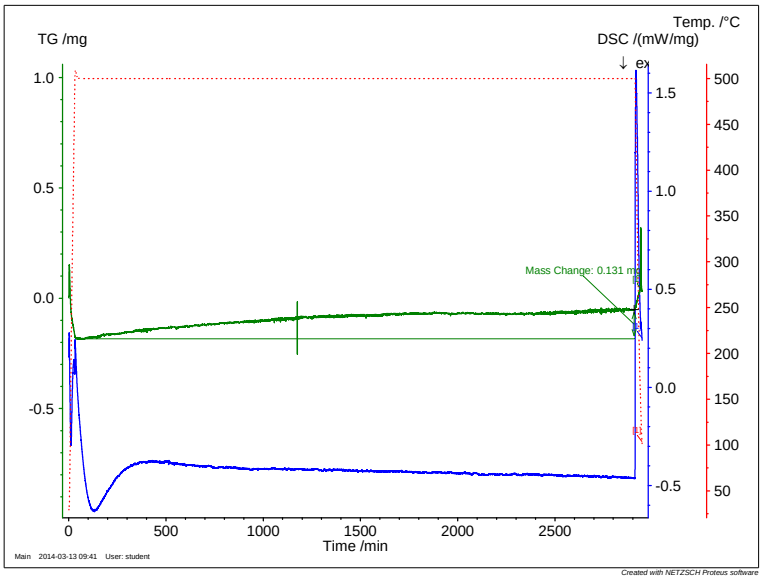

Figure 4.6: The first STA run at 500°C

This mass gain curve of Figure 4.6 looks normal and exhibits a smooth upwards slope over time during the isothermal section. However, because of the heating section in practice becoming omitted from this thermograph due to the scale, it is hard to determine where the curve starts. There is obviously some kind of faulty interference affecting the balance in the beginning of the experiment, which may serve to destabilize it and invalidate the whole result.

The curve in Figure 4.7 also shows an expected upwards slope during the whole isothermal section. Again, something is interfering with the balance somewhere in the heating section which may cause flawed results in the later sections.

The first STA run conducted at 600°C, seen in Figure 4.8 was a failure as it exhibited massive balance fluctuations for some unknown reasons. It is not shown here but can be found in the Appendix.

Since the first and second runs were failures, this one was used to exemplify the appearance of an oxidation curve at 600°C. Note that this curve also includes a balance anomaly during the heating section.

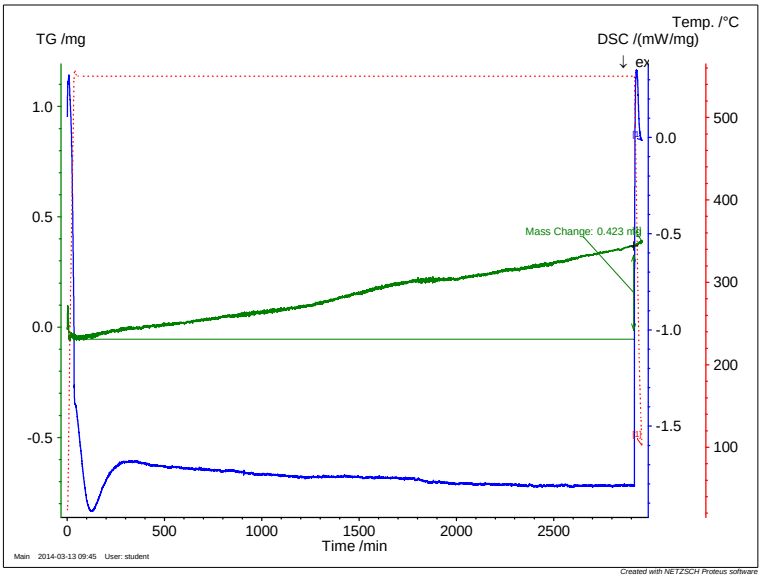

Figure 4.7: The first STA run at 625°C

Despite all 48-hour STA runs experienced some kind of errors in the beginning, the overall mass changes are at least increasing with increasing temperature. Further experiments should be conducted to verify this and to get rid of the balance fluctuations.

The figure below shows a combined plot of the first three 48-hour STA experiments. The samples held at higher temperatures exhibit a significantly higher mass increase, which is consistent with what theory predicts.

As is evident from the results in Figure 1 above, the oxidation is clearly more accentuated at higher temperatures. The mass increase is recorded as approximately $4mg/cm^2$ after 48 hours in the 600°C experiment, $1.5mg/cm^2$ in the 625°C experiment and $0.5mg/cm^2$ in the 500°C experiment. Furthermore, the oxidation curves show little to no indication of slowing down, assuming a linear increase in mass. The 500°C curve could be said to slow down as the mass gain is relatively constant after 1500 minutes. The oxidation rate of 625°and 600°C show a small rise in the vicinity of 1500 minutes, with unclear reason.

When comparing the mass gains halfway through the STA measurements, at 24 hours (1440 minutes), with the mass gains at 48 hours, the results become a bit clearer.

The mass gain of sample 1 shows a decrease in rate during the second half of the experiment whereas the mass gain is increased for sample 2 and just slowing down slightly at 600°C. The increase in mass gain for the second half of the experiment of sample 2, albeit small, can be attributed to the small bump in the curve at roughly 1500 minutes. The cause of this is unknown, and is most likely a measurement anomaly.

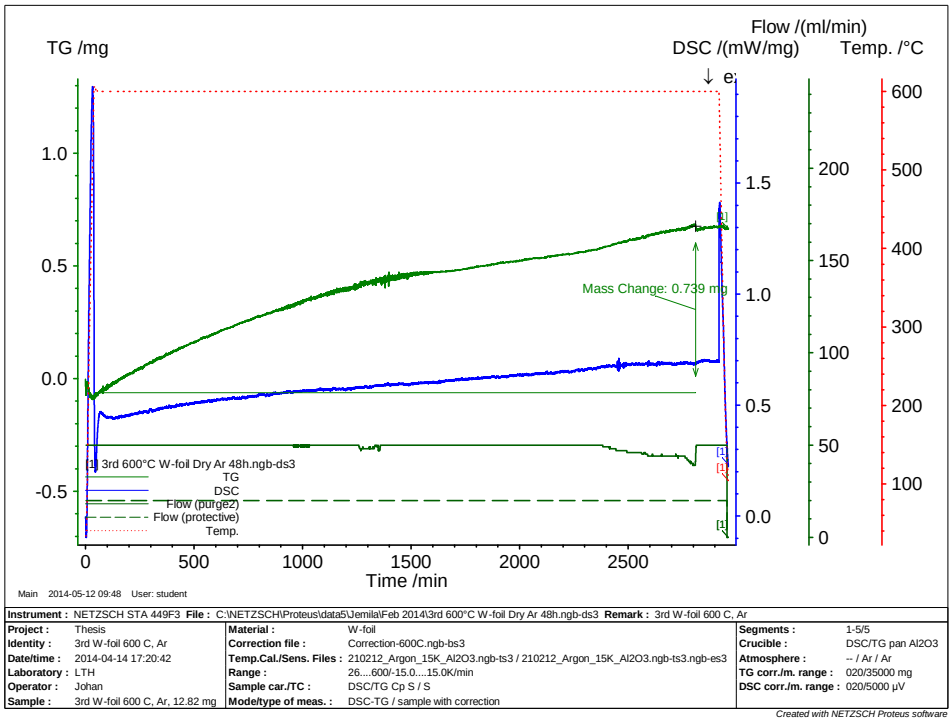

Figure 4.8: The third STA run at 600°C

Based on these results, it is fairly obvious that the mass gain is still prominent even after 48 hours. It is therefore reasonable to assume that longer oxidation measurements, e.g. for 96 hours, could give useful information on the oxidation behavior.

The noise which is seen on the 600°C curve is some kind of measurement anomaly which is superimposed on the oxidation curve. It does not seem to affect the overall slope of the curve over the time period and the noise eventually stops and regains a stable appearance again.

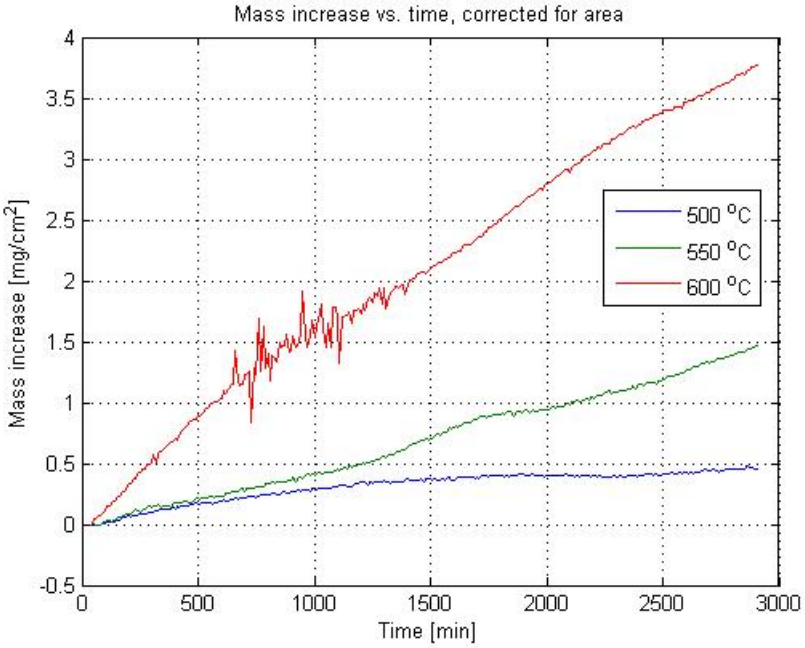

Figure 4.9: Combination of 48-hour STA runs

4.1.3 Summary of STA results

The mass change data for all 2-hour STA experiments as well as for all 48-hour experiments can be seen in 4.10 and 4.11. Table 4.1 below.

As opposed to the thermographs acquired directly as an output from the STA, these figures have had their irrelevant mass gain sections cropped out for a clearer view. This means that all mass gains that were found when the STA chamber temperature was below 200°C has been omitted. The reason for this is that a significant mass gain from oxidation below 200°C was deemed to be inconsistent with theory and was most likely a flawed result. The temperature limit was based on Lassner and Schubert's book which state that oxidation proceeds rapidly only after 200°C [3]. In light of this, only the relevant portion of the thermographs are present in these figures for a convenient comparison.

It is possible to acquire rate constants and activation energies from the STA results but these are deemed to inaccurate to give any meaningful contribution to the overall understanding of the oxidation process. Instead, the rate constants and activation energies are only presented for the TGA experiments.

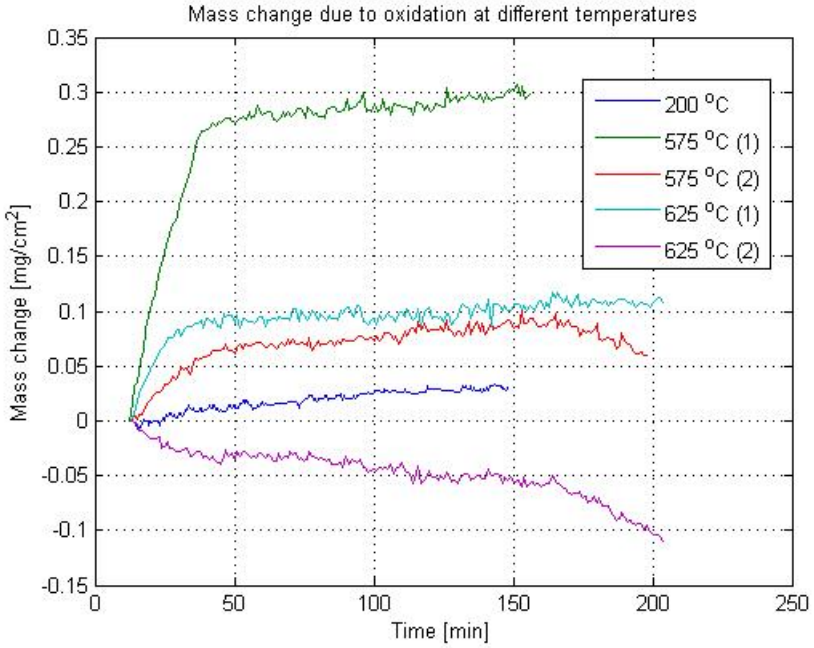

Figure 4.10: Mass change for all 2-hour STA experiments at different temperatures.

As duscussed previously, the first experiment conducted at 575°C and the second experiment conducted at 625°C can probably be discarded

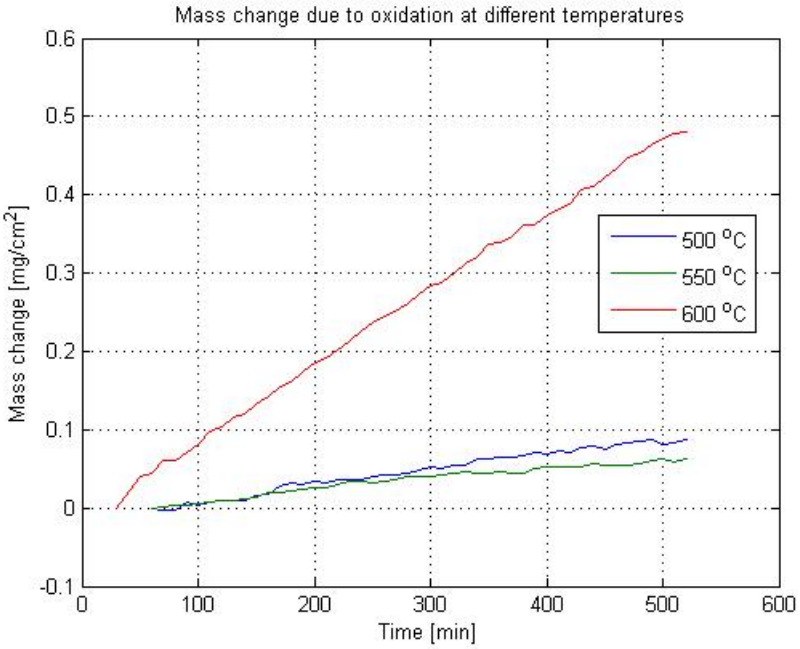

Figure 4.11: Mass change for all 48-hour STA experiments at different temperatures.

Sample number	Temperature [°C]	Absolute mass gain $[mg]$	Normalized mass gain $[mg/cm^2]$
1	200	0.02	0.0354
2	575	0.17	0.3006
3	625	0.06	0.1061
4	575	0.05	0.0884
5	625	-0.06	-0.1061

Table 4.1: Mass change of tungsten foils for all 2-hour STA experiments.

4.1.4 Sources of error

Some substantial sources of error may be encountered when performing STA measurements which affect the accuracy of the results to some extent. As mentioned both in the experimental setup section as well as in the beginning of this chapter, the buoyancy effect can cause significant errors in a thermograph. The buoyancy will affect the in-built analytical balance, and when gas flow is supplied to the STA, it may temporarily disturb the readings of the balance which is in turn sent to the computer and registered as a result. This works for both initiating a gas flow and cutting it, but it is more crucial to control it in the beginning of the measurements.

The effect of this buoyancy can be seen in most of the STA thermographs above, indicated as the unexpected changes in the mass gain curve. For example, in Figure 4.6 representing the mass gain at 500°C, the curve starts off by rapidly gaining and then losing an disproportional large amount of mass, which is impossible to explain in any other way. The sample cannot instantaneously gain a tenth of a milligram and then lose three tenths directly afterwards.

4.2 Thermogravimetric Analysis

The results from the oxidation experiments conducted with the TGA setup is presented in this section. Some sublimation experiments were also conducted with this setup but is presented in the Sublimation Analysis section.

Two types of samples were tested for their oxidation characteristics; unpolished samples and electropolished samples, both from TianLong Co. The unpolished samples had not undergone any surface treatments that could aid its resistance to oxidation and theory thus predicts that they will possibly be more severely damaged by oxygen attacks than the electropolished samples. Since the samples have a different geometry and surface quality than the samples used with the STA instrument, a comparison of the results is not easily done. The results are instead compared primarily with the results obtained from the same type of equipment.

Due to the large difference in mass gains between the relatively low temperature experiments and those conducted at higher temperatures, the results are divided into different figures. The atmosphere during all these experiments was helium with maximum 5 ppm oxygen.

Oxidation experiments were conducted in the temperature interval 400°–1000°C, although some higher temperature oxidation were also done during the sublimation analysis.

4.2.1 Unpolished samples

The unpolished samples had not undergone any surface treatments that could aid its resistance to oxidation and theory thus predicts that they will possibly be more severely damaged by oxygen attacks than the electropolished samples. It was found that this was indeed the case, as unpolished samples gained a slightly higher amount of mass during the exposure to oxygen.

At the relatively lower temperatures, it was sometimes difficult to observe a strict parabolic behavior of the oxidation curves, as seen in Figure 4.12. There appears to be a significant leap in mass gain when the temperature is raised from 600°to 700°C but should probably be attributed to the exponential dependence of temperature of the oxidation kinetics. The 700°C curve appears to have had some serious interference issues from the balance, but a typical oxidation curve can still be observed and this noise is neglected. The 725°C curve exhibits some kind of anomaly around the 40-minutes mark. The increase in oxidation rate for about twenty minutes in what appears to be an onset of a new parabola can possibly be a result of oxide spalling, but this could not be verified by visual inspection.

At the higher set of temperatures, it is much easier to see the parabolic behavior of the oxidation curves. Both the noise level and intereference with the balance is less pronounced when the mass gains are this large.

Table 4.2 summarizes the absolute and normalized mass gains of the unpolished TGA samples

Prior to further manipulation, e.g. for evaluating the rate constants, a polynomial is fitted to each oxidation curve as seen in Figures 4.15 to 4.17.

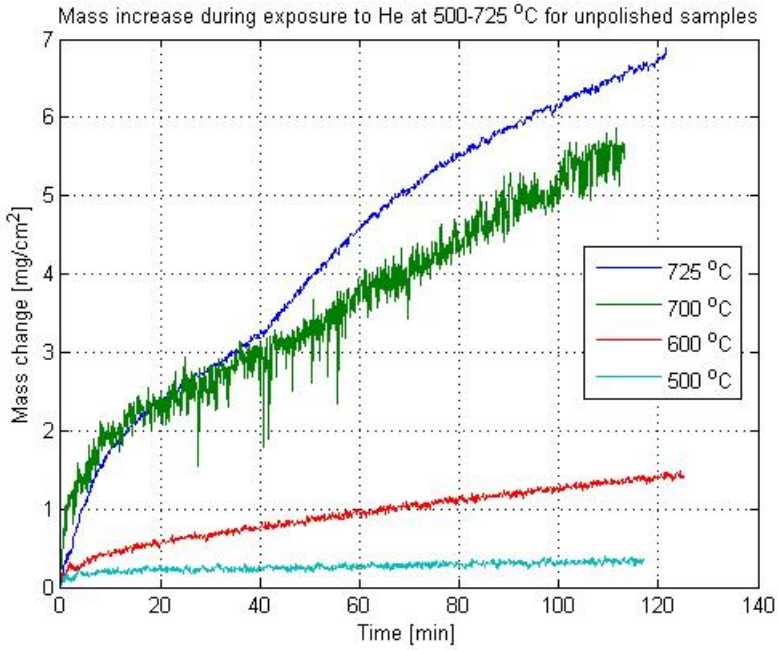

Figure 4.12: Oxidation curves from unpolished samples in He at 500°–725°C

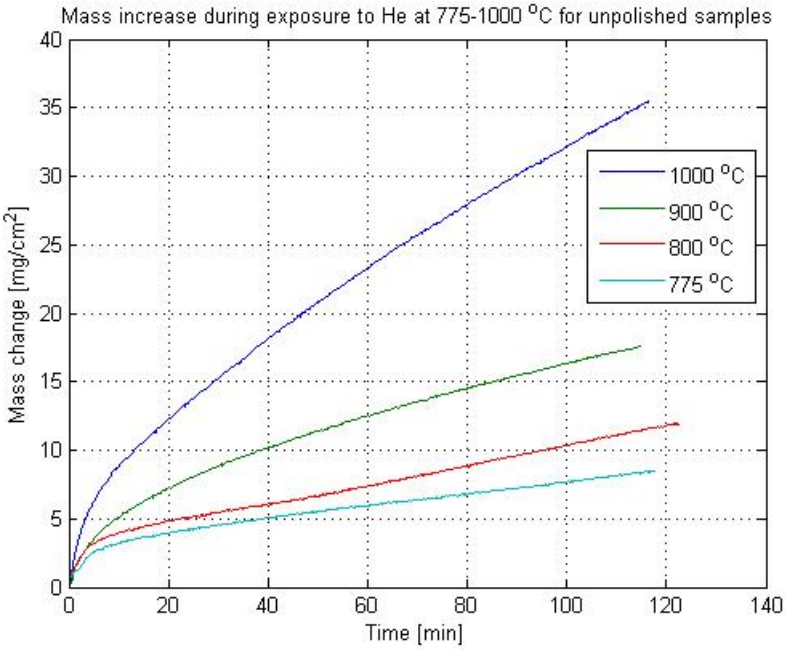

Figure 4.13: Oxidation curves from unpolished samples in He at 775°–1000°C

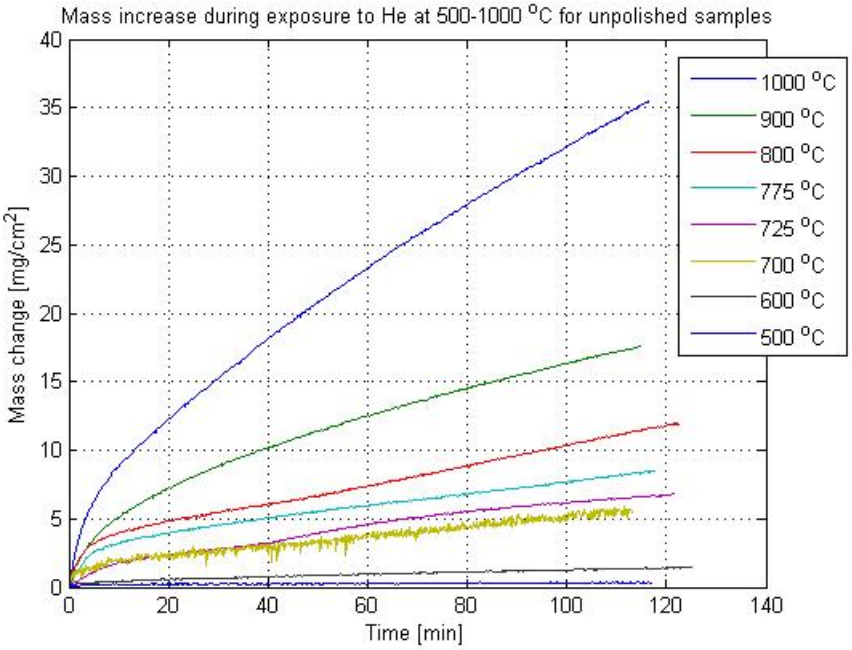

Figure 4.14: Oxidation curves from unpolished samples in He at 500°–1000°C

Sample number	Temperature [°C]	Absolute mass gain $[mg]$	Normalized mass gain $[mg/cm^2]$
1	500	2.79	0.34
2	600	11.66	1.43
3	700	45.23	5.54
4	725	56.33	6.90
5	775	69.54	8.51
6	800	96.79	11.85
7	900	143.53	17.57
8	1000	291.86	33.73

Table 4.2: Mass change of unpolished tungsten discs for TGA experiments

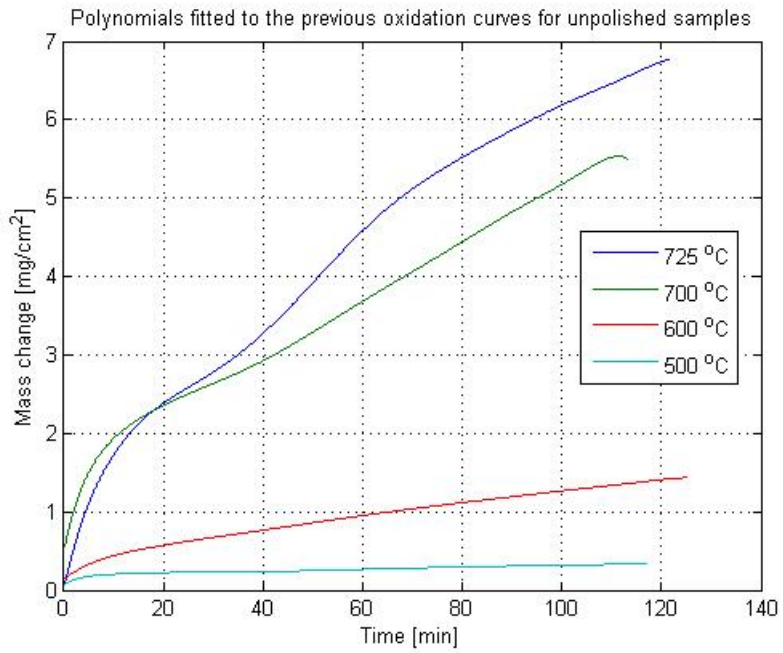

Figure 4.15: Polynomial fitted oxidation curves of unpolished samples at 500°–725°C

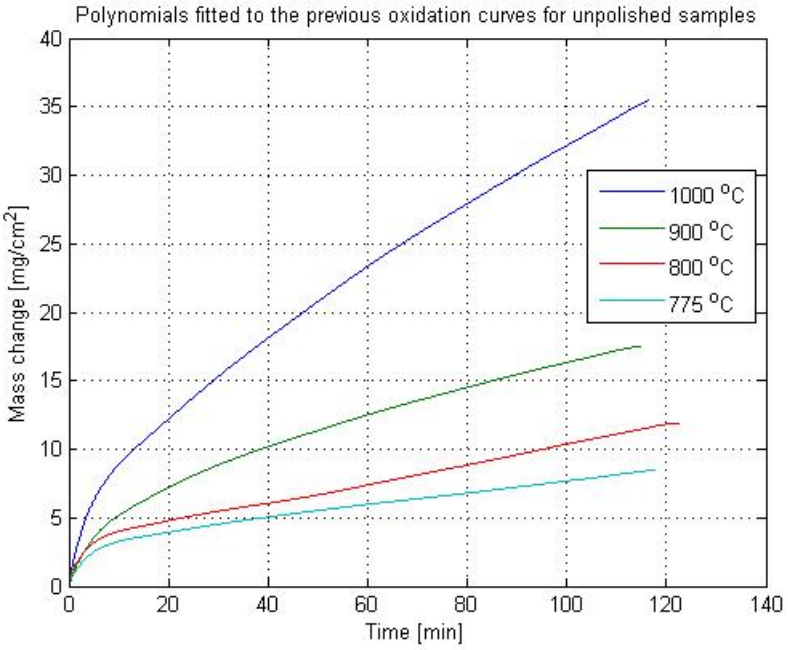

Figure 4.16: Polynomial fitted oxidation curves of unpolished samples at 775°–1000°C

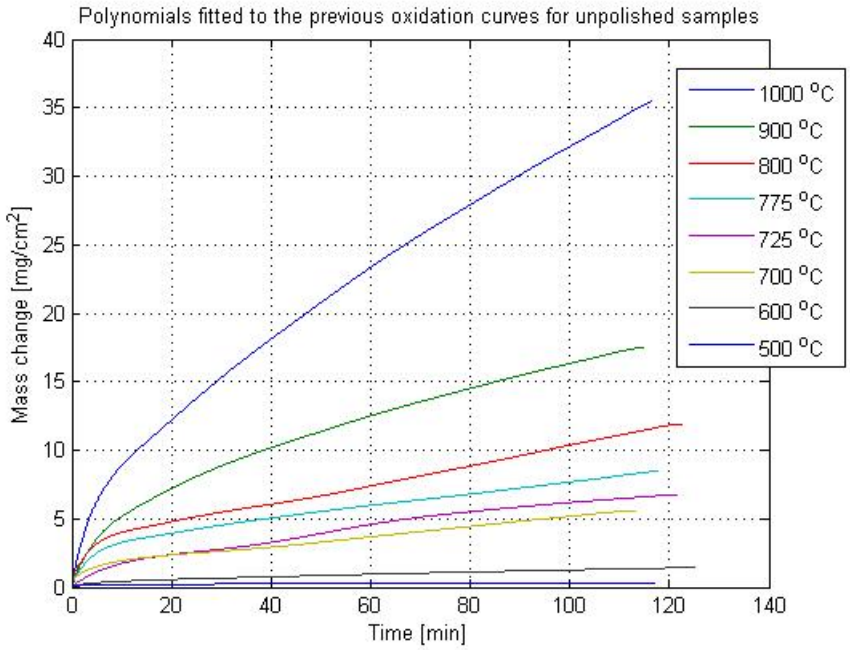

Figure 4.17: Polynomial fitted oxidation curves of unpolished samples at 500°–1000°C

4.2.2 Electropolished samples

The electropolished samples have undergone a treatment which raises their surface quality, thereby lowering their effective surface area which also lowers their susceptibility to oxidation. The electropolished samples are therefore expected to oxidize to a lesser extent than the unpolished samples.

Consistent with oxidation theory, the tungsten discs exposed to oxidizing environments at elevated temperatures are rapidly oxidized, even at a very low partial pressure of oxygen. The effect is significantly more profound at relatively higher temperatures and amounts to upwards of a 2 % weight gain in samples placed in a 1000°C tube furnace for 2 hours. Even though the oxidation rate diminishes as the oxide layer thickens and the oxidation curve transitions into a linear region, there is still a very steep mass gain per unit time.

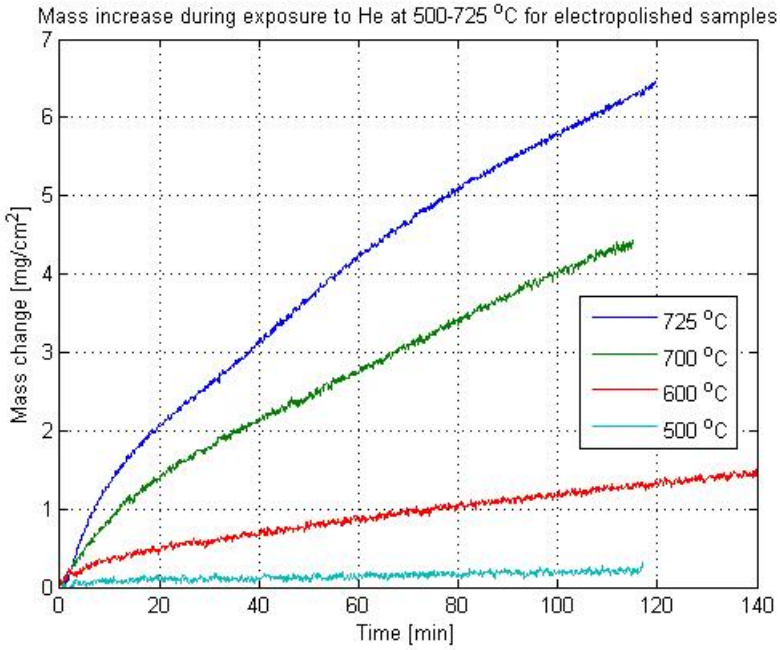

Figure 4.18: Oxidation curves from electropolished samples in He at 500°–725°C

The mass increase due to oxidation is seen to follow a parabolic curve from the beginning of the measurement to roughly 30 minutes in. At this point, the curve transitions into a region where the mass gain per unit time follows a linear relationship. This is true for the curves representing 700°, 900°and 1000°C, but does not hold for the 800°C curve seen below.

A closer look at this curve reveals that it does not follow a typical parabolic-to-linear curve as with the other temperatures but rather there is a distinct kink on the curve. This kink is thought to indicate that there is some kind of cracking process causing the oxide layer to spall and fall off. This leads to bare metal being exposed which in turns lead to an increase in oxidation rate.

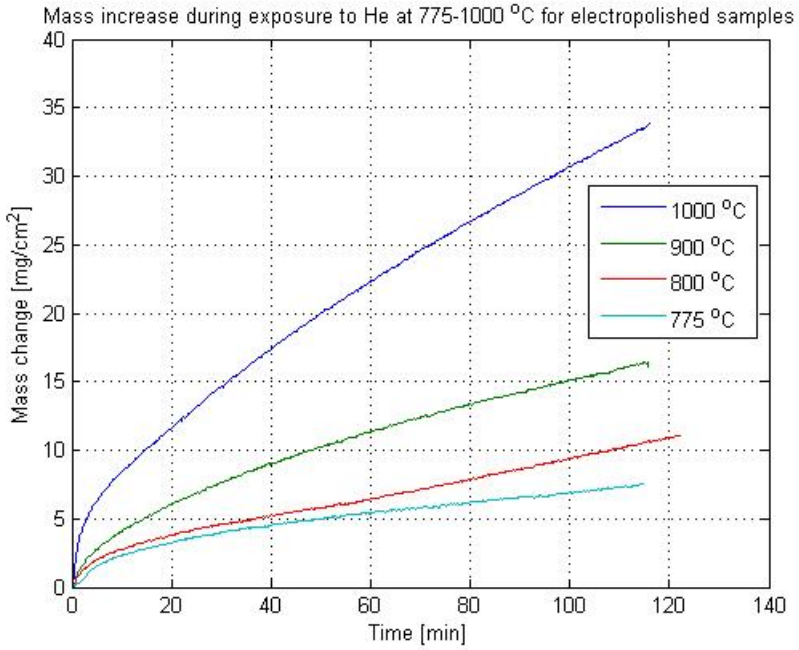

Figure 4.19: Oxidation curves from electropolished samples in He at 775°–1000°C

This result is consistent with what is predicted by theory as the loss of a protective oxide layer will increase the oxidation rate. It is reasonable to believe that some parts of the oxide cracks and spalls also at higher temperatures. This too would lead to a kink phenomenon on the curves but it is probable that its effect is relatively low compared with the rest of the oxidation, meaning it stays hidden under the rapid weight increase observed at these higher temperatures.

Table 4.3 below gives an overview of the mass gains of the electropolished samples.

Sample number	Temperature [°C]	Absolute mass gain $[mg]$	Normalized mass gain $[mg/cm^2]$
1	500	2.52	0.31
2	600	12.85	1.30
3	700	36.02	4.41
4	725	52.78	6.46
5	775	61.54	7.53
6	800	90.43	11.07
7	900	130.90	16.03
8	1000	271.00	33.18

Table 4.3: Mass change of electropolished tungsten discs during TGA experiments

The oxidation curves of the electropolished samples are also fitted with polynomials before they are further evaluated, seen in Figures 4.21 to 4.23.

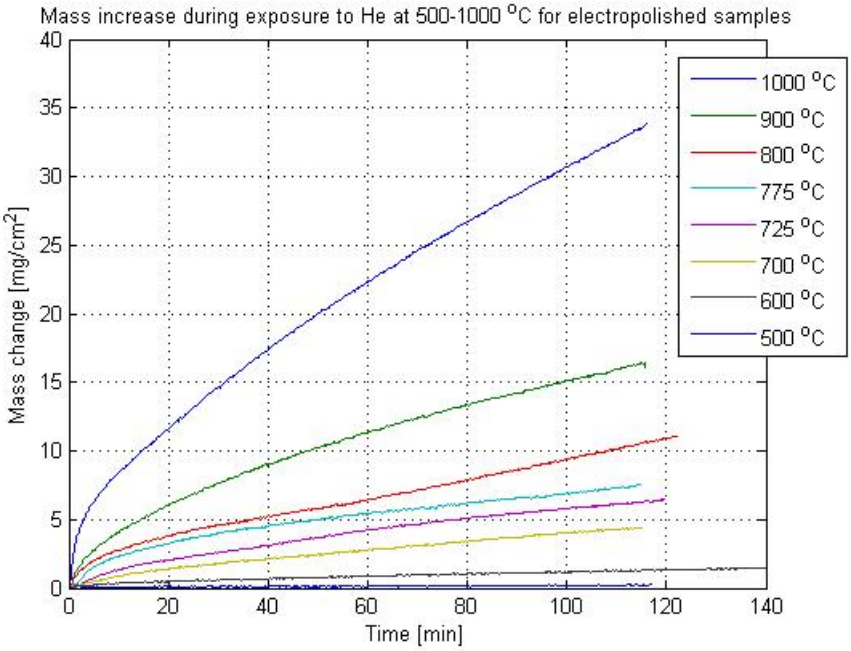

Figure 4.20: Oxidation curves from electropolished samples in He at 500°–1000°C

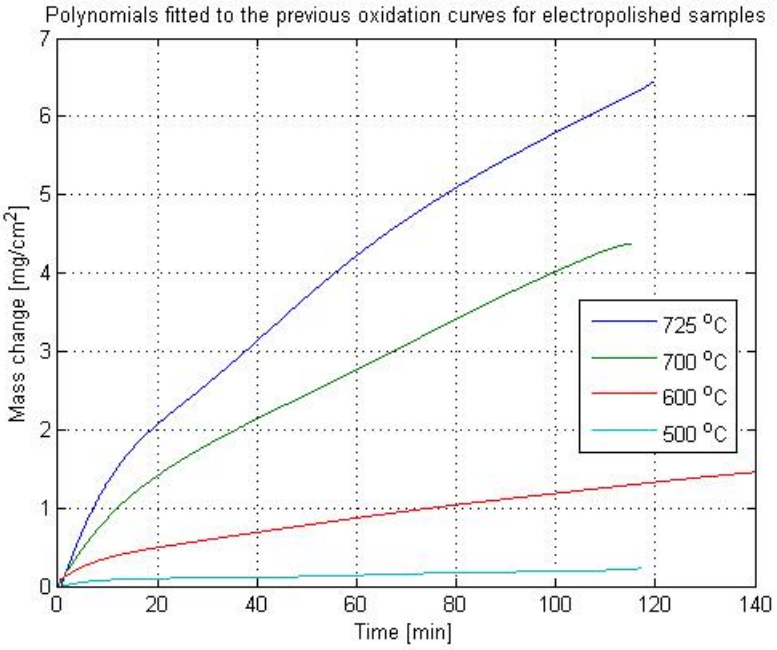

Figure 4.21: Polynomial fitted oxidation curves of electropolished samples at 500°–725°C

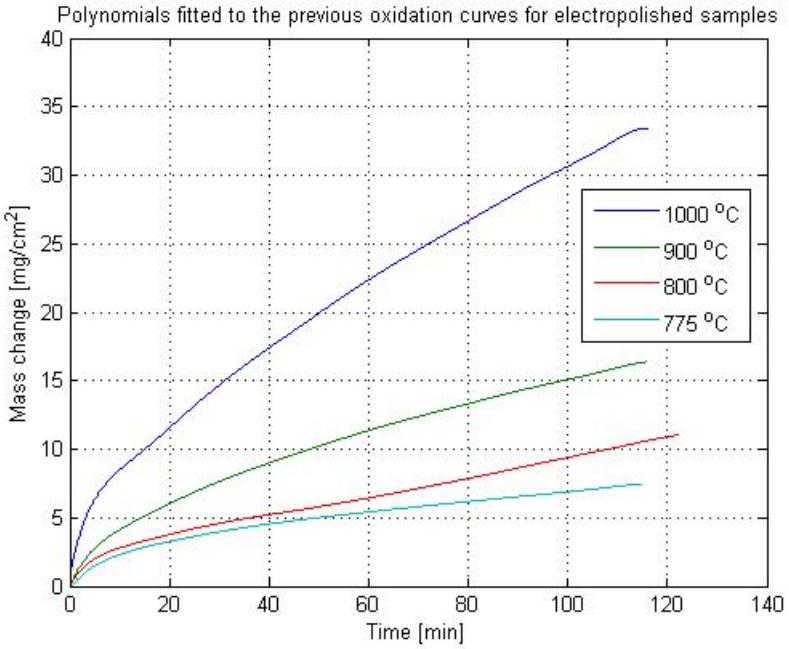

Figure 4.22: Polynomial fitted oxidation curves of electropolished samples at 775°–1000°C

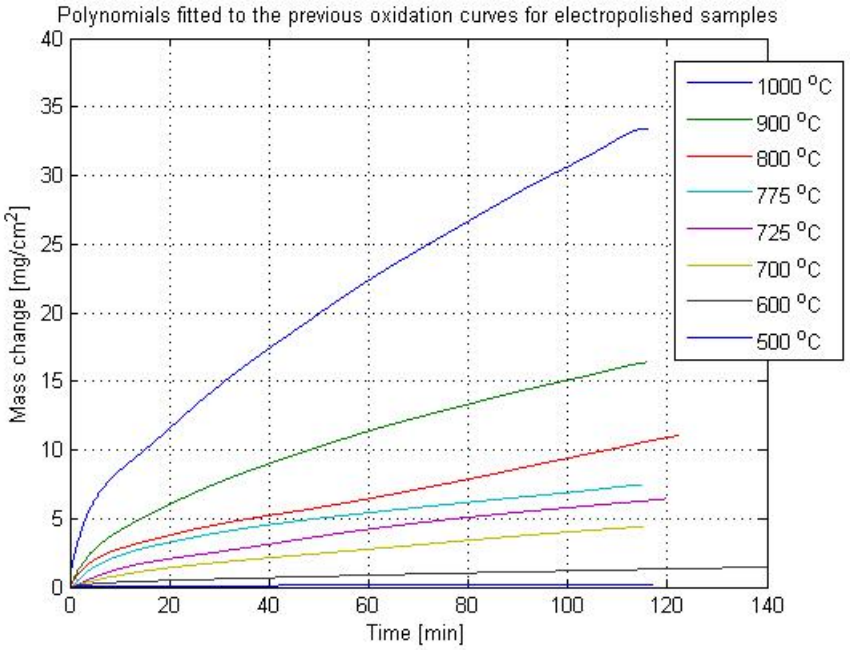

Figure 4.23: Polynomial fitted oxidation curves of electropolished samples at 500°–1000°C

4.2.3 Determination of the rate constants

One major goal of characterizing the oxidation behavior is to determine the relevant rate constants for the chemical processes involved in oxidation. The rate constants can be acquired by calculating the slope of the linear region in a plot of the squared mass gain per area versus time which was explained previously in the theoretical section.

As stated earlier, it is important but sometimes tricky to get a desired curve fitting. The whole determination of the parabolic rate constant is dependent on getting precisely the parabolic section. Each curve can have one or more anomalies as a result from spalling or cracking, which will distort the parabolic appearance.

To get around this problem, it is possible to assess the parabolic behavior of the oxidation curves by splitting them up in small segments, e.g. comprising 1 minute of the total measurement time or 20 data points and then see how the rate constants differ between each segment, but this is not done here.

The chemical reaction rate constants and the corresponding activation energy

Another kinetic parameter than can be established from these results is the activation energy for the chemical reaction between tungsten and oxygen, i.e. the formation of WO_3 from W and O. This can be acquired from the same general procedure with the exception that a polynomial is fitted to the first few points of the oxidation curve. At this stage, the sample does not contain any oxide and oxygen can rapidly attack the tungsten.

The main problem here is to determine where this region begins and ends. If the slope is determined from a section too early in the experiment, there might be significant interference from the balance but if the slope is determined too late, the oxide layer might be too thick which also distorts the results.

Figure 4.24 collects all available data points for the electropolished and unpolished samples. Note that only the rate constants corresponding to the five highest temperatures were deemed reliable enough to be incorporated into these plots and used for kinetic calculations.

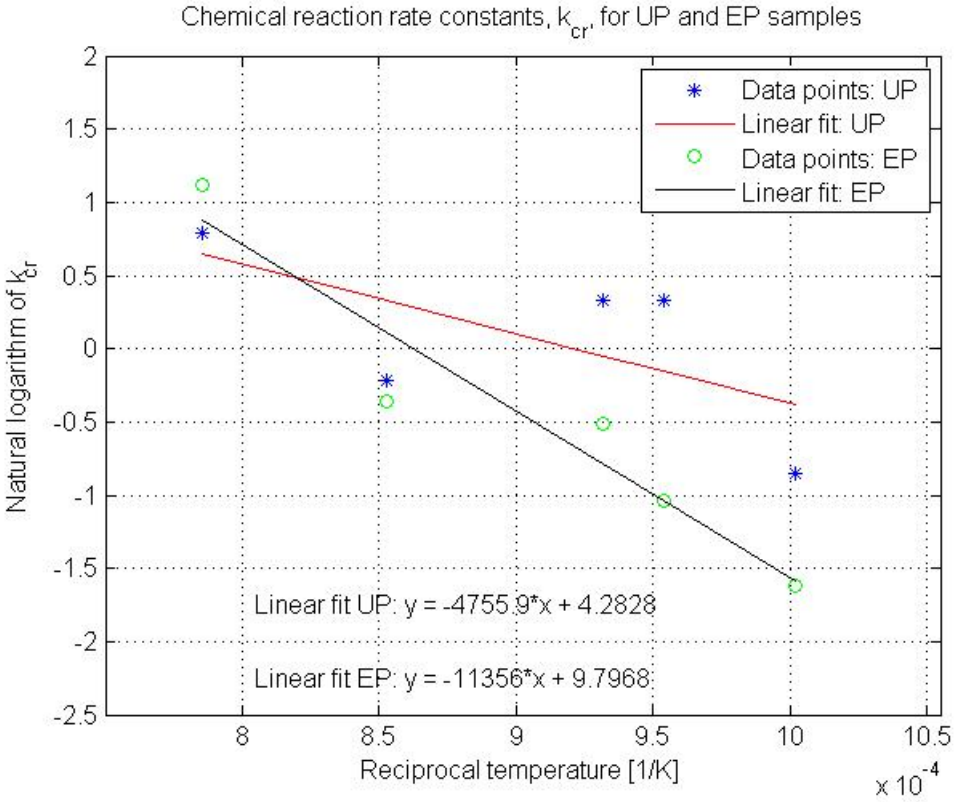

Figure 4.24: The chemical reaction rate constants for electropolished and unpolished samples.

The slope multiplied with the gas constant finally yields the activation energy.

$$Q_{cr,UP} = 40\frac{kJ}{mol} \tag{4.1}$$

$$Q_{cr,EP} = 94\frac{kJ}{mol} \tag{4.2}$$

The activation energy appears to be significantly higher for electropolished samples than for unpolished samples which is consistent with theory. However, there are some errors which must be taken into consideration before drawing any conclusions, e.g. abnormal deviations from the linear fit. Because of the uncertainties when choosing the starting point where oxidation is said to being, prior to any oxide scale formation, there will inevitably be some errors that are introduced.

Even though the data points in the graphs above show some deviation from the linear fit, they seem to follow this trend in the entire temperature range, and it is assumed that this representation is a somewhat good approximation to the true behavior.

The parabolic rate constants and the corresponding activation energy

The parabolic rate constant is a measure of the rate of mass addition to the sample during the period where ionic diffusion through the oxide layer is the rate limiting step in the oxidation reaction. The theory behind this is explained in the theoretical section concerning Wagner's model on oxidation. As explained in that section, the parabolic rate constant can only be extracted from experiments conducted below the sublimation temperature. Above this critical temperature, the rate constant will be a product of both the parabolic rate constant due to oxidation and the linear rate constant due to sublimation. Here, both unpolished and electropolished samples are analyzed and compared.

Figure 4.25 collects all available data points for the electropolished and unpolished samples.

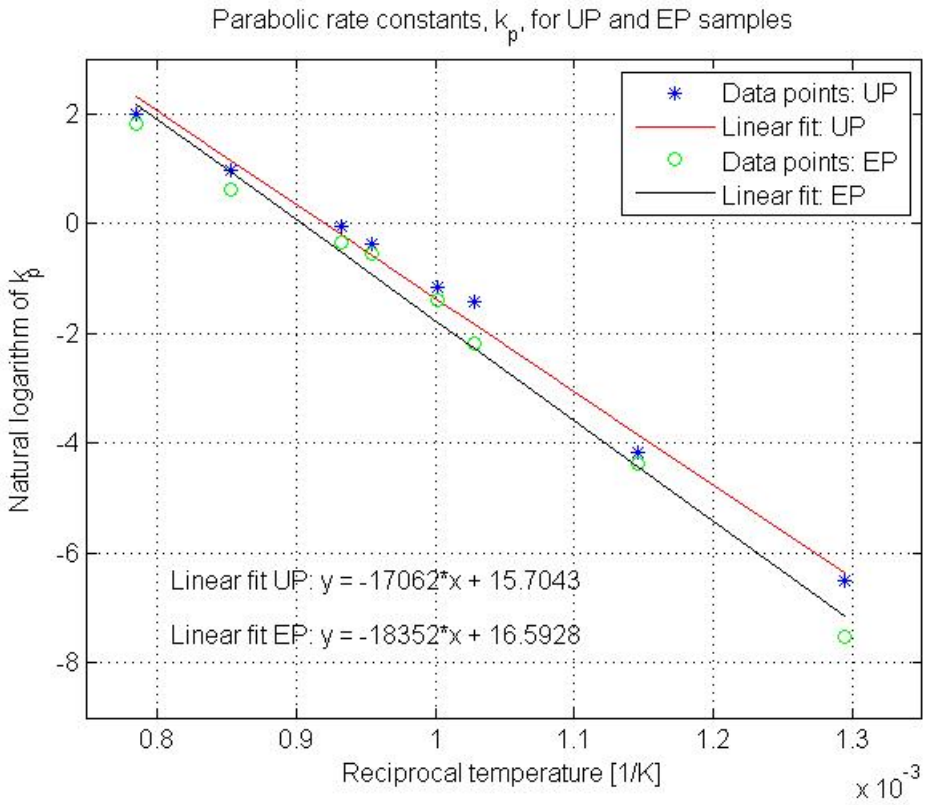

Figure 4.25: The parabolic rate constants for electropolished and unpolished samples

The slope multiplied with the gas constant finally yields the activation energy.

$$Q_{p,UP} = 142 \frac{kJ}{mol} \tag{4.3}$$

$$Q_{p,EP} = 153 \frac{kJ}{mol} \tag{4.4}$$

The linear fittings applied to these data points appear accurate in both cases but a few more data points would give a more precise value. The difference between

these results seem good, as electropolished samples are thought to have require a slightly higher activation energy than unpolished ones and may indicate that the supposed difference in chemical reaction activation energy may influence the oxidation behavior later on. Despite this, the values are slightly lower than those presented in other sources found in literature.

As stated previously in the literature survey section, there are numerous reported values of the activation energy for tungsten oxidation. The parabolic rate constant is most often reported but there are not very many sources for the oxidation reaction itself.

Gulbransen and Andrew investigated the oxidation kinetics of tungsten in the temperature interval 500°–1300°C [27]. Initially they found a heat of activation of 44500 cal/mol, i.e. 186 kJ/mol, which was also previously found by Gulbransen and Wysong [10] to explain the oxidation at 400°–500°C. Another research group that is mentioneded in the same article and is also mentioned in the NASA technical translation is Gorbunova and Arslambekov, which found that the heat of activation was dependent on surface preparation in the temperature range 390°–487°C. Electrolytically polished samples gave a heat of activation of 46500 cal/mol, i.e. 195 kJ/mol from parabolic rate constants, while mechanically polished surfaces yielded a heat of activation of 41000 cal/mol, i.e. 172 kJ/mol.

Gulbransen and Andrew also state that the value of 186 kJ/mol probably represents the heat of formation of defects and the heat of activation of diffusion of metal atoms for the early stage of oxidation when the oxide film is protecting the metal. The authors furthermore found out that the parabolic rate law constants could be fitted to two straight lines, separated at 750°C. The values below this temperature was found to have an activation energy of 54500 cal/mol, i.e. 228 kJ/mol. Above 750°C they reported a value of 32500 cal/mol, i.e. 136 kJ/mol. They motivate this separation with a transition stage in the oxidation process, but no further information is given.

It is worth noting that Gulbransen and Andrew conducted their experiments at oxygen pressures of $0.00132atm$ - $0.1atm$. Compared to the oxygen partial pressure of $10^{-6}atm$ used for almost all oxidation experiments in this thesis, it is difficult to estimate whether this may have influenced the oxidation kinetics. A relatively higher oxygen partial pressure may e.g. have aided in a more rapid mass transport of ions across the oxide scale, which could have affected the rate constants in an unforeseeable way.

The calculated values of activation energies from the experiments of this thesis are a bit lower than is reported from literature, but there is generally a decent correlation between the values. The activation energy of unpolished samples are slightly lower than electropolished samples, which is expected.

4.2.4 Summary of oxidation results with TGA

It was found that the tungsten disc samples gained a significant amount of mass during exposure to helium gas, with the mass addition being considerably larger in each increment of 100°C. Furthermore, it was shown that unpolished samples gained slightly more mass during the experiment period as compared to samples that were electropolished. This result is predicted as the electropolishing treatment is thought to passivate the metal surface to some extent. The effect can be seen in Figure 4.26 below.

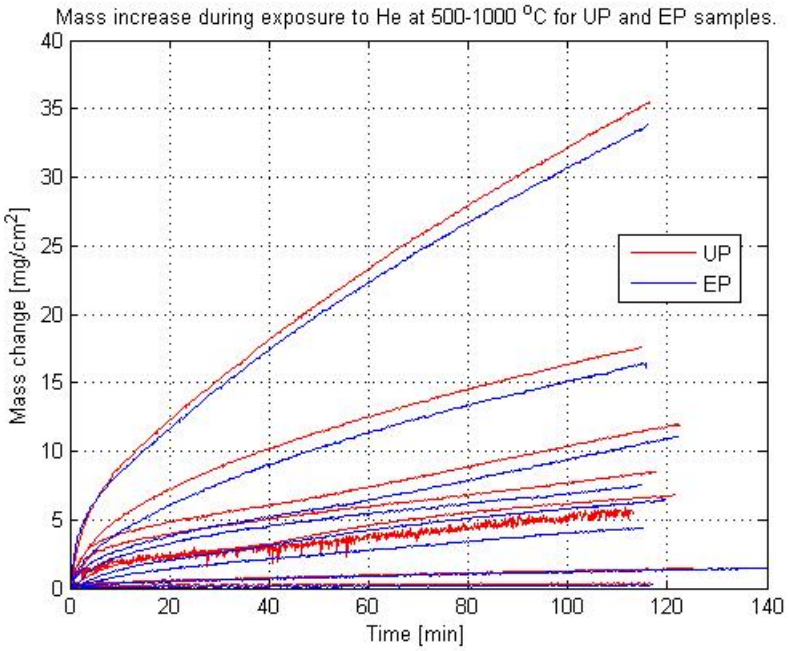

Figure 4.26: Comparison of oxidation between unpolished and electropolished samples.

The mass gain was typically around 6 % higher for unpolished samples at intermediate and high temperatures but at lower temperatures, e.g. 500°C, the difference was negligible.

In addition to the figures presented above, Table 4.4 summarizes the normalized mass gains of all TGA samples. Table 4.5 and Table 4.6 collects all rate constants, and Table 4.8 gives a short description of the appearances and other interesting information about the samples.

The most striking change the samples will undergo during the exposure to oxygen is a color change, easily visible to the naked eye. A brief selection of the samples in the range 600°to 900°C can be seen in Figure 4.27. These are electropolished samples, but the unpolished samples look almost identical.

Notice that the oxidation process appears to have started at 600°C but that the surface has not yet acquired the typical yellow color. At 1000°C, the oxide layer crumbles easily and falls off along the edges of the discs.

Sample number	Temperature [°C]	Normalized mass gain: UP $[mg/cm^2]$	Normalized mass gain: EP $[mg/cm^2]$
1	500	0.3416	0.3085
2	600	1.427	1.343
3	700	5.537	4.410
4	725	6.896	6.462
5	775	8.514	7.534
6	800	11.85	11.07
7	900	17.57	16.42
8	1000	35.46	33.82

Table 4.4: Mass change of unpolished tungsten discs for TGA experiments

Sample number	Temperature [°C]	Chemical reaction: UP $[mg^2/cm^4]$	Chemical reaction: EP $[mg^2/cm^4]$
4	725	0.4270	0.1985
5	775	1.3969	0.3543
6	800	1.3877	0.5960
7	900	0.8067	0.6945
8	1000	2.2077	3.0649

Table 4.5: Chemical reaction rate constants for tungsten discs, acquired from TGA experiments.

Increasing the temperature by 100°C will lead to dramatic changes in the rate of oxidation. The color and texture will also undergo very clearly visible changes as the tungsten disc loses its bright metallic luster and gains a matte dark yellow color with nuances of grey and green. The oxide tends to be adherent on discs that are oxidized at relatively low temperatures. At higher temperatures, 800°–1000°C, the oxide is very easily crumbled to oxide dust as it is handled and removed from the Chromaloy cage.

Sample number	Temperature [°C]	Parabolic: UP $[mg^2/cm^4]$	Parabolic: EP $[mg^2/cm^4]$
1	500	0.0015	0.0005373
2	600	0.0153	0.0126
3	700	0.2397	0.1126
4	725	0.3146	0.2509
5	775	0.6922	0.5804
6	800	0.9438	0.7008
7	900	2.6197	1.8512
8	1000	7.2938	6.0879

Table 4.6: Parabolic rate constants for tungsten discs, acquired from TGA experiments.

Sample type	Activation energy	Value $[kJ/mol]$
UP	Chemical reaction	118
EP	Chemical reaction	155
UP	Parabolic	142
EP	Parabolic	153

Table 4.7: Collection of activation energies for tungsten disc samples.

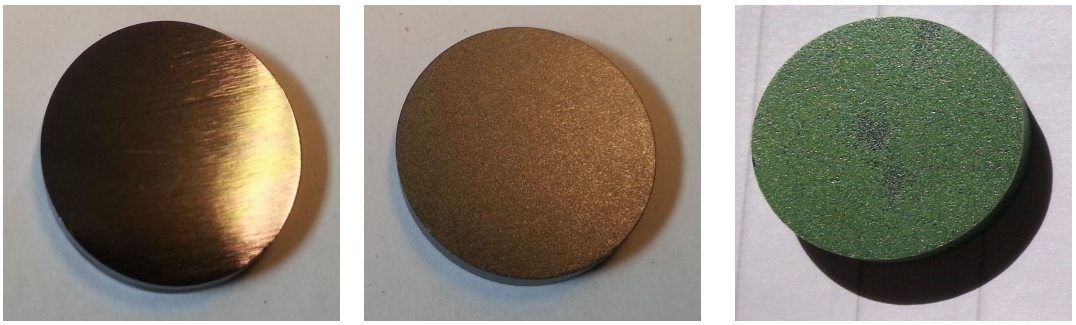

(a) 500°C (b) 600°C (c) 700°C

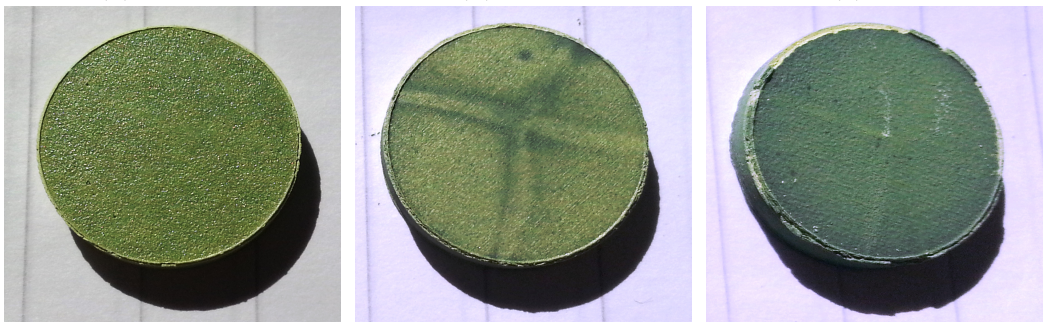

(d) 800°C (e) 900°C (f) 1000°C

Figure 4.27: Tungsten foils oxidized in the vertical tube furnace.

Sample number	Temperature [°C]	Color and texture
Reference	25	Bright grey, metallic luster, noticeable polishing marks
1	500	Blackened, metallic luster
2	600	Grey, matte surface finish, some visible pores
3	700	Green-yellow, slightly dark, surface dotted with pores
4	725	Dark yellow, green, surface porosity
5	775	Green-yellow, porosity
6	800	Dark yellow, significant porosity, oxide crumbles when handled.
7	900	Grey-green yellow, visible porosity, small geometrical changes.
8	1000	Grey-green yellow, extensive porosity, large geometrical changes, edges developing around the disc.

Table 4.8: Description of the color and texture of the samples after exposure to pure He gas at different temperatures.

4.2.5 Sources of error for TGA

The main source of errors for all TGA experiments is probably the analytical balance. During prolonged experiments, drift-phenomena can occur which could slightly distort the results. When working with the high-temperature furnace, the surrounding air will become heated and cause small flows of air which could interfere with the hanging device and the readings of the balance. Furthermore, the balance needs to be calibrated every now and then to ensure reliable results, but this calibration procedure sometimes failed when environmental interference became too pronounced, leading to some fluctuations in the balance readings.

4.2.6 Comparison of oxidation data from the STA and TGA setups

It is difficult to compare the results acquired from the STA and TGA setups due to the inherent differences of the two methods. While the STA setup should in theory provide a superior control of gas flow and greater mass sensitivity of the balance than the TGA setup, the two methods use different gas compositions, different samples, and operate at different temperatures.

Indeed, the results seem to lack in consistency as the results differ between the two setups. An STA result from 575°C show a mass gain of about $0.09 mg/cm^2$, and $0.10 mg/cm^2$ for a 625°C sample, whereas the corresponding values for the TGA setup are $1.30 mg/cm^2$ and $1.43 mg/cm^2$ for EP and UP samples respectively.

Consequently, it is probably best to analyze the results of the two methods on a separated basis.

4.3 Sublimation Analysis

The sublimation temperature, i.e. the temperature at which solid tungsten trioxide transitions into gaseous tungsten trioxide, is designated as an important parameter to factor into the design of the European Spallation Source. The reason for this is the risk of contamination in the cooling circuits as irradiated tungsten trioxide particles may leave the target surface after oxidation. The high-velocity flow of cooling helium gas will likely aid in oxide spalling and may ease the transport of gaseous oxide compounds through the cooling circuit.

The kinetics of sublimation can be hard to assess due to interference from the oxidation data. To get around this problem, a series of experiments were conducted in order to isolate the sublimation phenomenon. Tungsten trioxide powder of high purity was acquired and put in an STA crucible and was subsequently exposed to isothermal heat programs at different temperatures in both a regular high-temperature furnace as well as the vertical tube furnace with TGA capabilities and atmosphere control. The basic principle in these experiments is the same as for the oxidation experiments and utilizes the change in mass of the sample as an indication of what mechanisms are present. At some elevated temperature, the sublimation mechanism is initiated which results in a negative change in mass, i.e. a loss of material from the sample. The change is assumed to be only dependent on the sublimation. This is a valid assumption since the temperature and partial pressure of oxygen in the air is sufficiently high to keep the tungsten in its highest oxidation state, i.e. all powder is anticipated to be tungsten trioxide and no tungsten dioxide or any other non-stoichiometric oxide is thought to be present.

In addition to WO_3-powder being used, small circular pieces of tungsten foil were also used in both setups. As opposed to the powder, which was already in its highest oxidation state, the tungsten foils were oxidized rapidly in all experiments, after which they consisted of only WO_3 and was ready to sublime.

The results presented in this section are therefore thought to give an indication under what conditions tungsten trioxide may or may not be subject to sublimation.

The initial literature survey revealed that the sublimation temperature was around 750°C but that the impact of sublimation in terms of mass change becomes significant only at higher temperatures [3]. This was accepted at first and experiments were set up so as to verify this value, and possibly pin-point it further.

4.3.1 High-temperature furnace

It was suspected that some mass loss due to sublimation could take place even below 750°C, albeit very small changes and at low rates and some experiments were set up in a non-modified, high-temperature furnace in order to test whether low-temperature sublimation could occur. Tungsten trioxide powder with 99.8 % purity was used and placed inside an STA crucible without a lid. Roughly 100 mg of powder was used each time to get a significant reading of the balance. The atmosphere inside the furnace was regular air, and there was no gas flow. Prior to heating the powder, remnant water vapor was removed from the crucible by heating it at 200°C for approximately 24 hours.

Table 4.9 below gives an overview of the experiments.

Sample number	Temperature [°C]	Time [h]	Mass change [mg]
1	500	45	0
2	600	20	-0.01
3	700	26	-0.06
4	730	29	-0.08
5	740	24	-0.05
6	750	24	-0.05
7	760	24	-0.05

Table 4.9: Mass change during the first set of sublimation experiments.

The observed mass changes were deemed too small to have any meaning as they are likely to be within the noise level of the balance. Additionally, theory predicts that a linear loss of material is expected as soon as the sublimation temperature is reached. Given this set of observed mass changes, the results are discarded and it was concluded that no mass loss could be observed from these experiments where tungsten trioxide powder is subjected to heating up to 760°C in a stagnant air environment. The sublimation temperature was simply not reached under these conditions and low-temperature sublimation was ruled out. This result in particular gives indications that the normal operation of ESS should be on the safe side in terms of sublimation. However, as accident scenarios can bring the spallation target to higher temperatures, the sublimation temperature of tungsten oxide is still desirable to establish.

These results pointed out that the sublimation temperature may not be as well established previously thought and a new experiment was designed by simply raising

the temperature to 900°C. No mass change was observed at this point and the temperature was therefore raised to 1000°C, the maximum operating temperature of this furnace. No mass loss could be observed at this temperature either, and the conclusion was that sublimation will not occur below 1000°C given these conditions.

An interesting effect occurred when trying to sublime the WO_3-powder. At relatively high temperatures, above 900°C, some early stages of sintering appears to have taken place. When handled, the powder was not as fine as prior to the heating, and was markedly darker in color. As stated earlier however, no mass loss took place and this was the only noticeable change.

Concerned with these results, a more in-depth literature survey was performed in order to find more evidence of what was happening. Indeed, the sublimation temperature was not as well established as previously thought and one source points towards higher sublimation temperatures in the range 750°–1000°C where at least the sublimation becomes significant enough to have an impact on the sample mass [28].

It was also thought that the tendency for sublimation was dependent on whether the substrate material was a small piece of tungsten foil or tungsten trioxide powder. The tungsten foil would be oxidized rapidly in the air atmosphere at high temperature and this newly oxidized material was thought to be slightly more reactive than the WO_3 powder. Experiments performed both at 900°and 1000°C with tungsten foils proved that this was not the case at this temperature however, as both foils had only become oxidized and gained mass. As mass loss due to sublimation would have been lower than mass gain due to oxidation at these temperatures, the theoretical mass gain of a 100 % oxidized sample was calculated using simple chemical relations. This mass corresponded well with the new tungsten foil mass, and it was concluded that no sublimation had occurred.

An interesting aspect of the experiments was the delamination of the tungsten foils as they were exposed to temperatures above 900°C. Because of the rolling treatments of the parent tungsten material to produce the tungsten foil, each foil piece was made up of two layers. At room temperature, this is not visible to the naked eye but as the material is oxidized, a delamination process begins as oxygen ions move into and embrittles the foil. The result is that the two layers of the foil detach from each other and can be separated by a tweezer. The layers are extremely brittle however, and will almost immediately crumble to oxide dust if tehy are handled. An example of this delamination can be seen in Figure 4.28.

An untreated sample is shown for comparison. Note the matte dark green and gray color as well as the highly brittle rim around the edges of both layers, which fell off as the sample was removed from the crucible.

4.3.2 TGA setup with vertical tube furnace

Due to both the temperature and atmosphere control limitations of the regular furnace, the remainder of the sublimation experiments were designed to be used with the tube furnace, where previously only oxidation experiments had been done.

Figure 4.28: Delamination of rolled tungsten foil due to high-temperature oxidation.

Two experiments were designed using first tungsten foil and then WO_3-powder put in a small STA crucible. The crucible was suspended in a Chromaloy cage and with wires from an external balance. The samples were then heated up in air to 1100°C for 20 minutes, after which the temperature was lowered due to limitations of the heating elements, and kept at 1075°C for 1 hour and 40 minutes. The mass balance gave no good result from the continuous reading, as the noise level was relatively high and only a small mass gain could be observed. This change was attributed to the oxidation of the Chromaloy cage. The crucible with contents was weighed both before and after each experiment, and no mass change could be observed. The conclusion was that no mass loss due to sublimation had occurred in either tungsten foil or WO_3-powder at temperatures of up to 1100°C. Note that even though the temperature was at 1100°C for a relatively short period of time, it is thought that if the sublimation temperature would have been reached, significant mass loss would occur.

An experiment where tungsten foil was subjected to 1075°C in helium was conducted to test whether a very low oxygen partial pressure could aid in the sublimation reaction. It was determined that the oxygen partial pressure had no effect at this temperature, as no mass loss was observed.

Helium atmosphere contaminated with water vapor

Concern was raised whether small amounts of water vapor would affect the sublimation characteristics, as some evidence has been given for this by e.g. Belton [15].

Two consecutive experiments were designed for the TGA setup in the vertical tube furnace, with tungsten foil and WO_3-powder handled in the same way as previous experiments. This time however, the gas dryer attached to the setup was disconnected to enable an inherent small level of water vapor impurity mix with the helium gas before entering the furnace. The attempt was done to try to enhance the volatilization of the trioxide, allowing it to sublime more easily. The desired result, i.e. a mass loss, was not observed. It was hard to estimate how much water vapor was present in the helium when the dryer was disconnected.

Another set of two experiments with the same setup were conducted, but this time, the helium gas canister was connected to a series of looped tubes going through water tanks. This lead to a small water vapor partial pressure in the helium gas, equivalent to the saturation level of water vapor in helium at that particular temperature, i.e. room temperature in this case so that $p_{H_2O} = 0.0316atm$. The addition of a controlled level of water vapor could potentially enhance the sublimation kinetics of tungsten trioxide. Indeed, some mass loss was now observed, although at small values of around 2 mg during exposure to this modified atmosphere for 2 hours at 1075°C.

In an attempt to replicate this result and acquire a more pronounced mass loss, the experiment with the tungsten foil was repeated for a straight 5-hour run. The result was a definite mass loss of around 5 mg. This is a notable change in mass seeing as the initial foil mass was around 12.6 mg, i.e. the mass loss could have been upwards of 30-40 %. Additionally, there was visible dimensional changes of the top layer of the delaminated oxide structure could be observed, as seen in Figure 4.29.

Furthermore, the top delaminated layer was much thinner than the bottom one and both layers had a more complex surface roughness than samples in other experiments not subject to any water vapor containing helium. This might indicate that sublimation had started on both layers and was proceeding not only from the edges although the greatest mass loss was observed from the top layer.

An attempt to calculate the sublimation kinetics can be done based on these results. The two sublimation experiments yielded mass losses of around 2 mg for the 2-hour set up and around 5 mg for the 5-hour set up. The samples were thin tungsten foils with a surface area of 0.565 cm^2. Recognizing that the sublimation kinetics obey a linear rate law, i.e. a constant loss of material, the rate constant for sublimation can be calculated to $k_s = 1.77\ mg/cm^2h$. These calculations do not take into account the delamination of the tungsten foil, which can create a larger surface area available for sublimation, or the dimensional changes of the top layer of the foil, which lowers the surface area. Despite this, the result can serve as an indication of the sublimation kinetics of WO_3 under these conditions.

Figure 4.29: Evidence of sublimation of tungsten foil in water vapor containing He at 1075°C for 5 hours.

4.3.3 Summary of sublimation results

The literature search indicates that the sublimation temperature is not yet well established as several sources have different values. Additionally, it is difficult to compare the values since the experimental setups are quite diverse. Good correlation with previous reported values are not always found due to the large number of reported values.

The saturation of the helium gas with water vapor clearly enhanced the volatilization of tungsten oxide and made sublimation possible. It is however unclear what amount of water vapor is needed to achieve this result. The water vapor pressure in this setup was approximately 0.0316 atm as calculated in the experimental setup section and this is a relatively high contamination compared with the inherent oxygen impurity of the helium gas which is at maximum 5 ppm. It might be possible to enhance sublimation even at lower water vapor pressures but this was not investigated further.

After 5 hours of exposure to the water vapor saturated helium gas atmosphere at 1075°C, the tungsten foil showed a mass loss of upwards of 40% and this result indicates a significant sublimation process.

4.3.4 Sources of error for sublimation analysis

The crucible containing the tungsten trioxide powder and tungsten foil was of roughly the same mass as the powder and foil itself, meaning that the analytical balance should give an adequately accurate reading. The main errors in these experiments are instead related to e.g. the inevitable heat flow gradients that exist in the furnace, inducing an uneven temperature distribution. Other errors may be related to disturbances when handling the powder, transporting it, and opening and closing the furnace hatches. It is impossible to estimate the impact of these errors, but they are assumed to be sufficiently small for the purpose presented here.

4.4 High-temperature oxidation in air

A series of experiments were also carried out in small high-temperature furnaces with an air atmosphere. The partial pressure of oxygen is therefore taken as the same as that for air, $p_{O_2} = 0.21$, with a total air pressure of 1 atm. No continuous measurements of the mass gain can be performed when using these furnaces since they lack any internal balance or possibilities to attach an external one. Mass measurements are therefore carried out before and after each experiment. The results from these experiments were not used in any kinetic calculations but only serve as an indication of oxidation behavior of tungsten foils in an air environment.

Three samples were tested in separate ovens at 400°, 500°, and 600°C. The results are presented in Table 4.10 below.

Sample number	Temperature [°C]	Initial mass $[mg]$	Mass change $[mg]$	Normalized mass gain $[mg/cm^2]$
1	400	52.48	0.25	0.44
2	500	54.62	2.92	5.16
3	600	50.75	10.51	18.59

Table 4.10: Mass change of tungsten foil kept in air atmosphere at elevated temperatures for 48 hours.

These results show a positive mass gain after exposure to an oxidizing species at elevated temperature, as is predicted.

The final value of the mass gain of the sample at 400°C indicates it has acquired more oxygen compared with e.g. a 500°C sample in the STA which was exposed to the inert argon gas atmosphere, despite being kept at a temperature roughly 100°C lower. This in turn indicates that a markedly higher oxygen partial pressure has a profound influence on the oxidation kinetics.

The sample held at 500°C acquired a few milligrams of oxygen and shows a distinct increase in oxidation compared with the 400°C sample.

The sample held at 600°C is oxidized to a large extent, gaining roughly 10.51 mg of mass or around 20.7 % of its original mass. By comparing the mass gain

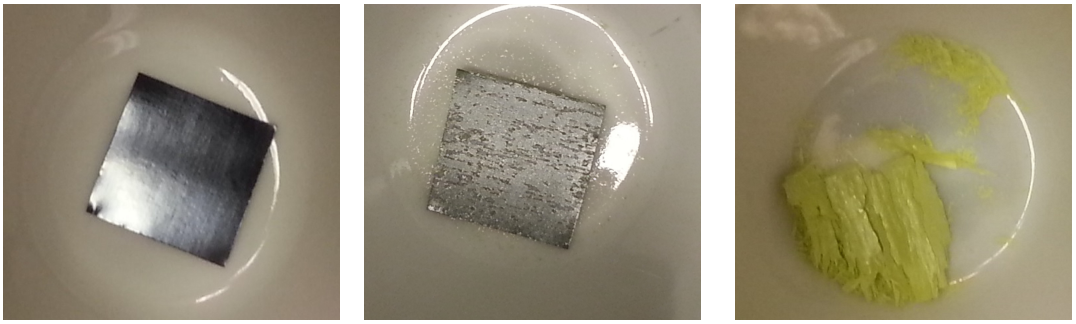

(a) 400°C (b) 500°C (c) 600°C

Figure 4.30: Tungsten foils oxidized in air.

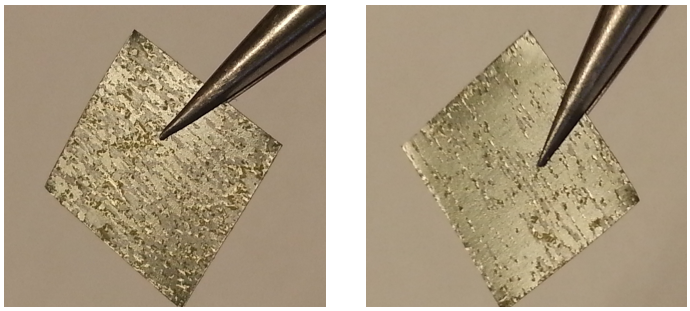

(a) Top view (b) Bottom view

Figure 4.31: Tungsten foil oxidized at in air at 500°C.

and original mass of the sample with the molar masses of oxygen and tungsten, it is possible to get a rough estimate of the extent of oxidation in the sample. In this case, there is a good correlation with the predicted theoretical mass gain so this sample was fully oxidized WO_3 at the end of the experiment.

The appearance of each sample after oxidation can be seen in Figure 4.30.

At 400°C, the tungsten sample exhibits a dark grey color with the metallic luster still present whereas at higher temperatures, oxide particles form on the surface and the metallic shine fades. At 600°C, the sample is completely oxidized and consists of a bright yellow powder. At first, the dimensions of the foil were intact but as soon as the crucible was lifted, the structure crumbled and oxide flakes slided past each other to become a formless mass of tungsten trioxide.

It is assumed that both sides of the tungsten foil is oxidized and while this is true, the top side is exposed to a larger amount of oxygen and is consequently more oxidized as seen in Figure 4.31.

An error which may arise during these oxidation experiments are related to the relative masses of the crucibles and the foil samples. Since the masses of the crucibles themselves are very large in comparison with the masses of the foil samples, the overall mass change may be hard to detect as it could drown in the noise of the large total mass of the crucible and sample combined.

Chapter 5

Kinetic Modelling

There are basically two major processes affecting tungsten in the temperature interval between room temperature and 1000°C.

The first one is the oxidation process, referring to the binding of oxygen species to the metal surface, forming different kinds of tungsten oxide species. The formation of these oxides is governed by the second law of thermodynamics stating that it must be thermodynamically favorable for the oxide to form, i.e. the free energy change of the system must be negative upon formation of the oxide. This thermodynamic reasoning indicates at what temperatures an oxide will spontaneously form, and what type of oxides can form, based on thermodynamic data which can be extracted from e.g. HSC-like computer programs.

However, the thermodynamics of the oxide formation does not state how fast the different oxides will form. An oxide may very well form at room temperature but at such a low rate that it is not going to be a problem for the spallation target in ESS. Therefore, it is crucial to construct a kinetic model describing this behavior at different temperatures. With this information, the life expectancy of the tungsten slabs at ESS could possibly be predicted.

The situation is further complicated by the fact that the different tungsten oxides go through a phase transition at sufficiently high temperatures. At this point the tungsten trioxide will begin to sublimate and leave the oxidized tungsten slab as oxide particles. This process is based on the thermodynamic equation describing the equilibrium between the solid tungsten trioxide slab and the gaseous tungsten trioxide particles.

$$WO_3(s) \leftrightarrow WO_3(g) \tag{5.1}$$

The sublimation will occur at a temperature specified by the thermodynamic relation, but will not give any information about the rate of sublimation, as in the case of oxide formation. At around 750 C, it is predicted that the sublimation of tungsten trioxide is initiated. At this temperature, the sublimation rate will be extremely low in relation to how fast the remaining metal is oxidized to WO_2. At a higher temperature, the oxidation rate becomes progressively higher but at the same time, sublimation also increases. Eventually, sublimation will be the predominating process which will occur, thus removing the oxide layer faster than fresh metal is

oxidized. This in turn will lead to a large amount of free tungsten trioxide particles in the surroundings, contaminating the system, and tungsten being oxidized and immediately being vaporized and leaving again. This will impose security risks at ESS which makes it vital to acquire knowledge of this sublimation process and its equilibrium with oxidation. There will probably be required to construct two different kinetic models based on the process. One of the main reasons to include this modeling section in this thesis is the idea that it might help with further lifetime assessments of tungsten based components subjected to similar environmental conditions. The inherent superimposition of the oxidation and sublimation results can render results hard to interpret. These complications may be minimized or even eliminated to some extent should accurate kinetic data be available, and more importantly, combined into a kinetic model. The model could subsequently be used to describe various high temperature applications in a more accurate way. For example, a tungsten component in a similar environment will be subjected to both extensive oxidation as well as sublimation. If one would want to know how aggressive the oxidation will be, then the sublimation effect in terms of mass loss must be subtracted from the result. This would work in a similar way if the sublimation is the important mechanism.

An attempt to modeling the oxidation kinetics of alloys has been made by Tedmon [29]. The article is focused on taking the volatilization phenomena into account when assessing the oxidation kinetics.

Stringer [30] established some basic kinetic models for the formation of Cr-scales on alloys. It is stated that below 1200 C, the mass gain of the sample follows a parabolic law: $x^2 = k_p t$. At higher T or at very long times, there are deviations from this model. There exists a maximum weight at some point after which the sample loses mass. Stringer refers to two methods that can be used when determining the kinetics, a graphical method developed by Lewis, and an analytical method developed by Tedmon.

5.1 The Tedmon model

The kinetic model developed by Tedmon is based on a combination of the oxidation and sublimation phenomena that is affecting the thickness of the oxide. The rate of growth for the oxide scale follows a parabolic relationship, where x is the oxide thickness, kp is the rate constant, and t is the time.

$$x^2 = k_p t \tag{5.2}$$

The derivative of this expression yields the instantaneous rate of growth

$$\frac{dx}{dt} = \frac{k_p}{2x} \tag{5.3}$$

This is consistent with classical oxidation theory describing the diffusion controlled process in which different ions migrate and form an external oxide. As the thickness

of the oxide increases, the rate of growth diminishes and eventually comes to a halt. This will only occur at very long times and very large oxide thickness.

However, at high temperatures, there is also the sublimation phenomenon which must be taken into consideration as this leads to a mass loss. This is due to solid oxide transitioning into a volatile gaseous form and can be expressed by a linear loss constant

$$\frac{dx}{dt} = -k_e \tag{5.4}$$

The two processes are competing and will simultaneously lead to oxide growth, i.e. the oxide interface eating its way into the sample, and mass loss due to volatile species leaving the sample. The combination of these two rate laws will take the form

$$\frac{dx}{dt} = \frac{k_p}{2x} - k_e \tag{5.5}$$

Integrating this expression will give the time dependence

$$-\frac{x}{k_e} - \frac{k_p}{2k_e^2} - \ln\left[\frac{k_p}{2} - k_e x\right] + C = t \tag{5.6}$$

To evaluate the integration constant C, the boundary condition that x=0 at t=0 can be applied.

$$t = \frac{k_p}{2k_e^2} \cdot \frac{-2k_e}{k_p} \cdot x - \ln\left[1 - \frac{2k_e}{k_d}x\right] \tag{5.7}$$

The rate of oxide growth decreases with increasing thickness and eventually reaches zero, this indicating that a maximum oxide thickness is reached. This means that the ionic transports to the gas/oxide interface is exactly balanced by the mass loss due to sublimation. This is obvious as the limiting thickness x_f can be expressed at the thickness where the rate of thickening through oxidation is equal to the rate of thinning by sublimation.

$$x_f = \frac{k_p}{2k_e} \tag{5.8}$$

For the scale to reach a fraction of the limiting thickness, $0 <= n <= 1$, it can be shown that

$$t_n = \frac{x_f}{k_e}(-n - log(1-n)) \tag{5.9}$$

When combining activation energies, there should be some kind of transition of its value as the sublimation temperature is reached. This would indicate that below 750°C, the activation energy is equal only to the activation energy of the oxidation process and is not affected by the sublimation phenomena. Over 750°C, the activation energy represents both the oxidation reaction and the sublimation reaction.

It has been demonstrated by Blackburn et al. [28] that the oxidation rate is independent of sublimation rate.

Chapter 6

Conclusions

In this thesis, the characteristics of tungsten oxidation and tungsten oxide sublimation were evaluated over a wide range of experimental conditions. Samples of tungsten foil, tungsten discs and tungsten trioxide powder was used as the basis for experiments conducted in a variety of different atmospheres and at different temperatures. The atmospheres all had a small amount of oxygen impurity in it, $p_{O_2} \leq$ 5 ppm, which inevitably oxidizes the tungsten samples.

6.1 STA experiments

The STA experiments were quite tricky to acquire good data from as there were large differences between samples, even when they were tested at the same temperature. An accurate interpretation is therefore complicated. Additionally, the expected parabolic regions were hard to distinguish from the rest of the curve and consequently the rate constants and activation energies were hard to determine.

Still, the STA experiments yield some information about the linear characteristics that the oxidation curve exhibits after some time. The long experiments indicated an almost linear increase in mass per unit time over the whole 48 hour test period.

At 200°C, some oxidation was observed according to the STA thermograph but this may be subject to interference from the internal balance of the STA instrument due to its sensitivity and noise level since the mass gain was so low.

At 575°–625°C, the absolute mass gain of a sample was about 0.5 % after 2 hours.

6.2 TGA experiments

The TGA experiments for oxidation constituted the majority of data which was treated in this thesis and were also the basis for all kinetic calculations when determining the rate constants and activation energies.

Owing to the larger tungsten disc samples, the effect of oxidation became more noticeable and gave a more significant reading on the balance, far beyond its sensi-

tivity and noise level.

The oxidation curves show a close resemblance to smooth parabolas for the most part over the temperature range 500°–1000°C, which is consistent with theory. When each oxidation curve is fitted with polynomials and subsequently squared, deviations become more pronounced as some segments of each curve have a slope that is either steeper or lower than the slope of the linear curve that is fitted to the squared polynomials.

Although this difference is small for most segments, there are some segments that stand out. This complicates the determination of rate constants as choosing the correct segment is crucial to acquiring an accurate value. With care, the segments can be chosen to a satisfactory level of accuracy but this is a point that must be made.

As explained in the chapter on theory, oxides of different composition are expected when tungsten samples are oxidized at 500°, 600°or 700°–1000°C. The reason is the emerging formation of the complex transitional layer oxides at above around 600°C. Several tungsten oxides with only a minute difference in composition is formed on top of each other as oxygen is continuously penetrating the tungsten oxide structure. It is worth noting that the oxide layer closest to the pure tungsten metal is tungsten dioxide, WO_2 whereas the outermost oxide layer facing the environment is tungsten trioxide, WO_3. This is true throughout the whole temperature interval of 500°–1000°C. Despite this, the colors of WO_3 differ whether it is formed at 500°or 1000°C, giving the oxide a shining black appearance or a matte green-yellow appearance, respectively.

The kinetic calculations performed for the TGA experiments gave the activation energies for the chemical reaction to 40 and 94 kJ/mol for UP and EP samples, respectively. The activation energies for the parabolic oxidation were determined to 142 and 153 kJ/mol for UP and EP samples, respectively.

6.3 Sublimation analysis

The sublimation experiments were focused on enabling tungsten trioxide to transition into a gaseous state and leave the solid starting material. Tungsten foils and WO_3-powder were used for this in a variety of difference atmospheres and at different temperatures. The sublimation experiments were initially designed based on the assumption that tungsten trioxide sublimates at around 750°C as was found in some literature.

By a series of experiments using WO_3-powder in air in the temperature range 500°-760°C, any low-temperature sublimation could be ruled out as the powder had undergone no mass loss after the length of each experiment time. This indicated a conflict between reported literature values of the sublimation temperature and more extensive literature survey was needed.

Subsequent experiments were set up in a similar air environment at increasingly higher temperatures of 800°, 900°and 1000°C. Still, no evidence of mass loss due to sublimation was observed, and the temperature limit of this equipment was reached.

New experiments were designed to go beyond this temperature and both tungsten foil and WO_3-powder was tested up to 1100°C. Despite these high temperatures, no sublimation was observed.

Concern was raised as to whether or not the partial pressure of oxygen would influence the sublimation characteristics as some literature had indicated this. The previous experiments were redone in an atmosphere of pure helium but no sublimation was observed at this stage either.

Lastly, a water vapor containing helium atmosphere saturated with water could finally enhance the sublimation to such a point that a clear mass loss was observed at 1075°C in this modified atmosphere. The water vapor pressure was approximately 0.0316 atm in this setup which is markedly higher than the oxygen impurity of 5 ppm inherently present in the helium gas. From this result, the rate constant for sublimation was determined to be 1.77 mg/cm^2h. It is possible that a lower water vapor pressure can also enhance the sublimation but this was not further investigated.

Although the results presented in this thesis are obtained with specialized laboratory equipment under monitored conditions, the correlation between the results and the operation of the spallation target at ESS may be difficult. The conditions at ESS have a significant complexity which cannot be easily reproduced and the results should therefore only serve as an indication of what happens with tungsten and tungsten oxides under conditions which are similar to the ones in ESS.

Still, some results may be relevant to the design of the target system in ESS, e.g. the sublimation temperature of tungsten trioxide. This was, as mentioned previously, determined to be 1075°C in a water-saturated helium atmosphere.

Other results could be utilized to a lesser extent by confirming the oxidation kinetics in a helium atmosphere in a wide temperature range which covers both the normal operation of ESS as well as some accident scenarios.

6.4 Suggestions for future work

There are still a lot of question marks regarding the oxidation of tungsten under certain conditions, and maybe most importantly, it is difficult to estimate just how large impact on the results those question marks may have.

It is impossible to construct an experiment which replicates all the conditions that are present in the target system of ESS, and impossible to take every small physical or chemical effect into account for what is happening.

Some suggestions for what could be further looked at:

- The effect of thermal cycling on the oxidation behavior and how the thermal stresses from temperature cycling influence oxide cracking and spalling processes.
- The effects of high speed He-cooling gas flowing past the target and how this influences the oxidation behavior.

- The effect which different crystallographic planes may have on the oxidation and sublimation characteristics.

Appendix A

STA thermographs

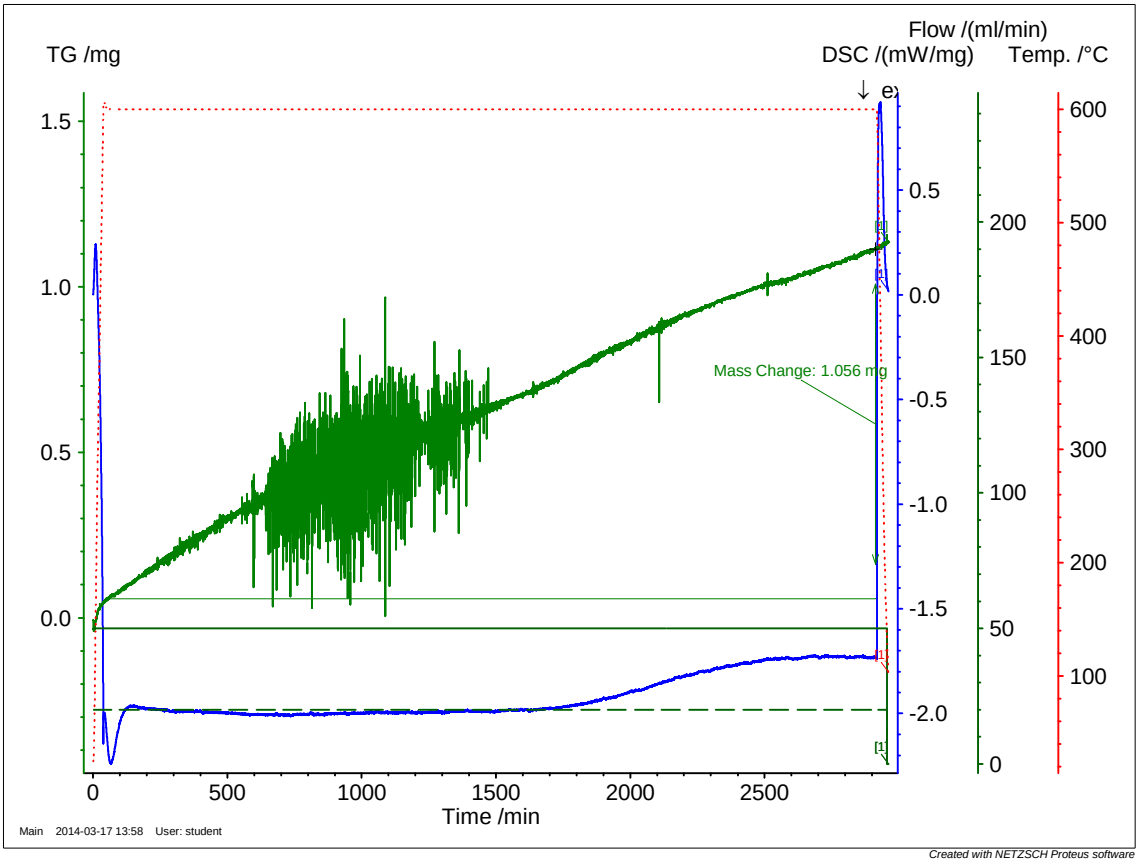

Figure A.1: The first STA run at 600°C.

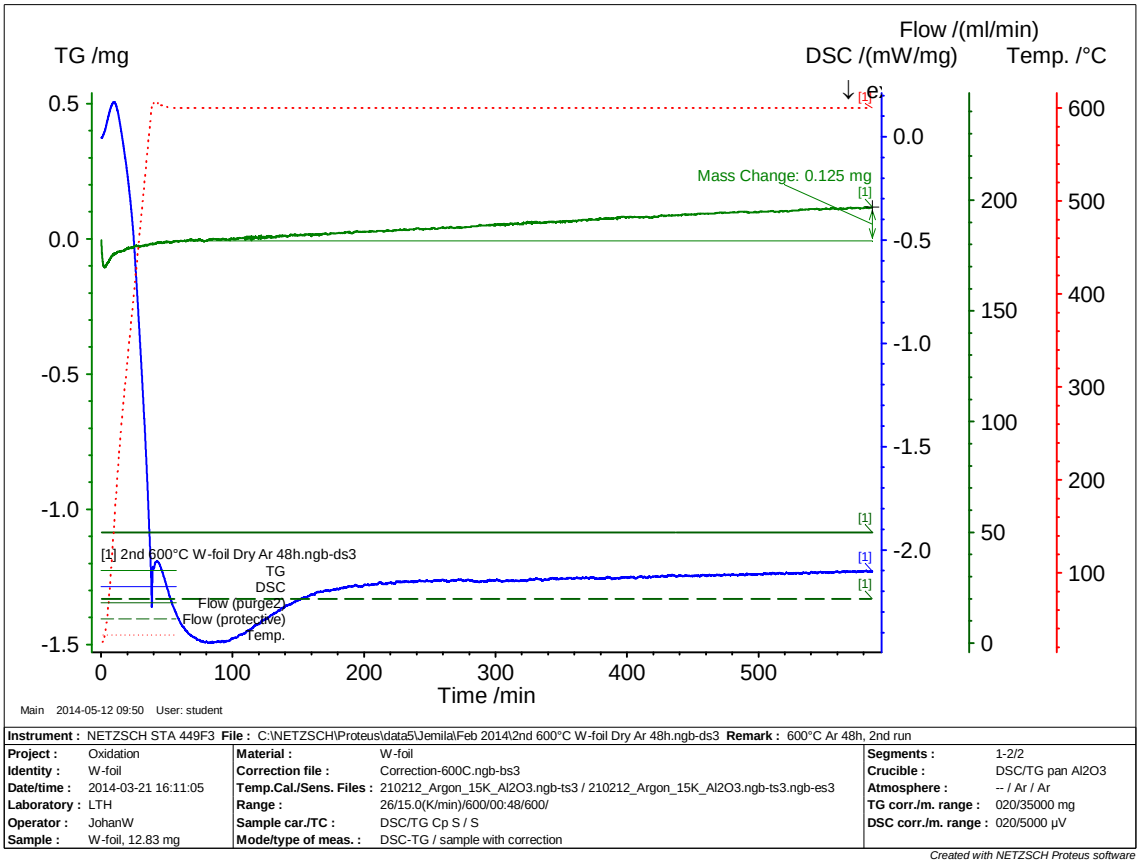

Figure A.2: The second STA run at 600°C.

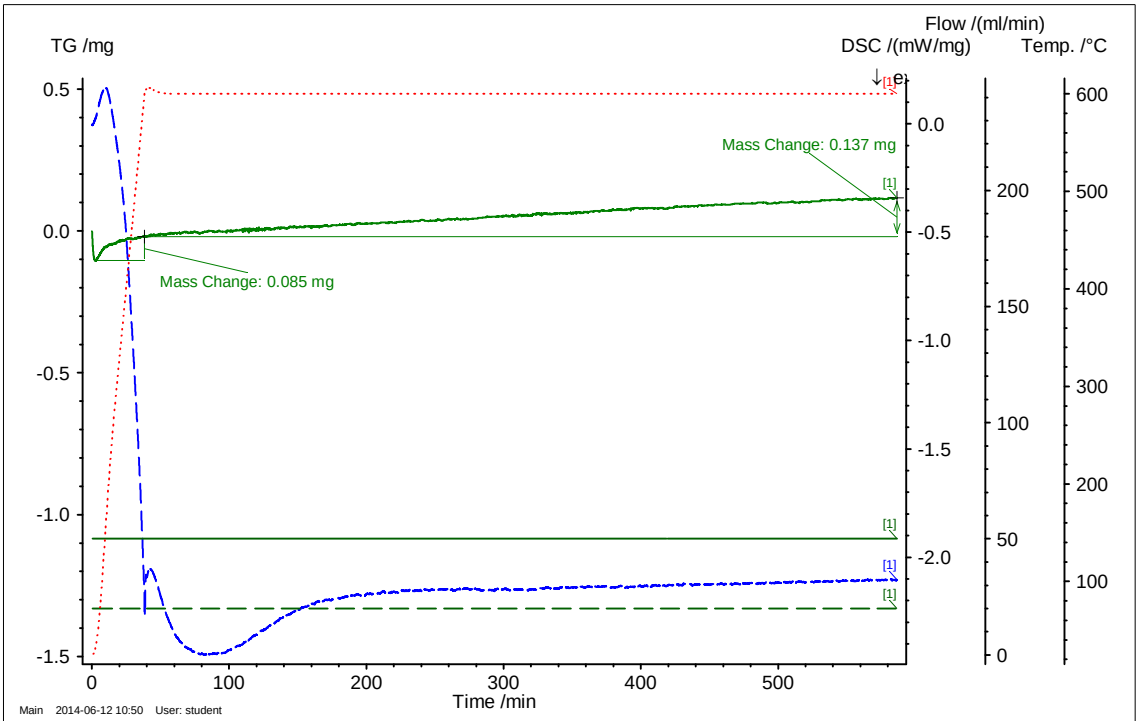

Figure A.3: Segment of the second STA run.

Bibliography

[1] Team Henning Larsen Architects. The latest conceptual rendering of the ESS, September 2014.

[2] Neil Birks, Gerald H. Meier, and Frederick S. Pettit. *Introduction to the High Temperature Oxidation of Metals, 2nd Edition*. 2006.

[3] Erik Lassner and Wolf-Dieter Schubert. *Tungsten - Properties, Chemistry, Technology of the Element, Alloys, and Chemical Compounds*. 1999.

[4] ASM International. *ASM Handbook, Volume 3 - Alloy Phase Diagrams*. 1992.

[5] S Peggs. ESS technical design report - Target station. 2013.

[6] G. W. Meetham and M. H. Van de Voorde. Materials for high-temperature engineering applications. 2000.

[7] S. Peggs and R. Kreier. ESS Technical Design Report. Technical report, 2012.

[8] Michael Rieth. Functional Tungsten Materials for the ESS Target. Technical report, 2012.

[9] V. Ye. Ivanov, Ye. P. Nechiporenko, L. N. Yefimenko, and M. I. Yurchenko. High Temperature Oxidation Protection of Tungsten. Technical report, 1968.

[10] E. A. Gulbransen and W. S. Wysong. Thin Oxide Films on Tungsten. (September):611–627, 1947.

[11] Roger J. Mortimer. Electrochromic Materials. *Annual Review of Materials Research*, 41(1):241–268, August 2011.

[12] C. G. Granqvist. Electrochromic oxides: A unified view. *Journal of Solid State Ionics*, pages 678–685, 1994.

[13] John Stanley Dunn. The Oxidation of Tungsten: Evidence for the Complexity of Tungstic Oxide, WO3. *Journal of the Chemical Society*, pages 1149–1150, 1929.

[14] D. N. Poluboyarinov, N. T. Andrinnov, I. Ya. Guzman, and E. S. Lukin. Volatilization of porous oxide ceramics at high temperatures. Technical Report 11, 1966.

[15] G. R. Belton and R. L. McCarron. The Volatilization of Tungsten in the Presence of Water Vapor. *The Journal of Phsyical Chemistry*, 33(2):1852–1856, 1962.

[16] I. Hargittai, M. Hargittai, V. P. Spiridonov, and E. V. Erokhin. An electron diffraction study on the vapors of tungsten trioxide. *Journal of Molecular Structure*, 8:31–41, 1971.

[17] Watt Wo Webb, T John, and Carl Wagner. Oxidation of Tungsten. 103(2):107–111, 1956.

[18] R. E. Smallman and A. H. W. Ngan. *Physical Metallurgy and Advanced Materials*. 2007.

[19] H. A. Wriedt. The O-W (Oxygen-Tungsten) system. *Bulletin of Alloy Phase Diagrams*, 10(4):368–384, 1989.

[20] E. A. Kellet and S. E. Rogers. The Structure of Oxide Layers on Tungsten. 1963.

[21] S. C. Cifuentes, M. A. Monge, and P. Pérez. On the oxidation mechanism of pure tungsten in the temperature range 600°–800°C. *Corrosion Science*, 57:114–121, April 2012.

[22] A. L. Pergament and G. B. Stefanovich. Phase composition of anodic oxide films on transition metals: a thermodynamic approach. *Journal of Thin Solid Films*, 322(1-2):33–36, June 1998.

[23] Donald L. Smith. *Thin-film deposition - Principles & practice*. 1995.

[24] J.R. Davis. *Heat-Resistant Materials - ASM Specialty Handbook*. 1997.

[25] D. V. Kostomarov, Kh. S. Bagdasarov, and E. V. Antonov. Formation of complex tungsten oxides at high temperatures. *Doklady Chemistry*, 442(2):37–39, March 2012.

[26] D. V. Kostomarov, Kh. S. Bagdasarov, and E. V. Antonov. Formation of complex oxides in the W-O2 system at temperatures from 2000 to 2500 K and a pressure of 10ˆ5 Pa. *Inorganic Materials*, 48(11):1115–1119, October 2012.

[27] E. A. Gulbransen and K. F. Andrew. Kinetics of the Oxidation of Pure Tungsten from 500^oC - 1300^oC. *Journal of the Electrochemical Society*, 107(7):619–628, 1960.

[28] P. E. Blackburn, K. F. Andrew, E. A. Gulbransen, and F. A. Brassart. Oxidation of Tungsten and Tungsten Based Alloys. Technical report, 1961.

[29] C. S. Tedmon. The Effect of Oxide Volatilization on the Oxidation Kinetics of Cr and Fe-Cr Alloys. *Journal of the Electrochemical Society*, (1926):766–768, 1966.

[30] J Stringer. The Functional Form of Rate Curves for the High- Temperature Oxidation of Dispersion-Containing Alloys Forming Cr203 Scales. *Oxidation of Metals*, 5(1):49–58, 1972.